Romanian Authority for Nuclear Activities
Institute of Nuclear Research-Pitesti

Gesellschaft für Anlagen- und Reaktorsicherheit (GRS) mbH

Comparison of long-term safety of repositories for spent CANDU or LWR fuels in hard rock

GRS - 196
SCN-NT 261/2003

Romanian Authority for Nuclear Activities
Institute of Nuclear Research-Pitesti

Gesellschaft für Anlagen- und Reaktorsicherheit (GRS) mbH

Comparison of long-term safety of repositories for spent CANDU or LWR fuels in hard rock

Dieter Buhmann
Margarit Pavelescu (SCN)
Alice Ionescu (SCN)
Andrei Rizoiu (SCN)
Richard Storck

Dezember 2003

Remarks:

This work has been financially supported by a linkage grant of the scientific part of the North Atlantic Treaty Organisation (NATO) under contract no. EST.CLG 977810. Work has been carried out by Gesellschaft für Anlagen- und Reaktorsicherheit (GRS) mbH in cooperation with Institute for Nuclear Research (SCN) in Romania. Only the authors are responsible for the contents of this report.

GRS - 196
SCN-NT 261/2003
ISBN 3-931995-64-X

Deskriptoren:
Aktiver Abfall, Endlager, Felsformation, Grundwasser, Langzeitsicherheit, Sicherheitsanalyse, Strahlenexposition, Umweltbelastung, Uran

Table of contents

1 Introduction

A long-term safety analysis for direct disposal of spent nuclear fuel from power plants of CANDU type has been performed. The results are compared with previous results for disposal of spent LWR fuel. Additional parameter variations have been performed for both fuel types. CANDU reactors use natural uranium as nuclear fuel, while LWR fuel elements are made of enriched Uranium. The study was jointly performed by a Romanian institute and a German company. Thus, the input data for the calculations are taken from the corresponding national data bases.

In the present study, disposal is assumed to take place in a granite formation. The long-term safety of repositories in such formations has been investigated in detail in a recent project of the European Commission, called Spent fuel disposal Performance Assessment (SPA project) [3]. Results of the German participant of that project regarding spent LWR fuel have been published in detail separately [13]. The latter report is the basis for the actual investigations.

After contact with groundwater, the radionuclides disposed of in the repository are assumed to be released from the spent fuel elements and to be transported through the repository system by diffusive and advective flow. Other release paths are not dealt with in this study. After transport of the radionuclides to the biosphere a radiation exposure to man occurs. The consequences of the potential release of radionuclides are mainly discussed in terms of annual radiation exposures, i.e. effective doses.

The consequences are calculated by a deterministic method applying computer codes of the computer code package EMOS [5], all of them in the version 1.01. Release from the near field is calculated by GRAPOS, transport in the geosphere by CHETMAD, and the radiation exposure in the biosphere by EXMAS. Uncertainties of the input parameters are treated by local parameter variations.

The repositories for spent CANDU or LWR fuel elements are assumed to be different mainly in the data of the source term for spent fuel and the size of the underground facilities. Differences in the amount of waste of both countries are also taken into account. A common model of the source term is applied for both types of fuel.

A similar exercise as the present one has been performed by the same team and published recently [6]. In that publication the long-term aspects of disposal in a salt formation have been dealt with. One of the main results was, that differences in the calculated radiation exposures are mainly due to the lower heat production of CANDU fuel elements. But the overall behaviour of the repositories was similar for CANDU and LWR fuel.

In chapters 2 and 3, all input data for the calculations are compiled for CANDU and LWR fuel. The compilation is based on report [13], i.e. the following tables give a summary of that report concerning LWR fuel, supplemented by the information needed for CANDU fuel. Chapter 4 gives the calculated results for the reference case with best estimate values of the input parameters and Chapter 5 for the parameter variations.

2 Repository design in granite formations

The general concept for disposal of spent fuel elements in granite is similar for CANDU and LWR. The containers with spent fuel are placed centrally in cylindrical emplacement boreholes, and are surrounded by cylindrical buffer material. The buffer is assumed to enclose the containers entirely. Thus, there is no advective flow through the buffer and the release of radionuclides in this part of the repository system is only by diffusion. Flow of water around the buffer is assumed to be possible through the excavation damaged zone (EDZ) of the borehole. If a connection exists between the EDZ and a major water conducting fault in the granite body, then radionuclides can be transported advectively from the EDZ towards the biosphere.

A concept of a potential repository in a granite formation in Germany is proposed in the GEISHA project report [15] and considered as reference concept in the present study. The repository is assumed to be at a depth of 900 m. A suitable host rock is characterized by a large block of low-permeable crystalline material. Assuming the repository to be placed in a rock mountain (see Figure 2.1) the repository can be accessed by a tunnel. If the mine is deep underground, it may be accessed by a shaft, as shown in Figure 2.2.

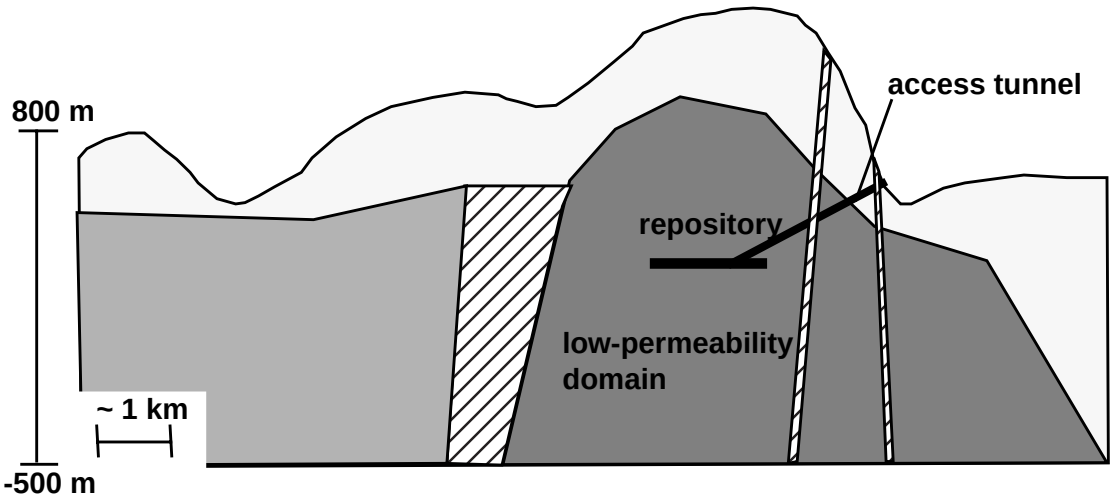

Fig. 2.1 Sketch of a repository in granitic mountains

General data for both fuel types are compiled in Table 2.1. In the following, the main characteristics of the disposal concepts for both fuel types are presented.

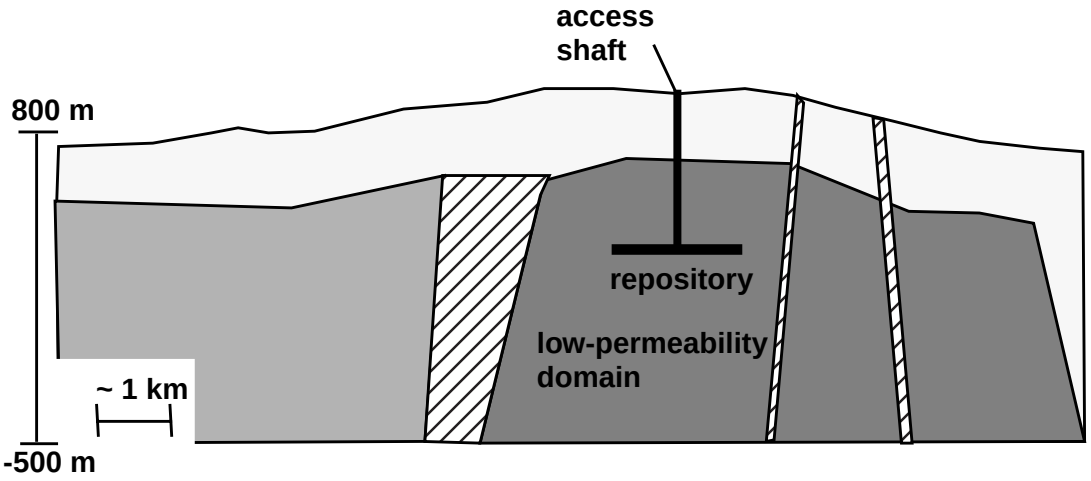

Fig. 2.2 Sketch of a repository in flat regions

Tab. 2.1 General data of disposal systems

Design considerations		CANDU fuel	LWR fuel
Fuel			
Type of spent fuel		Used-fuel bundles from CANDU 6 reactors	Used-fuel bundles from PWR reactors
Initial enrichment		Natural uranium	3.6% U-235
Fuel burnup		7.93 GWd/t_{HM} (685 GJ/kg U)	45 GWd/t_{HM}
Fuel inventory:	number of bundles	518 400	46 815
	mass of uranium	9 828 t_U	74 998 t_U
Fuel cooling time		10 y	60 y
Container			
Container shell material		Grade-2 Ti	Fine grain steel 15MnNi6.3
Container lifetime		$1.5 \cdot 10^3$ y	10^3 y
Dimensions:	length	2.246 m	4.9 m
	diameter	0.633 m	0.53 m
	thickness	6.35 mm	0.1 m
Volume for dissolution		534 l	300 l
Number of waste containers		7 200	15 605[a]
Number of bundles per container		72	3

Tab. 2.1 General data of disposal systems

Emplacement method		
	Boreholes drilled into the floors of the vault, surrounded by buffer	
Buffer		
Material	Compacted bentonite clay and silica sand (50:50)	Compacted bentonite clay
Solid dry density (minimum)	1856 kg/m^3	2760 kg/m^3
Porosity	0.10	0.38
Height	5.0 m	6.3 m
Inner bentonite radius, r_{in}	0.37 m	0.265 m
Outer bentonite radius, r_{out}	0.62 m	0.6 m
Excavation damaged zone (EDZ)		
Thickness	Not explicitly evaluated in the post-closure assessment - would have no significant effect in this disposal system	
Porosity		
Flow rate through rock per deposition hole	0.223 l/y	9 l/y
Flow rate through EDZ of one deposition hole	0.0223 l/y	1 l/y
Vault design and layout		
Vault depth	500 m	500 m
Area	0.19 km^2	1.0 km^2
Number of storage drifts	25 (234 m long and 8 m wide)	745 (215 m long and 4 m wide)

a. Only 25% of all the containers are taken into account in the performance assessment

2.1 Repository design for spent LWR fuel

The repository for LWR spent fuel is designed as a system of horizontal storage tunnels at one level schematically shown in Figure 2.3.

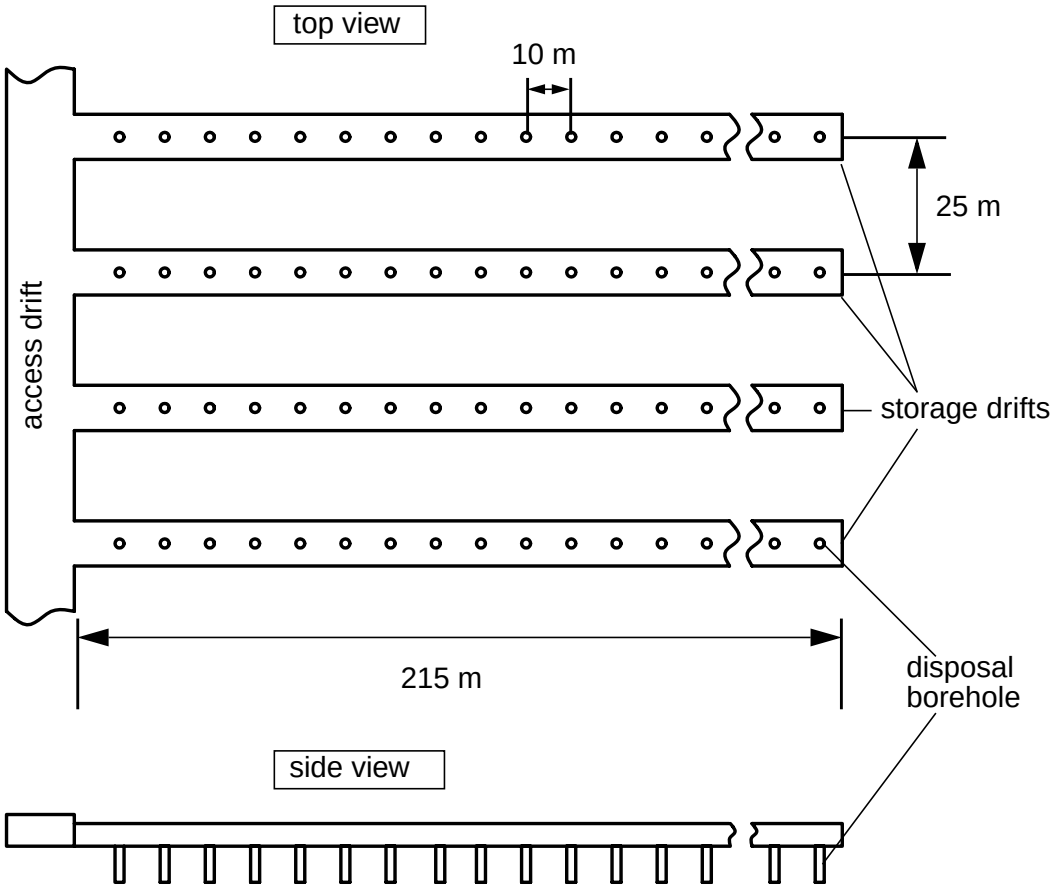

Fig. 2.3 Schematic view of the hypothetical repository for spent LWR fuel in a granite formation [13]

A total of 15 605 containers are disposed of in 8.3 m deep vertical holes drilled into the floors of the drifts. The containers are surrounded by a buffer of compacted bentonite. As shown in Figure 2.4, only one container is disposed of per borehole. A minimum spacing of 10 metres between the boreholes is necessary to keep the maximum temperature of the bentonite below 100°C, since at such a temperature it is guaranteed that the bentonite will be stable and keep its barrier function. The distance between the storage drifts is 25 metres.

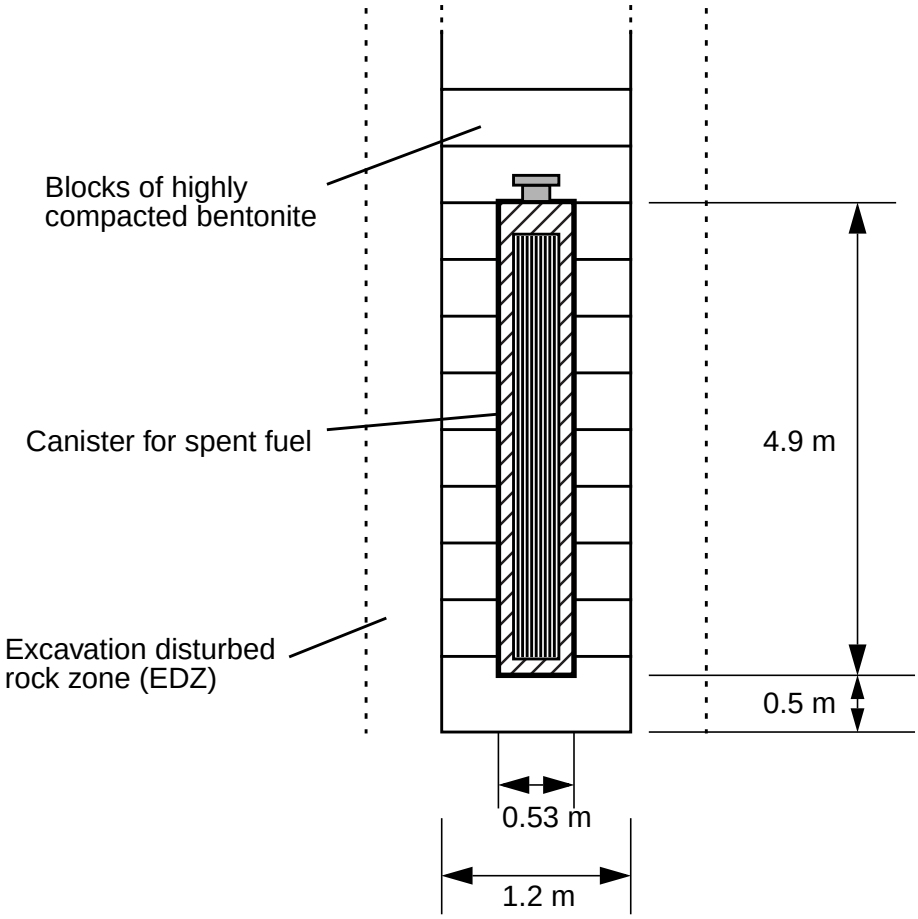

Fig. 2.4 Disposal borehole with LWR canister, buffer and EDZ

2.2 Repository design for spent CANDU fuel

In the case of CANDU fuel, the disposal concept is similar, the differences only appear in the borehole arrangement in the disposal rooms. The layout of the repository for CANDU fuel follows the Canadian emplacement concept [11]. Thus, boreholes are arranged in a network of three rows abreast the room and 96 columns lengthwise. The width of a disposal room is 8 m, the distance of the centers of two adjacent boreholes is 2.1 m. The concept is shown in Figure 2.5.

The repository consists of 25 disposal rooms, in which 7200 containers are disposed of. This quantity represents the equivalent of 5000 bundles per year and unit, arising from 2 nuclear units similar to the one in Cernavoda for a period of 50 years [14]. The distance between disposal rooms is 30 m. The outer radius of a Ti container is 0.37 m, the outer radius of the buffer is 0.62 m.

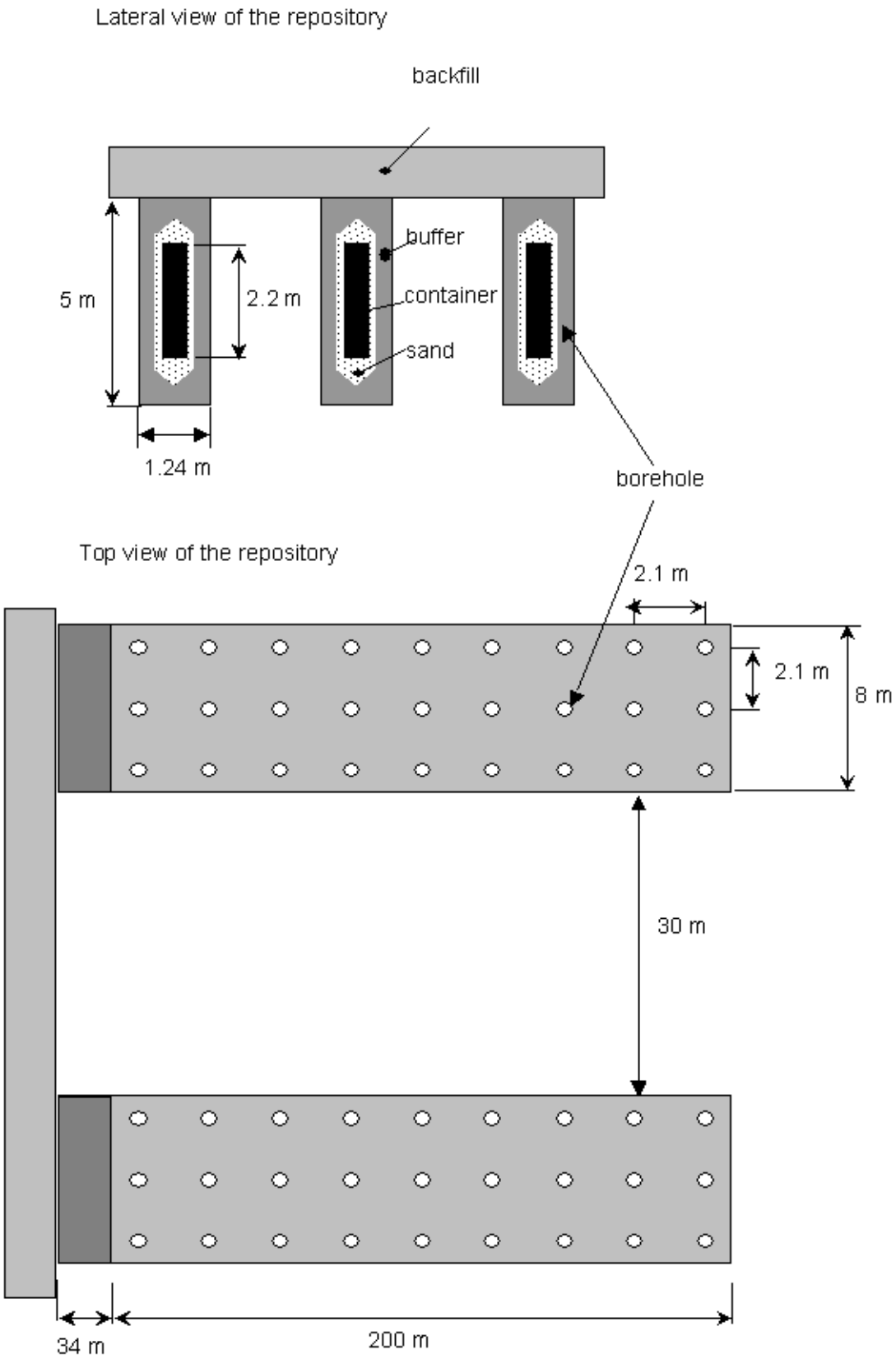

Fig. 2.5 Borehole emplacement of spent CANDU fuel in granite formations

3 Models and data

In this chapter, the models and data for the near field, the far field, and the biosphere are compiled. This description is a short version of the appropriate chapters in Ref. [13], supplemented by data for spent CANDU fuel.

3.1 Near-field model

The near-field model describes the release of radionuclides and their transport through the engineered barriers of the near field to the water-conducting zones of the geosphere. A schematic representation of the near-field is given in Figure 3.1.

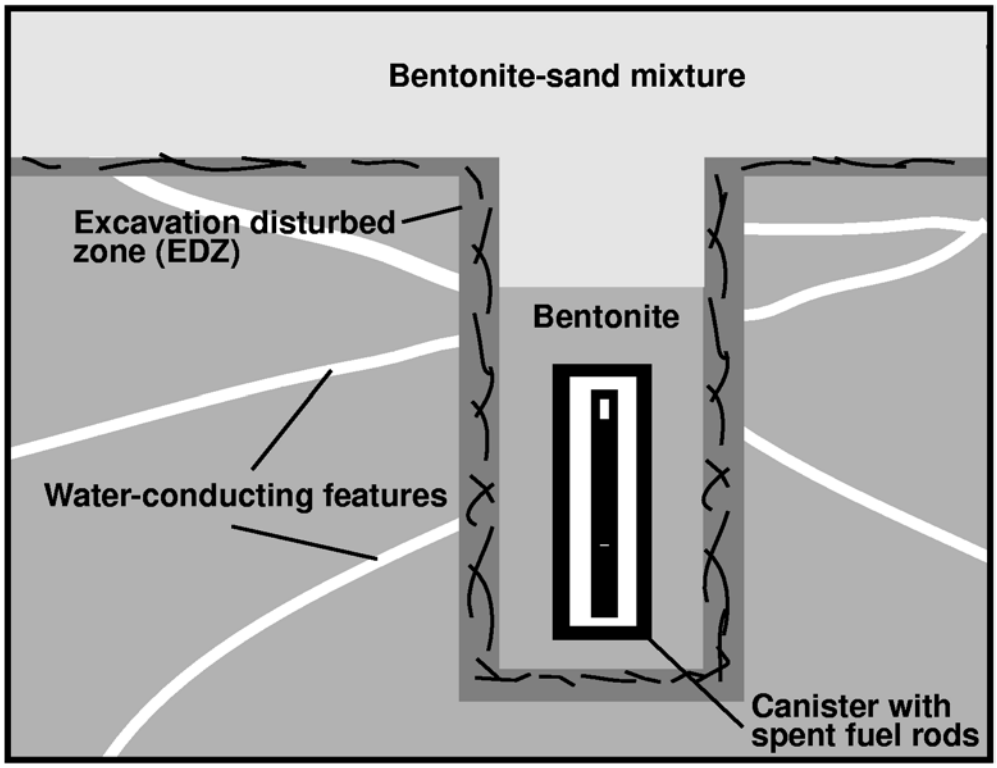

Fig. 3.1 Schematic representation of the near-field [13]

The following components of the engineered barriers have been taken into account in the conceptual near-field model:

- the spent-fuel matrix,

- the massive steel container, and
- the highly compacted bentonite buffer.

When the spent-fuel matrix becomes dissolved, the radionuclides may be mobilised in the water phase or immobilised in other phases caused by processes such as precipitation/dissolution and sorption. The radionuclides may diffuse through the bentonite barrier and reach water-conducting zones of the far-field. A schematic representation of the transport mechanisms considered in the near field is given in Figure 3.2.

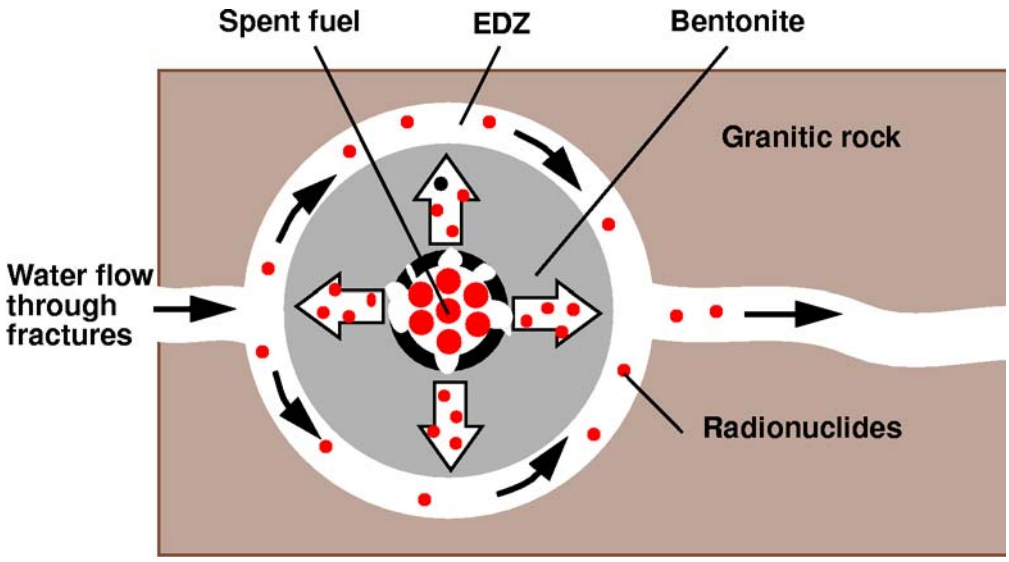

Fig. 3.2 Schematic representation of the mechanisms modelled in the near-field transport code GRAPOS [13]

3.1.1 Mobilisation of radionuclides from spent fuel

Before the container failure, the activities of radionuclides will change due to radioactive decay and ingrowth only. For the *i*th radionuclide with decay constant λ^i the change of inventory A^i is given by the following differential equation:

$$\frac{\partial}{\partial t}A^i(t) \;=\; -\lambda^i\left(A^i(t) - \sum\nolimits_k A^k(t)\right), \qquad (3.1)$$

where the index k denotes the parent radionuclides of the *i*th radionuclide.

In calculating the release of radionuclides from the waste matrix a potential barrier effect of the container or cladding is neglected. Therefore, the radionuclide release into the volume of dissolution starts immediately after failure of the first container. The mobilisation process is modelled according to the common source term model developed in the SPA project [3]. The source term model distinguishes between the inventory in the gap, the metallic parts, and the fuel matrix. The metallic parts include the cladding and the structural parts of the fuel element. For the gap inventory an instantaneous release, whereas for the metallic part and the fuel matrix a constant degradation rate is assumed (cf. chapter 3.2.5).

The release $S^i(t)$ of nuclide i is described by

$$S^i(t) \;=\; n_c(t) \sum_x \alpha_{x,\ e(i)}\, r_x A^i(t)\ , \qquad (3.2)$$

where r_x is the constant release rate in the respective region x (gap, metal parts, matrix), $a_{x,\ e(i)}$ the element-specific fraction of the so called “hypothetical inventory” $A^i(t)$ of the ith nuclide in region x, and $n_c(t)$ is the number of failed containers at the time t. The “hypothetical inventory” $A^i(t)$ corresponds to the initial inventory changed only by radioactive decay and ingrowth.

3.1.2 Solubility limits and the waste-bentonite interface

After container failure the interior of the container becomes water-saturated and then the radionuclides are mobilized. In the model a hypothetical “volume of dissolution” V_{dis} is assumed, into which radionuclides are released. The change in the inventory M^i in this volume is given by the differential equation

$$\begin{aligned} \frac{\partial}{\partial t} M^i(t) \;=\; & -\lambda^i \left[M^i(t) - \sum\nolimits_k M^k(t) \right] + S^i(t) \\ & -2\pi r_{\mathrm{in}} h \varepsilon_b D_b \frac{\partial}{\partial r} C^i(t) \Big|_{r \,=\, r_{\mathrm{in}}}, \end{aligned} \qquad (3.3)$$

where r is the radial distance, r_{in} the inner radius of the buffer, and h the axial length of a waste container. The terms on the right-hand side represent radioactive decay and ingrowth, release from spent fuel, and diffusion into the bentonite, respectively. The release from spent fuel $S^i(t)$ is given in equation 3.2. ε_b is the diffusion porosity and D_b the diffusion coefficient in bentonite

The boundary condition at the inner interface of the bentonite is defined by the radionuclide concentration in the hypothetical volume of dissolution V_{dis}. Including the solubility limits $L^{e(i)}$, the concentration C^i of the *i*th radionuclide at the inner interface of the bentonite is determined by

$$C^i\Big|_{r\,=\,r_{\mathrm{in}}} \;=\; \min\left(\frac{M^i}{V_{\mathrm{dis}}},\; \frac{M^i}{M_{\mathrm{el}}^{e(i)}} L^{e(i)}\right) , \qquad (3.4)$$

where $M_{\mathrm{el}}^{e(i)}$ is the number of moles of element *e* of which the radionuclide *i* is an isotope.

3.1.3 Diffusion through the bentonite

The radionuclides are assumed to be transported through the bentonite only by diffusion. For the calculation of this diffusive transport the geometry is simplified in such a way that only one-dimensional radial diffusion is considered. Then the governing equation for the transport through the bentonite is given by

$$R^i \frac{\partial C^i}{\partial t} \;=\; D_b \left[\frac{1}{r}\frac{\partial}{\partial r}\left(r\frac{\partial C^i}{\partial r}\right)\right] - \lambda^i \left[R^i C^i - \sum\nolimits_k R^k C^k\right] . \qquad (3.5)$$

The index k denotes the parent radionuclides of the *i*th radionuclide. Assuming linear sorption yields the following retardation factor R^i:

$$R^i \;=\; 1 + \frac{1-\varepsilon_b}{\varepsilon_b}\rho_b K_d^{e(i)} \qquad (3.6)$$

with the density of bentonite ρ_b, the bentonite porosity ε_b, and the element-specific distribution coefficient for bentonite $K_d^{e(i)}$. No solubility limits are applied during the transport through the bentonite. This means that the dissolved amount of daughter nuclides formed during the diffusion process by decay of their parents may exceed the solubility limits.

3.1.4 Release to the host rock

At the interface between the bentonite and the excavation-disturbed zone (EDZ) which is intersected by water-conducting features of the granitic rock, the so called “mixing tank” boundary condition is used. In that case, the diffusive flux across the bentonite-host rock interface is determined in such a way that the diffusive flux is equal to the mass flux by advection in the excavation-disturbed zone:

$$2\pi r_{\text{out}} h \varepsilon_b D_b \frac{\partial C^i}{\partial r}\bigg|_{r = r_{\text{out}}} = Q_{\text{EDZ}} C^i. \qquad (3.7)$$

The groundwater flow Q_{EDZ} through an excavation-disturbed zone of a deposition hole is controlled by the total water flow *Q* through the repository area by $Q = F_{\text{nc}} \sum_n Q_{\text{EDZ}}$. The fraction of the water flow around a deposition hole entering the excavation-disturbed zone is determined by the parameter F_{nc}.

3.2 Near field data

In the following, the concept specific data for the near field are presented, i.e. flow rate in the EDZ, waste inventories, source term data and diffusion parameters. The geometrical data of the repository and of the containers have been presented in Chapter 2. The remaining data are common for both concepts and are available from literature [11], [13].

The radionuclide migration data (pore diffusion coefficients) and geochemical parameters (sorption and solubility) are considered to be the same for both fuel types. This is because similar geochemical conditions are expected to appear in both cases.

3.2.1 Flow rate in the EDZ

According to SPA calculations, the total flow rate in the geosphere, corresponding to a repository area of 4.0 km^2 for spent LWR fuel, is 140 m^3 /yi.e. the Darcy velocity is $3.5 \cdot 10^{-5}$ m/y [13].

In the case of spent CANDU fuel, the total area is much smaller. It results as 191 520 m^2, which corresponds to 26.6 m^2 repository area per container [11]. Accordingly, the total flow rate through the entire CANDU repository is 6.7 m^3 /y The active area of the repository, meaning the area of all emplacement chambers, is 46 000 m^2 .It means that 24% of flow is through the chambers (1.6 m^3/y), i.e. $2.2 \cdot 10^{-4}$ m^3 /y(0.22 l/y) per container. It is conservatively assumed, as in the SPA calculations, that 10% of the total flow is through the EDZ.

3.2.2 Bentonite porosity

For spent LWR fuel, the data of the SPA project are used. For spent CANDU fuel, according to Canadian specifications, the buffer volume per container is 4.9 m^3. The void volume in the buffer is divided into 400 l empty volume and 100 l occupied by water [11]. In total, in 4.9 m^3 of buffer there are 500 l of void space, yielding a porosity of 0.1 for the bentonite buffer.

3.2.3 Bentonite dry density

For spent LWR fuel, the data of the SPA project are used. For spent CANDU fuel, the bentonite dry bulk density ρ_b, defined as ratio of the solid mass and the sum of the volumes of the solid rock matrix and the pore volume, is 1670 kg/m^3. The relation between the bulk density and the dry density ρ_d (the ratio between the solid mass and the volume of the solid rock matrix) is given by:

$$\rho_d = \frac{\rho_b}{1 - \varepsilon} \qquad (3.8)$$

With these values, the buffer dry density results as 1856 kg/m^3 for CANDU repository.

3.2.4 Waste packages and inventories

Sketches of the waste packages used for the purpose of this study are shown in Figures 3.3 and 3.4. Table 2.1 contains a compilation of all data relevant for the modelling of the containers. Table 3.1 contains a list of radionuclide inventories in the spent fuel of CANDU and LWR type, respectively.

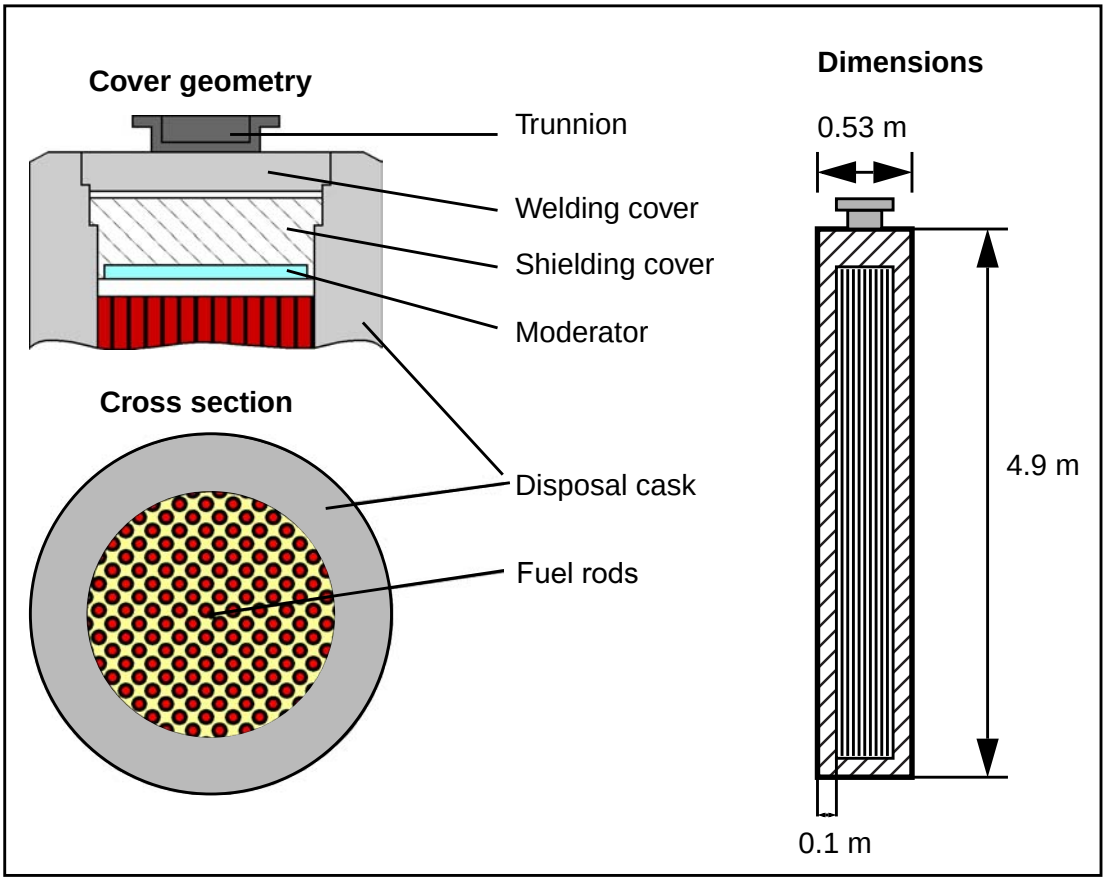

Fig. 3.3 Schematic view of an LWR waste container for borehole disposal

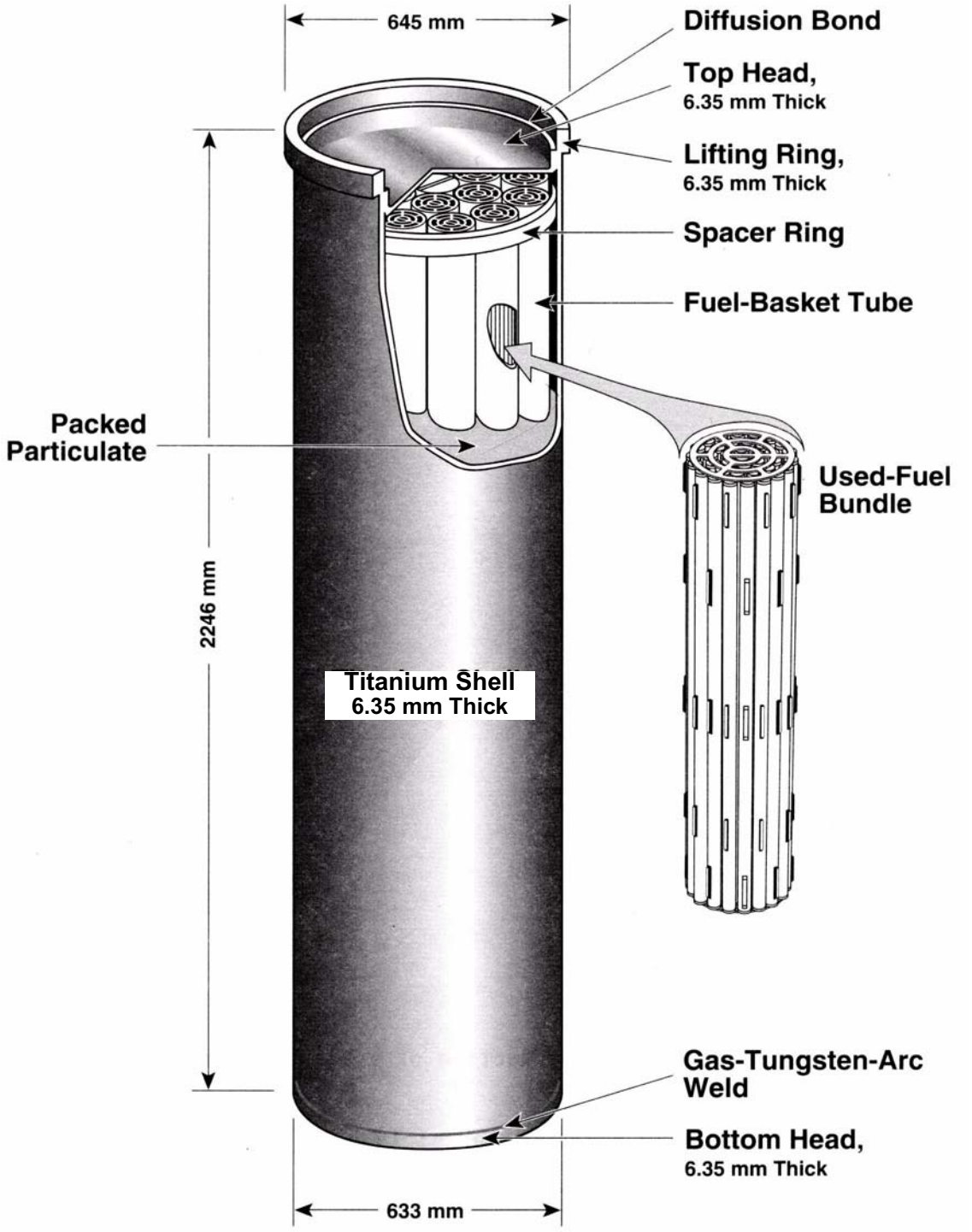

Fig. 3.4 The Packed-Particulate, supported shell container for spent CANDU fuel. The basket is assumed to be ceramic or a metal that produces little H_2 upon corrosion. The particulate material is assumed to contain small amounts of magnetite to scavange residual oxygen inside the container.

Tab. 3.1 Inventory of long-term relevant radionuclides in spent fuel and metal parts immediately after discharge (Bq/container)

Nuclide	Half-live [years]	CANDU fuel			LWR-UO_2 fuel		
		spent fuel	metal parts	total	spent fuel	metal parts	total
C-14	$5.73 \cdot 10^{+03}$	$5.82 \cdot 10^{+10}$	$1.02 \cdot 10^{+10}$	$6.84 \cdot 10^{+10}$	$1.28 \cdot 10^{+07}$	$3.32 \cdot 10^{+07}$	$4.60 \cdot 10^{+07}$
Cl-36	$3.00 \cdot 10^{+05}$	$2.33 \cdot 10^{-04}$	-	$2.33 \cdot 10^{-04}$	$6.10 \cdot 10^{+05}$	$5.25 \cdot 10^{+01}$	$6.10 \cdot 10^{+05}$
Ca-41	$1.40 \cdot 10^{+05}$	$2.31 \cdot 10^{+08}$	-	$2.31 \cdot 10^{+08}$	$3.01 \cdot 10^{+04}$	-	$3.01 \cdot 10^{+04}$
Ni-59	$8.00 \cdot 10^{+04}$	$8.53 \cdot 10^{+08}$	$2.44 \cdot 10^{+08}$	$1.10 \cdot 10^{+09}$	$6.97 \cdot 10^{+04}$	$5.08 \cdot 10^{+08}$	$5.08 \cdot 10^{+08}$
Ni-63	$9.20 \cdot 10^{+01}$	$1.21 \cdot 10^{+11}$	$3.46 \cdot 10^{+10}$	$1.55 \cdot 10^{+11}$	$1.09 \cdot 10^{+07}$	$7.21 \cdot 10^{+10}$	$7.21 \cdot 10^{+10}$
Se-79	$6.50 \cdot 10^{+04}$	$4.55 \cdot 10^{+09}$	-	$4.55 \cdot 10^{+09}$	$1.86 \cdot 10^{+07}$	-	$1.86 \cdot 10^{+07}$
Rb-87	$4.88 \cdot 10^{+10}$	$2.55 \cdot 10^{+13}$	-	$2.55 \cdot 10^{+13}$	$1.05 \cdot 10^{+03}$	-	$1.05 \cdot 10^{+03}$
Sr-90	$2.88 \cdot 10^{+01}$	$8.89 \cdot 10^{+14}$	$1.17 \cdot 10^{+07}$	$8.89 \cdot 10^{+14}$	$3.74 \cdot 10^{+12}$	$1.37 \cdot 10^{+05}$	$3.74 \cdot 10^{+12}$
Mo-93	$3.50 \cdot 10^{+03}$	$8.38 \cdot 10^{+06}$	$1.29 \cdot 10^{+07}$	$2.13 \cdot 10^{+07}$	$7.16 \cdot 10^{+03}$	$4.29 \cdot 10^{+06}$	$4.30 \cdot 10^{+06}$
Zr-93	$1.50 \cdot 10^{+06}$	$2.13 \cdot 10^{+10}$	$2.28 \cdot 10^{+09}$	$2.36 \cdot 10^{+10}$	$8.95 \cdot 10^{+07}$	$9.24 \cdot 10^{+06}$	$9.87 \cdot 10^{+07}$
Nb-94	$2.03 \cdot 10^{+04}$	$2.22 \cdot 10^{+06}$	$5.63 \cdot 10^{+08}$	$5.65 \cdot 10^{+08}$	$8.24 \cdot 10^{+03}$	$8.49 \cdot 10^{+07}$	$8.49 \cdot 10^{+07}$
Tc-99	$2.10 \cdot 10^{+05}$	$1.72 \cdot 10^{+11}$	$2.18 \cdot 10^{+06}$	$1.72 \cdot 10^{+11}$	$6.45 \cdot 10^{+08}$	$6.87 \cdot 10^{+05}$	$6.46 \cdot 10^{+08}$
Pd-107	$7.00 \cdot 10^{+06}$	$1.41 \cdot 10^{+09}$	-	$1.41 \cdot 10^{+09}$	$5.20 \cdot 10^{+06}$	-	$5.20 \cdot 10^{+06}$
Sn-126	$1.00 \cdot 10^{+05}$	$7.07 \cdot 10^{+09}$	-	$7.07 \cdot 10^{+09}$	$2.79 \cdot 10^{+07}$	-	$2.79 \cdot 10^{+07}$
I-129	$1.70 \cdot 10^{+07}$	$3.85 \cdot 10^{+08}$	$9.09 \cdot 10^{-07}$	$3.85 \cdot 10^{+08}$	$1.52 \cdot 10^{+06}$	-	$1.52 \cdot 10^{+06}$
Cs-135	$2.30 \cdot 10^{+06}$	$1.35 \cdot 10^{+09}$	-	$1.35 \cdot 10^{+09}$	$1.59 \cdot 10^{+07}$	-	$1.59 \cdot 10^{+07}$
Cs-137	$3.00 \cdot 10^{+01}$	$1.31 \cdot 10^{+15}$	-	$1.31 \cdot 10^{+15}$	$5.37 \cdot 10^{+12}$	-	$5.37 \cdot 10^{+12}$
Sm-147	$1.06 \cdot 10^{+11}$	$7.13 \cdot 10^{+03}$	-	$7.13 \cdot 10^{+03}$	$6.70 \cdot 10^{+01}$	-	$6.70 \cdot 10^{+01}$
Sm-151	$8.70 \cdot 10^{+01}$	$2.96 \cdot 10^{+12}$	-	$2.96 \cdot 10^{+12}$	$1.25 \cdot 10^{+10}$	-	$1.25 \cdot 10^{+10}$
Ra-226	$1.60 \cdot 10^{+03}$	$1.11 \cdot 10^{+01}$	-	$1.11 \cdot 10^{+01}$	$7.90 \cdot 10^{-01}$	-	$7.90 \cdot 10^{-01}$
Th-229	$7.30 \cdot 10^{+03}$	$7.73 \cdot 10^{+00}$	-	$7.73 \cdot 10^{+00}$	$7.95 \cdot 10^{+00}$	-	$7.95 \cdot 10^{+00}$
Th-230	$8.00 \cdot 10^{+04}$	$7.48 \cdot 10^{+04}$	-	$7.48 \cdot 10^{+04}$	$6.00 \cdot 10^{+02}$	-	$6.00 \cdot 10^{+02}$
Pa-231	$3.25 \cdot 10^{+04}$	$2.65 \cdot 10^{+04}$	-	$2.65 \cdot 10^{+04}$	$1.24 \cdot 10^{+03}$	-	$1.24 \cdot 10^{+03}$
Th-232	$1.41 \cdot 10^{+10}$	$4.60 \cdot 10^{-02}$	-	$4.60 \cdot 10^{-02}$	$1.31 \cdot 10^{-03}$	-	$1.31 \cdot 10^{-03}$
U-232	$7.20 \cdot 10^{+01}$	$5.35 \cdot 10^{+06}$	-	$5.35 \cdot 10^{+06}$	$7.72 \cdot 10^{+03}$	-	$7.72 \cdot 10^{+03}$
U-233	$1.62 \cdot 10^{+05}$	$4.53 \cdot 10^{+04}$	-	$4.53 \cdot 10^{+04}$	$2.57 \cdot 10^{+03}$	-	$2.57 \cdot 10^{+03}$
U-234	$2.47 \cdot 10^{+05}$	$1.35 \cdot 10^{+10}$	-	$1.35 \cdot 10^{+10}$	$3.10 \cdot 10^{+07}$	-	$3.10 \cdot 10^{+07}$
U-235	$7.10 \cdot 10^{+08}$	$2.20 \cdot 10^{+08}$	-	$2.20 \cdot 10^{+08}$	$4.85 \cdot 10^{+05}$	-	$4.85 \cdot 10^{+05}$
U-236	$2.39 \cdot 10^{+07}$	$2.51 \cdot 10^{+09}$	-	$2.51 \cdot 10^{+09}$	$1.19 \cdot 10^{+07}$	-	$1.19 \cdot 10^{+07}$

Tab. 3.1 Inventory of long-term relevant radionuclides in spent fuel and metal parts immediately after discharge (Bq/container)

Nuclide	Half-live [years]	CANDU fuel			LWR-UO_2 fuel		
		spent fuel	metal parts	total	spent fuel	metal parts	total
Np-237	$2.14 \cdot 10^{+06}$	$1.26 \cdot 10^{+09}$	-	$1.26 \cdot 10^{+09}$	$1.64 \cdot 10^{+07}$	-	$1.64 \cdot 10^{+07}$
Pu-238	$8.78 \cdot 10^{+01}$	$1.67 \cdot 10^{+10}$	-	$1.67 \cdot 10^{+10}$	$1.63 \cdot 10^{+11}$	-	$1.63 \cdot 10^{+11}$
U-238	$4.51 \cdot 10^{+09}$	$3.99 \cdot 10^{+12}$	-	$3.99 \cdot 10^{+12}$	$1.16 \cdot 10^{+07}$	-	$1.16 \cdot 10^{+07}$
Pu-239	$2.44 \cdot 10^{+04}$	$8.29 \cdot 10^{+12}$	-	$8.29 \cdot 10^{+12}$	$1.31 \cdot 10^{+10}$	-	$1.31 \cdot 10^{+10}$
Pu-240	$6.76 \cdot 10^{+03}$	$1.19 \cdot 10^{+13}$	-	$1.19 \cdot 10^{+13}$	$2.39 \cdot 10^{+10}$	-	$2.39 \cdot 10^{+10}$
Am-241	$4.33 \cdot 10^{+02}$	$2.94 \cdot 10^{+11}$	-	$2.94 \cdot 10^{+11}$	$6.43 \cdot 10^{+09}$	-	$6.43 \cdot 10^{+09}$
Pu-241	$1.44 \cdot 10^{+01}$	$1.17 \cdot 10^{+15}$	-	$1.17 \cdot 10^{+15}$	$5.79 \cdot 10^{+12}$	-	$5.79 \cdot 10^{+12}$
Am-242*	$1.52 \cdot 10^{+02}$	$1.15 \cdot 10^{+10}$	-	$1.15 \cdot 10^{+10}$	$1.91 \cdot 10^{+08}$	-	$1.91 \cdot 10^{+08}$
Pu-242	$3.87 \cdot 10^{+05}$	$1.20 \cdot 10^{+10}$	-	$1.20 \cdot 10^{+10}$	$1.15 \cdot 10^{+08}$	-	$1.15 \cdot 10^{+08}$
Am-243	$7.65 \cdot 10^{+03}$	$2.63 \cdot 10^{+10}$	-	$2.63 \cdot 10^{+10}$	$1.33 \cdot 10^{+09}$	-	$1.33 \cdot 10^{+09}$
Cm-244	$1.81 \cdot 10^{+01}$	$8.85 \cdot 10^{+11}$	-	$8.85 \cdot 10^{+11}$	$2.16 \cdot 10^{+11}$	-	$2.16 \cdot 10^{+11}$
Pu-244	$8.28 \cdot 10^{+07}$	$7.67 \cdot 10^{+02}$	-	$7.67 \cdot 10^{+02}$	$4.34 \cdot 10^{+01}$	-	$4.34 \cdot 10^{+01}$
Cm-245	$8.27 \cdot 10^{+03}$	$1.67 \cdot 10^{+07}$	-	$1.67 \cdot 10^{+07}$	$1.70 \cdot 10^{+07}$	-	$1.70 \cdot 10^{+07}$
Cm-246	$4.71 \cdot 10^{+03}$	$2.91 \cdot 10^{+06}$	-	$2.91 \cdot 10^{+06}$	$4.25 \cdot 10^{+07}$	-	$4.25 \cdot 10^{+07}$
Cm-247	$1.64 \cdot 10^{+07}$	$3.04 \cdot 10^{+00}$	-	$3.04 \cdot 10^{+00}$	$9.34 \cdot 10^{+01}$	-	$9.34 \cdot 10^{+01}$
Cm-248	$3.52 \cdot 10^{+05}$	$3.45 \cdot 10^{+00}$	-	$3.45 \cdot 10^{+00}$	$2.91 \cdot 10^{+05}$	-	$2.91 \cdot 10^{+05}$

3.2.5 Source term

The relevant data for the source term are shown in Table 2.1 for both fuel types. Radionuclide mobilization out of the container takes into account the following processes:

- Container failure

  A constant distribution, which implies instantaneous failure of all containers after 1500 y, is assumed for Titanium containers (see [11]).

- Degradation of fuel matrix at a constant rate

For CANDU fuel, the degradation of the fuel matrix is based on an oxidative model (Werme 1990) [11]. The fractional leaching rate of $9 \cdot 10^{-5}$ a^{-1}, given by the above mentioned model, is used. That means that the fuel matrix completely degrades after about 10^4 years. A more reliable model, based also on oxidative leaching and taking into account α radiolysis (Shoesmith & Sunder 1991) gives a maximum leaching rate of the fuel matrix of 10^{-10} g/(cm^2·day) [11]. The degradation time of the fuel pellet is calculated following the NAGRA methodology [12]. The cylindrical pellet is replaced by an equivalent sphere, in such a way that the ratio between the total lateral area and the volume to be kept constant. The equivalent sphere dissolves with a constant rate F. In the end, the leaching time is calculated by

$$T = \frac{\rho R_0}{F} \qquad (3.9)$$

where ρ is the density of the matrix (10 600 kg/m^3) and R_0 is the radius of the equivalent sphere. The fuel pellet is 15.3 mm high and has a diameter of 12.15 mm.

As a result, the dissolution time of the CANDU fuel pellet is $3.8 \cdot 10^8$ years. In the following, for CANDU fuel the first estimation of the dissolution time will be used as a best estimate value. The second value will be dealt with in a sensitivity study.

- Instant release fractions of spent fuel

  In the spent fuel bundles, a fractional amount of radionuclides is present in cracks in the fuel, in gaps between fuel pellets, and in gaps between pellets and the zircaloy cladding. This fractional amount, called ‘instant release fraction’, is assumed to be available for release the moment a container fails. The instant release fractions of the radionuclides are given in Table 3.2.

- Release of activation products within the cladding material at a constant degradation rate

Tab. 3.2 Instant release fractions

LWR fuel	CANDU fuel
0.5% of Ni, Mo, Nb, Ra, actinides	0.1% of Ni, Mo, Nb
1% of Se, Sm, Sr, Ca	0.8% of actinides
2% of Tc, Pd, Sn, C	1% of Sm
5% of Cs, I, Rb, Zr, Cl	2% of Pd, Sn
	3% of C, Sr, Zr
	5% of Cl, Rb
	6% of Tc
	8% of Se, I, Cs

For the Zircalloy cladding of CANDU fuel a value of 10^{-3} y^{-1} is taken for the degradation rate, the same as the one used for LWR fuel. Given the small amounts of the cladding, the contribution to release, which originates from inventories in the cladding is less important. The element-specific fractions of the activation products, which are assumed to be in the metal parts, are given in Table 3.3.

Tab. 3.3 Element specific fractions in the metal parts

Element	LWR fuel	CANDU fuel
C	72.2 %	97.3 %
Ni	99.5 %	99.9 %
Zr	9.4 %	9.6 %
Mo	99.5 %	99.9 %
Nb	99.5 %	99.9 %
Tc	0.1 %	0.1 %
Rb	95 %	-

3.2.6 Diffusion

The diffusion of radionuclides in compacted bentonite is described by an element-specific apparent diffusion coefficient D_a which is defined as the quotient of pore diffusion and retention according to

$$D_a = \frac{D_b}{1 + (1 - \varepsilon_b)\rho_b K_d / \varepsilon_b}, \qquad (3.10)$$

where ρ_b is the bentonite solid density and K_d the distribution coefficient for the bentonite. The pore diffusion coefficient takes into account retardation effects due to the tortuosity of the pore space and exclusion effects of ions. The diffusion porosity in the bentonite buffer is 0.1.

For CANDU fuel, the intrinsic diffusion coefficient for the bentonite buffer is uniformly distributed in the range 10^{-11} m^2/s to 10^{-10} m^2/s [11]. The pore diffusion coefficient can be calculated as the ratio between the intrinsic diffusion coefficient and the porosity. According to the calculated buffer porosity, the pore diffusion coefficient is in the range 10^{-10} m^2/s to 10^{-9} m^2/s. For the reference case, a median value of $5 \cdot 10^{-10}$ m^2/s has been chosen, which is the same as in the SPA calculations for LWR fuel.

3.2.7 Sorption

The distribution coefficients are taken from the Kristallin-I study [12]. The Swiss data collection procedure is transferable because similar bentonite barriers are assumed in the Swiss and the German studies. It is likely that the intruding water will equilibrate with bentonite before it comes into contact with the waste. Under these assumptions geochemical calculations have been performed in and sorption values have been estimated in [16]. In Table 3.4, sorption values are given for all relevant nuclides. Distribution coefficients for those elements which have not been considered in Kristallin-I were derived from studies mentioned in foot-notes. If oxidising conditions occur in the near field, it is assumed that Se, Mo and Tc do not sorb onto the bentonite. For U and Np, values of

$5 \cdot 10^{-3}$ m^3/kg from the Finnish study TVO-96 are used, in agreement with distribution coefficients between $5 \cdot 10^{-3}$ and 0.6 m^3/kg documented for uranium in the NEA data base ISIRS.

Tab. 3.4 Distribution coefficients in bentonite in [m^3/kg]; r denotes the same data as used in the reference case

Element	Reference	Conservative	oxidizing
	reducing		
C[a]	$1.0 \cdot 10^{-2}$	0	r
Cl [a]	0	r	r
Ca [a]	$2.0 \cdot 10^{-1}$	$2.0 \cdot 10^{-2}$	r
Ni	$1.0 \cdot 10^{0}$	$1.0 \cdot 10^{-1}$	0
Se	$5.0 \cdot 10^{-3}$	$1.0 \cdot 10^{-3}$	0
Sr	$1.0 \cdot 10^{-2}$	$1.0 \cdot 10^{-3}$	r
Zr	$1.0 \cdot 10^{0}$	$1.0 \cdot 10^{-1}$	r
Nb	$1.0 \cdot 10^{0}$	$1.0 \cdot 10^{-1}$	r
Mo[b]	$5.0 \cdot 10^{-3}$	$1.0 \cdot 10^{-3}$	r
Tc	$1.0 \cdot 10^{-1}$	$5.0 \cdot 10^{-2}$	0
Pd	$1.0 \cdot 10^{0}$	$1.0 \cdot 10^{-1}$	r
Sn	$1.0 \cdot 10^{0}$	$1.0 \cdot 10^{-1}$	r
I [a]	$5.0 \cdot 10^{-3}$	$1.0 \cdot 10^{-3}$	r
Cs, Rb[c]	$1.0 \cdot 10^{-2}$	$1.0 \cdot 10^{-3}$	r
Sm[d]	$5.0 \cdot 10^{0}$	$5.0 \cdot 10^{-1}$	r
Ra	$1.0 \cdot 10^{-2}$	$1.0 \cdot 10^{-3}$	r
U	$5.0 \cdot 10^{0}$	$5.0 \cdot 10^{-1}$	$5.0 \cdot 10^{3}$
Am	$5.0 \cdot 10^{0}$	$5.0 \cdot 10^{-1}$	r
Cm	$5.0 \cdot 10^{0}$	$5.0 \cdot 10^{-1}$	r
Pu	$5.0 \cdot 10^{0}$	$5.0 \cdot 10^{-1}$	r
Np	$5.0 \cdot 10^{0}$	$5.0 \cdot 10^{-1}$	$5.0 \cdot 10^{3}$
Th	$5.0 \cdot 10^{0}$	$5.0 \cdot 10^{-1}$	r
Pa	$1.0 \cdot 10^{0}$	$1.0 \cdot 10^{-1}$	r

a. data from SKI
b. Mo is assumed to exist as MoO42- or polyanion. Sorption values of Se are used
c. Data of Cs are used for Rb
d. Data of the tetravalent actinides are used

3.2.8 Solubility limits

For the repository in granite, reducing conditions are assumed because of the high Fe content of the containers and reducing species in bentonite and groundwater. An alkaline pH value (8-9) after equilibration of the groundwater with the bentonite is assumed, based on calculations of Curti [7]. As mentioned above, typical waters in deep granitic formations in Germany are more like those observed in Swiss studies than for example in the Scandinavian or Canadian formations [15].

The Swiss data collection procedure is transferable because a similar bentonite barrier is assumed and the water will equilibrate with bentonite before it makes contact with the waste. Consequently, all data except that for Rb, Sr, Mo and Ra are taken from the Swiss study Kristallin-I [12]. Rb, Sr and Mo have not been considered in the crystalline study and the values for Ra are not transferable to the conditions for the repository with disposed spent fuel elements. Best estimate values and upper limits (as conservative values) have been taken from the studies SAM and PACOMA determined for areas with alkaline conditions. No probabilistic calculations are performed, hence, only best estimate and conservative values are given in Table 3.5.

Tab. 3.5 Solubility limits in the near field for reducing conditions; r denotes the same data as used in the reference case

Element	$L_{e(i)}$ [mol/l]		
	Best estimate	Conservative	
	Reducing		Oxidizing
C, Cl, I, Cs, Rb, Ni	high	high	r
Ca[a]	$1.0 \cdot 10^{-2}$	high	r
Se	$1.0 \cdot 10^{-8}$	$6.0 \cdot 10^{-7}$	high
Sr	$1.0 \cdot 10^{-5}$	$1.0 \cdot 10^{-4}$	r
Zr	$5.0 \cdot 10^{-9}$	$5.0 \cdot 10^{-7}$	r
Nb	$1.0 \cdot 10^{-3}$	$1.0 \cdot 10^{-3}$	r
Mo	$1.0 \cdot 10^{-4}$	$1.0 \cdot 10^{-1}$	r
Tc	$1.0 \cdot 10^{-7}$	high	high
Pd	$1.0 \cdot 10^{-11}$	$1.0 \cdot 10^{-6}$	r
Sn	$1.0 \cdot 10^{-5}$	$1.0 \cdot 10^{-5}$	r
Sm	$1.0 \cdot 10^{-5}$	$1.0 \cdot 10^{-5}$	r
Ra	$1.0 \cdot 10^{-6}$	$1.0 \cdot 10^{-4}$	r
U	$1.0 \cdot 10^{-7}$	$7.0 \cdot 10^{-5}$	high
Am	$1.0 \cdot 10^{-5}$	$1.0 \cdot 10^{-5}$	r
Cm	$1.0 \cdot 10^{-5}$	$1.0 \cdot 10^{-5}$	r
Pu	$1.0 \cdot 10^{-8}$	$1.0 \cdot 10^{-6}$	r
Np	$1.0 \cdot 10^{-10}$	$1.0 \cdot 10^{-8}$	$1.0 \cdot 10^{-9}$
Th	$5.0 \cdot 10^{-9}$	$1.0 \cdot 10^{-7}$	r
Pa	$1.0 \cdot 10^{-10}$	$1.0 \cdot 10^{-7}$	r

a. from Projekt Gewähr

3.3 General characteristics of the far field

The far field is the geosphere outside the EDZ up to the biosphere. Figure 3.5 gives a schematic view of the far field in granite. The emplacement drifts and boreholes, denoted as repository, are assumed to be situated in an area of the granite body without major water conducting faults. Thus, the far field transport between the repository and such a major water conducting fault is modelled assuming fracture flow through small water conducting features with matrix diffusion into the wall rock. The radionuclide transport through the geosphere is modelled by a unidimensional advective-dispersive transport equation, taking into account sorption and radioactive decay. The main parameters for these transport calculations are listed in Table 3.6.

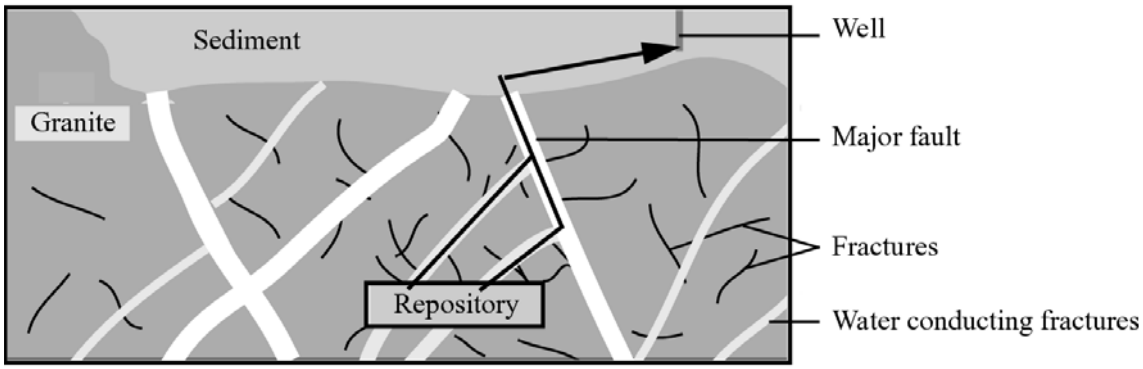

Fig. 3.5 Schematic view of the far field [13]

The sorption data of granite for the Swiss study Kristallin-I [12] have been used in our study. The best estimate and the conservative data for crystalline rock are shown in Table 3.7. Rb, Mo and Sm were not considered in Kristallin-I. Their distribution coefficients have been derived from chemical homologous elements as indicated in Table 3.7.

Tab. 3.6 Selected far field data

Parameter		Value
Length of transport path	[m]	200
Darcy velocity	[m/y]	$3.5 \cdot 10^{-5}$
Water travel time	[y]	50
Peclet number	[-]	10
Kinematic porosity	[-]	$8 \cdot 10^{-6}$
Discharge flow from the far field	[m^3/y]	140
Width of flow channels per area	[m/m^2]	0.01
Aperture	[m]	$8.0 \cdot 10^{-4}$
Porosity of altered wall rock	[-]	0.005
Penetration depth	[m]	0.02
Pore diffusion coefficient	[m^2/y]	$1.0 \cdot 10^{-3}$

Tab. 3.7 Distribution coefficients in granite in [m^3/kg]

Element	reference	conserv.	Element	reference	conserv.
Cl	0	0	Sn	$5.0 \cdot 10^{-1}$	$5.0 \cdot 10^{-2}$
C	$1.0 \cdot 10^{-3}$	0	Cs	$4.2 \cdot 10^{-2}$	$8.4 \cdot 10^{-3}$
Ca	$1.0 \cdot 10^{-2}$	$1.0 \cdot 10^{-3}$	Sm[a]	$5.0 \cdot 10^{+0}$	$5.0 \cdot 10^{-1}$
I	$1.0 \cdot 10^{-3}$	0	Ra	$5.0 \cdot 10^{-1}$	$1.0 \cdot 10^{-1}$
Ni	$5.0 \cdot 10^{-1}$	$5.0 \cdot 10^{-2}$	U	$1.0 \cdot 10^{+0}$	$5.0 \cdot 10^{-2}$
Se	$1.0 \cdot 10^{-2}$	$1.0 \cdot 10^{-3}$	Am	$5.0 \cdot 10^{+0}$	$1.0 \cdot 10^{+0}$
Rb[b]	$4.2 \cdot 10^{-2}$	$8.4 \cdot 10^{-3}$	Cm	$5.0 \cdot 10^{+0}$	$5.0 \cdot 10^{-1}$
Sr	$1.0 \cdot 10^{-2}$	$1.0 \cdot 10^{-3}$	Pu	$5.0 \cdot 10^{+0}$	$5.0 \cdot 10^{-1}$
Zr	$1.0 \cdot 10^{+0}$	$1.0 \cdot 10^{-1}$	Np	$1.0 \cdot 10^{+0}$	$5.0 \cdot 10^{-2}$
Nb	$1.0 \cdot 10^{+0}$	$1.0 \cdot 10^{-1}$	Th	$1.0 \cdot 10^{+0}$	$1.0 \cdot 10^{-1}$
Mo[c]	$1.0 \cdot 10^{-2}$	$1.0 \cdot 10^{-3}$	Pa	$1.0 \cdot 10^{+0}$	$1.0 \cdot 10^{-1}$
Tc	$5.0 \cdot 10^{-1}$	$5.0 \cdot 10^{-2}$	Pb	$5.0 \cdot 10^{-1}$	$5.0 \cdot 10^{-2}$
Pd	$5.0 \cdot 10^{-1}$	$5.0 \cdot 10^{-2}$			

a. Data of the tetravalent actinides are used.
b. Data of Cs are used.
c. Mo is assumed to be in the anionic state as MoO_4^{2-} and weakly sorbing. Data of Se (SeO_3^{2-}) are used.

3.4 General characteristics of the biosphere

In Ref. [13] a detailed biosphere analysis has been performed taking into account exposition paths via drinking water, various ingestion pathways (incl. irrigation), and external radiation. Biosphere dose conversion factors have been derived from the biosphere transport calculations using national data and previous ICRP dose factors [8], [9].

The biosphere dose conversion factors are compiled in Table 3.9. Applying these factors, a radionuclide concentration in biosphere water can be converted to a dose. The ingestion dose coefficients used for calculating radiotoxicities are also listed in Table 3.9, column 'IDC-SPIN'. They are based on new ICRP values, as listed in column 'ICRP 72' [10]. The dilution factors listed in Table 3.8 were applied to calculate concentrations in the biosphere water from concentrations at the end of near field.

Tab. 3.8 Parameter of the biosphere

Parameter	Value
Volumetric flow in the biosphere [m^3/y]	$8.0 \cdot 10^6$
Dilution factor from near field to biosphere	$2.1 \cdot 10^6$

Tab. 3.9 Nuclide-specific data for the biosphere calculation

Radio-nuclide	Half-life [y]	Ingestion dose coefficient [Sv/Bq]		Biosphere dose conversion factor [(Sv:y)/(Bq:m^3)]
		ICRP72	IDC-SPIN	SPA-GRS
C-14	$5.733 \cdot 10^{03}$	$5.80 \cdot 10^{-10}$	$5.80 \cdot 10^{-10}$	$1.00 \cdot 10^{-7}$
Cl-36	$3.012 \cdot 10^{05}$	$9.30 \cdot 10^{-10}$	$9.30 \cdot 10^{-10}$	$2.60 \cdot 10^{-8}$
Ca-41	$8.100 \cdot 10^{04}$	$1.90 \cdot 10^{-10}$	$1.90 \cdot 10^{-10}$	$3.10 \cdot 10^{-9}$
Ni-59	$8.000 \cdot 10^{04}$	$6.30 \cdot 10^{-11}$	$6.30 \cdot 10^{-11}$	$1.70 \cdot 10^{-9}$
Ni-63	$9.200 \cdot 10^{01}$	$1.50 \cdot 10^{-10}$	$1.50 \cdot 10^{-10}$	$1.10 \cdot 10^{-9}$
Se-79	$1.100 \cdot 10^{06}$	$2.90 \cdot 10^{-09}$	$2.90 \cdot 10^{-09}$	$2.30 \cdot 10^{-7}$
Rb-87	$4.699 \cdot 10^{10}$	$1.50 \cdot 10^{-09}$	$1.50 \cdot 10^{-09}$	$1.30 \cdot 10^{-7}$
Sr-90	$2.914 \cdot 10^{01}$	$2.80 \cdot 10^{-08}$	$3.07 \cdot 10^{-08}$	$2.00 \cdot 10^{-7}$
Zr-93	$1.531 \cdot 10^{06}$	$1.10 \cdot 10^{-09}$	$1.22 \cdot 10^{-09}$	$6.00 \cdot 10^{-9}$
Nb-94	$2.031 \cdot 10^{04}$	$1.70 \cdot 10^{-09}$	$1.70 \cdot 10^{-09}$	$9.20 \cdot 10^{-8}$
Mo-93	$3.501 \cdot 10^{03}$	$3.10 \cdot 10^{-09}$	$3.22 \cdot 10^{-09}$	$2.80 \cdot 10^{-8}$
Tc-99	$2.132 \cdot 10^{05}$	$6.40 \cdot 10^{-10}$	$6.40 \cdot 10^{-10}$	$4.90 \cdot 10^{-9}$
Pd-107	$6.501 \cdot 10^{06}$	$3.70 \cdot 10^{-11}$	$3.70 \cdot 10^{-11}$	$3.00 \cdot 10^{-10}$
Sn-126	$1.001 \cdot 10^{05}$	$4.70 \cdot 10^{-09}$	$5.07 \cdot 10^{-09}$	$8.70 \cdot 10^{-6}$
I-129	$1.571 \cdot 10^{07}$	$1.10 \cdot 10^{-07}$	$1.10 \cdot 10^{-07}$	$3.70 \cdot 10^{-7}$
Cs-135	$2.301 \cdot 10^{06}$	$2.00 \cdot 10^{-09}$	$2.00 \cdot 10^{-09}$	$8.60 \cdot 10^{-8}$
Cs-137	$3.002 \cdot 10^{01}$	$1.30 \cdot 10^{-08}$	$1.30 \cdot 10^{-08}$	$1.30 \cdot 10^{-6}$
Sm-147	$1.071 \cdot 10^{11}$	$4.90 \cdot 10^{-08}$	$4.90 \cdot 10^{-08}$	$1.60 \cdot 10^{-7}$
Sm-151	$9.006 \cdot 10^{01}$	$9.80 \cdot 10^{-11}$	$9.80 \cdot 10^{-11}$	$3.00 \cdot 10^{-10}$
Ho-166m	$1.200 \cdot 10^{03}$	$2.00 \cdot 10^{-09}$	$2.00 \cdot 10^{-09}$	Not used
Cm-248	$3.393 \cdot 10^{05}$	$7.70 \cdot 10^{-07}$	$7.70 \cdot 10^{-07}$	$9.80 \cdot 10^{-6}$
Pu-244	$8.267 \cdot 10^{07}$	$2.40 \cdot 10^{-07}$	$2.41 \cdot 10^{-07}$	$3.40 \cdot 10^{-6}$
Cm-244	$1.812 \cdot 10^{01}$	$1.20 \cdot 10^{-07}$	$1.20 \cdot 10^{-07}$	$1.40 \cdot 10^{-6}$
Pu-240	$6.542 \cdot 10^{03}$	$2.50 \cdot 10^{-07}$	$2.50 \cdot 10^{-07}$	$2.20 \cdot 10^{-6}$
Np-236*	$1.540 \cdot 10^{05}$	$1.70 \cdot 10^{-08}$	$2.48 \cdot 10^{-08}$	$6.20 \cdot 10^{-6}$
U-236	$2.343 \cdot 10^{07}$	$4.70 \cdot 10^{-08}$	$4.70 \cdot 10^{-08}$	$2.20 \cdot 10^{-7}$
Th-232	$1.406 \cdot 10^{10}$	$2.30 \cdot 10^{-07}$	$1.06 \cdot 10^{-06}$	$1.10 \cdot 10^{-5}$
U-232	$7.204 \cdot 10^{01}$	$3.30 \cdot 10^{-07}$	$4.73 \cdot 10^{-07}$	$5.20 \cdot 10^{-6}$
Cm-245	$8.505 \cdot 10^{03}$	$2.10 \cdot 10^{-07}$	$2.10 \cdot 10^{-07}$	$3.00 \cdot 10^{-6}$
Pu-241	$1.441 \cdot 10^{01}$	$4.80 \cdot 10^{-09}$	$4.80 \cdot 10^{-09}$	$4.30 \cdot 10^{-8}$

Tab. 3.9 Nuclide-specific data for the biosphere calculation

Radio-nuclide	Half-life [y]	Ingestion dose coefficient [Sv/Bq]		Biosphere dose conversion factor [(Sv:y)/(Bq:m^3)]
		ICRP72	IDC-SPIN	SPA-GRS
Am-241	$4.325 \cdot 10^{02}$	$2.00 \cdot 10^{-07}$	$2.00 \cdot 10^{-07}$	$2.70 \cdot 10^{-6}$
Np-237	$2.141 \cdot 10^{06}$	$1.10 \cdot 10^{-07}$	$1.11 \cdot 10^{-07}$	$6.20 \cdot 10^{-6}$
U-233	$1.586 \cdot 10^{05}$	$5.10 \cdot 10^{-08}$	$5.10 \cdot 10^{-08}$	$2.80 \cdot 10^{-7}$
Th-229	$7.344 \cdot 10^{03}$	$4.90 \cdot 10^{-07}$	$6.13 \cdot 10^{-07}$	$5.40 \cdot 10^{-6}$
Cm-246	$4.734 \cdot 10^{03}$	$2.10 \cdot 10^{-07}$	$2.10 \cdot 10^{-07}$	$2.60 \cdot 10^{-6}$
Pu-242	$3.872 \cdot 10^{05}$	$2.40 \cdot 10^{-07}$	$2.40 \cdot 10^{-07}$	$2.10 \cdot 10^{-6}$
Am-242m	$1.521 \cdot 10^{02}$	$1.90 \cdot 10^{-07}$	$2.00 \cdot 10^{-07}$	$2.60 \cdot 10^{-6}$
Pu-238	$8.780 \cdot 10^{01}$	$2.30 \cdot 10^{-07}$	$2.30 \cdot 10^{-07}$	$2.00 \cdot 10^{-6}$
U-238	$4.471 \cdot 10^{09}$	$4.50 \cdot 10^{-08}$	$4.84 \cdot 10^{-08}$	$3.10 \cdot 10^{-7}$
U-234	$2.447 \cdot 10^{05}$	$4.90 \cdot 10^{-08}$	$4.90 \cdot 10^{-08}$	$2.40 \cdot 10^{-7}$
Th-230	$7.705 \cdot 10^{04}$	$2.10 \cdot 10^{-07}$	$2.10 \cdot 10^{-07}$	$2.40 \cdot 10^{-6}$
Ra-226	$1.601 \cdot 10^{03}$	$2.80 \cdot 10^{-07}$	$2.17 \cdot 10^{-06}$	$1.50 \cdot 10^{-5}$
Cm-247	$1.561 \cdot 10^{07}$	$1.90 \cdot 10^{-07}$	$1.90 \cdot 10^{-07}$	$3.80 \cdot 10^{-6}$
Am-243	$7.385 \cdot 10^{03}$	$2.00 \cdot 10^{-07}$	$2.01 \cdot 10^{-07}$	$3.50 \cdot 10^{-6}$
Pu-239	$2.408 \cdot 10^{04}$	$2.50 \cdot 10^{-07}$	$2.50 \cdot 10^{-07}$	$2.20 \cdot 10^{-6}$
U-235	$7.043 \cdot 10^{08}$	$4.70 \cdot 10^{-08}$	$4.73 \cdot 10^{-08}$	$9.40 \cdot 10^{-7}$
Pa-231	$3.279 \cdot 10^{04}$	$7.10 \cdot 10^{-07}$	$1.92 \cdot 10^{-06}$	$1.30 \cdot 10^{-5}$

(*) Np-236 → U-236 (91%); Np-236 → Pu-236 → U-232 (9%)

4 Results

In the following, results of the calculations for the reference case are presented for LWR spent fuel, and for CANDU spent fuel respectively. The results for LWR spent fuel are taken from [13]. The results of parameter variations are presented in chapter 5.

4.1 LWR fuel

4.1.1 Near-field

The maximum release rates of radionuclides from the waste forms into the canister interior (“volume of dissolution”) and from the near-field into the geosphere are presented in Table 4.1. The release rates into the geosphere are shown in Figures 4.1 - 4.3. The results are presented for a group of 3900 canisters each containing 1.602 t_{hm}. The radionuclide release rates from this group of canisters, corresponding to 25 % of the total number of disposed canisters and a repository area of 1 km^2, define the portion of mass which enters into the most relevant flow pathway between the repository and the biosphere.

For all nuclides except Th-229, the maximum release rates of the waste forms (gap, metal parts, fuel matrix) occur at the time of canister failure (1000 years). This peak is caused by the instantaneous released fraction (IRF) from the gap. After 2100 years the release rates from the waste forms are controlled by the matrix-released fraction (MRF) whose inventory contains for most nuclides the main part of the waste. The release rates and the inventories of some daughter nuclides in the actinide chains continue to increase beyond 2100 years due to the decay of precursors.

The near-field results for the reference case lead to the following conclusions:

- The maximum release rates from the near-field into the geosphere are dominated by C-14, Ni-59, Mo-93, and Ra-226.

- The instantaneous release pulses from the waste forms of the non-solubility-limited and non- or weakly-sorbing nuclides, Cl-36, C-14, I-129, and Mo-93, are reduced by

diffusion through the bentonite buffer before entering the geosphere. For example, the maximum annual release rate of I-129 is $3.8 \cdot 10^{-4}$ times the IRF inventory.

- The release rates of Se, Zr, Tc, Pd, Ra, U, Pu, Np, Th, and Pa are governed by the solubility limits. In the cases of Zr, Tc, Pd, U, Np, and Pa major portions of the nuclides released from the waste forms precipitate in the canister interior.

- The solubility limits of Ca, Nb, Sr, Mo, Sn, Sm, Am, and Cm are so high that they do not affect the release rates significantly.

- The maximum release rates of Ra-226 and Pa-231 originate from the decay of their parents Th-230 and U-235, respectively. The decay of Th-230 and U-235 released from the waste forms but precipitated in the canister interior results in nearly constant release rates for the daughter nuclides even after the complete degradation of the waste forms.

Tab. 4.1 Maximum release rates from the waste forms and from the near-field into the geosphere in the reference case

Nuclide	Release from waste forms			Release from near-field	
	IRF [Bq/y]	$t_{max,MRF}$ [y]	MRF [Bq/y]	t_{max} [y]	[Bq/y]
C -14	$1.6 \cdot 10^{12}$	$2.1 \cdot 10^{3}$	$6.0 \cdot 10^{7}$	$2.1 \cdot 10^{3}$	$2.1 \cdot 10^{9}$
Cl-36	$1.9 \cdot 10^{11}$	$2.1 \cdot 10^{3}$	$3.6 \cdot 10^{6}$	$1.0 \cdot 10^{3}$	$9.5 \cdot 10^{7}$
Ca-41	$1.9 \cdot 10^{9}$	$2.1 \cdot 10^{3}$	$1.8 \cdot 10^{5}$	$1.3 \cdot 10^{5}$	$7.0 \cdot 10^{3}$
Ni-59	$1.9 \cdot 10^{13}$	--	--	$1.4 \cdot 10^{4}$	$3.7 \cdot 10^{8}$
Ni-63	$9.2 \cdot 10^{11}$	--	--	$2.0 \cdot 10^{3}$	$7.1 \cdot 10^{0}$
Se-79	$1.2 \cdot 10^{12}$	$2.1 \cdot 10^{3}$	$1.1 \cdot 10^{8}$	$1.7 \cdot 10^{3}$	$7.9 \cdot 10^{6}$
Rb-87	$3.3 \cdot 10^{8}$	$2.1 \cdot 10^{3}$	$6.2 \cdot 10^{3}$	$2.2 \cdot 10^{3}$	$6.2 \cdot 10^{3}$
Sr-90	$2.6 \cdot 10^{6}$	--	--	$1.0 \cdot 10^{3}$	$5.8 \cdot 10^{0}$
Zr-93	$2.8 \cdot 10^{13}$	$2.1 \cdot 10^{3}$	$5.3 \cdot 10^{8}$	$1.1 \cdot 10^{5}$	$1.7 \cdot 10^{5}$
Mo-93	$1.3 \cdot 10^{11}$	--	--	$2.0 \cdot 10^{3}$	$4.6 \cdot 10^{8}$
Nb-94	$3.1 \cdot 10^{12}$	--	--	$1.1 \cdot 10^{4}$	$4.5 \cdot 10^{7}$
Tc-99	$8.0 \cdot 10^{13}$	$2.1 \cdot 10^{3}$	$3.9 \cdot 10^{9}$	$1.2 \cdot 10^{4}$	$2.4 \cdot 10^{7}$
Pd-107	$6.5 \cdot 10^{11}$	$2.1 \cdot 10^{3}$	$3.2 \cdot 10^{7}$	$1.4 \cdot 10^{5}$	$7.9 \cdot 10^{1}$
Sn-126	$3.5 \cdot 10^{12}$	$2.1 \cdot 10^{3}$	$1.7 \cdot 10^{8}$	$1.1 \cdot 10^{5}$	$1.4 \cdot 10^{6}$

Tab. 4.1 Maximum release rates from the waste forms and from the near-field into the geosphere in the reference case

Nuclide	Release from waste forms			Release from near-field	
	IRF [Bq/y]	$t_{max,MRF}$ [y]	MRF [Bq/y]	t_{max} [y]	[Bq/y]
I-129	$4.8 \cdot 10^{11}$	$2.1 \cdot 10^{3}$	$9.0 \cdot 10^{6}$	$1.1 \cdot 10^{3}$	$1.2 \cdot 10^{7}$
Cs-135	$4.8 \cdot 10^{12}$	$2.1 \cdot 10^{3}$	$9.1 \cdot 10^{7}$	$1.8 \cdot 10^{5}$	$8.4 \cdot 10^{7}$
Cs-137	$3.9 \cdot 10^{7}$	--	--	$1.0 \cdot 10^{3}$	$8.9 \cdot 10^{1}$
Sm-147	$4.2 \cdot 10^{6}$	$2.1 \cdot 10^{3}$	$4.1 \cdot 10^{2}$	$1.0 \cdot 10^{6}$	$4.5 \cdot 10^{1}$
Sm-151	$2.2 \cdot 10^{11}$	$2.1 \cdot 10^{3}$	$4.0 \cdot 10^{3}$	--	--
Cm-248	$9.1 \cdot 10^{6}$	$2.1 \cdot 10^{3}$	$1.8 \cdot 10^{3}$	$5.1 \cdot 10^{5}$	$8.5 \cdot 10^{0}$
Pu 244	$1.4 \cdot 10^{6}$	$5.3 \cdot 10^{5}$	$2.7 \cdot 10^{2}$	$1.6 \cdot 10^{6}$	$7.4 \cdot 10^{0}$
Pu-240	$6.8 \cdot 10^{14}$	$2.1 \cdot 10^{3}$	$1.2 \cdot 10^{11}$	$2.4 \cdot 10^{4}$	$2.4 \cdot 10^{5}$
U-236	$3.9 \cdot 10^{11}$	$3.7 \cdot 10^{4}$	$1.2 \cdot 10^{8}$	$4.5 \cdot 10^{5}$	$1.8 \cdot 10^{3}$
Th-232	$2.0 \cdot 10^{4}$	$9.8 \cdot 10^{5}$	$5.6 \cdot 10^{3}$	$1.0 \cdot 10^{7}$	$1.8 \cdot 10^{1}$
U-232	$9.0 \cdot 10^{5}$	--	--	--	--
Cm-245	$4.9 \cdot 10^{11}$	$2.1 \cdot 10^{3}$	$8.8 \cdot 10^{7}$	$2.6 \cdot 10^{4}$	$3.0 \cdot 10^{3}$
Pu-241	$4.9 \cdot 10^{11}$	$2.1 \cdot 10^{3}$	$8.9 \cdot 10^{7}$	$2.6 \cdot 10^{4}$	$3.0 \cdot 10^{3}$
Am-241	$1.2 \cdot 10^{15}$	$2.1 \cdot 10^{3}$	$3.9 \cdot 10^{10}$	$2.6 \cdot 10^{4}$	$3.1 \cdot 10^{3}$
Np-237	$1.5 \cdot 10^{12}$	$4.1 \cdot 10^{3}$	$3.5 \cdot 10^{8}$	$5.0 \cdot 10^{5}$	$2.3 \cdot 10^{3}$
U-233	$5.4 \cdot 10^{9}$	$5.9 \cdot 10^{5}$	$2.9 \cdot 10^{8}$	$7.3 \cdot 10^{5}$	$3.8 \cdot 10^{3}$
Th-229	$2.3 \cdot 10^{8}$	$6.0 \cdot 10^{5}$	$2.9 \cdot 10^{8}$	$1.6 \cdot 10^{5}$	$7.0 \cdot 10^{4}$
Cm-246	$1.1 \cdot 10^{12}$	$2.1 \cdot 10^{3}$	$1.9 \cdot 10^{8}$	$1.8 \cdot 10^{4}$	$1.8 \cdot 10^{3}$
Pu-242	$3.6 \cdot 10^{12}$	$2.1 \cdot 10^{3}$	$7.1 \cdot 10^{8}$	$5.4 \cdot 10^{5}$	$1.1 \cdot 10^{6}$
Am-242	$4.8 \cdot 10^{10}$	$2.1 \cdot 10^{3}$	$5.7 \cdot 10^{4}$	--	--
U-238	$3.6 \cdot 10^{11}$	$2.3 \cdot 10^{4}$	$7.2 \cdot 10^{7}$	$7.5 \cdot 10^{5}$	$1.1 \cdot 10^{3}$
Pu-238	$1.3 \cdot 10^{12}$	$2.1 \cdot 10^{3}$	$1.7 \cdot 10^{5}$	--	--
U-234	$2.8 \cdot 10^{12}$	$2.1 \cdot 10^{3}$	$5.5 \cdot 10^{8}$	$1.8 \cdot 10^{5}$	$4.7 \cdot 10^{3}$
Th-230	$2.4 \cdot 10^{10}$	$2.0 \cdot 10^{5}$	$3.4 \cdot 10^{8}$	$2.2 \cdot 10^{5}$	$9.7 \cdot 10^{5}$
Ra-226	$4.6 \cdot 10^{9}$	$2.0 \cdot 10^{5}$	$3.4 \cdot 10^{8}$	$5.4 \cdot 10^{5}$	$1.5 \cdot 10^{9}$
Cm-247	$2.9 \cdot 10^{6}$	$2.1 \cdot 10^{3}$	$5.8 \cdot 10^{2}$	$1.0 \cdot 10^{6}$	$1.5 \cdot 10^{1}$
Am-243	$3.8 \cdot 10^{13}$	$2.1 \cdot 10^{3}$	$6.7 \cdot 10^{9}$	$2.3 \cdot 10^{4}$	$1.7 \cdot 10^{5}$
Pu-239	$4.0 \cdot 10^{14}$	$2.1 \cdot 10^{3}$	$7.7 \cdot 10^{10}$	$6.4 \cdot 10^{4}$	$2.5 \cdot 10^{6}$
U-235	$1.6 \cdot 10^{10}$	$2.0 \cdot 10^{5}$	$5.9 \cdot 10^{6}$	$1.3 \cdot 10^{5}$	$2.8 \cdot 10^{2}$
Pa-231	$3.8 \cdot 10^{8}$	$3.5 \cdot 10^{5}$	$5.9 \cdot 10^{6}$	$2.2 \cdot 10^{5}$	$1.1 \cdot 10^{5}$

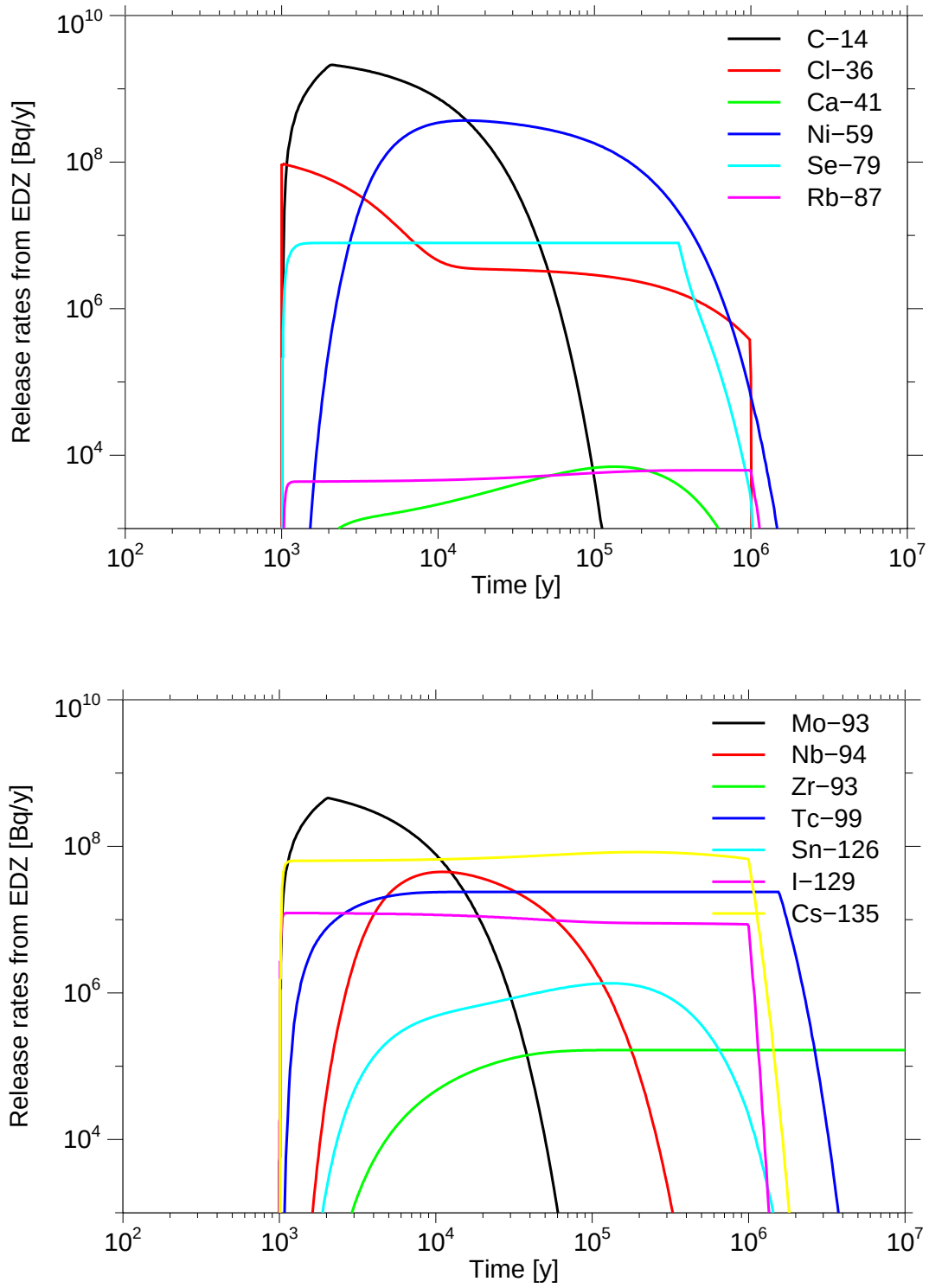

Fig. 4.1 Release rates of fission and activation products from the near-field into the geosphere. LWR, reference case

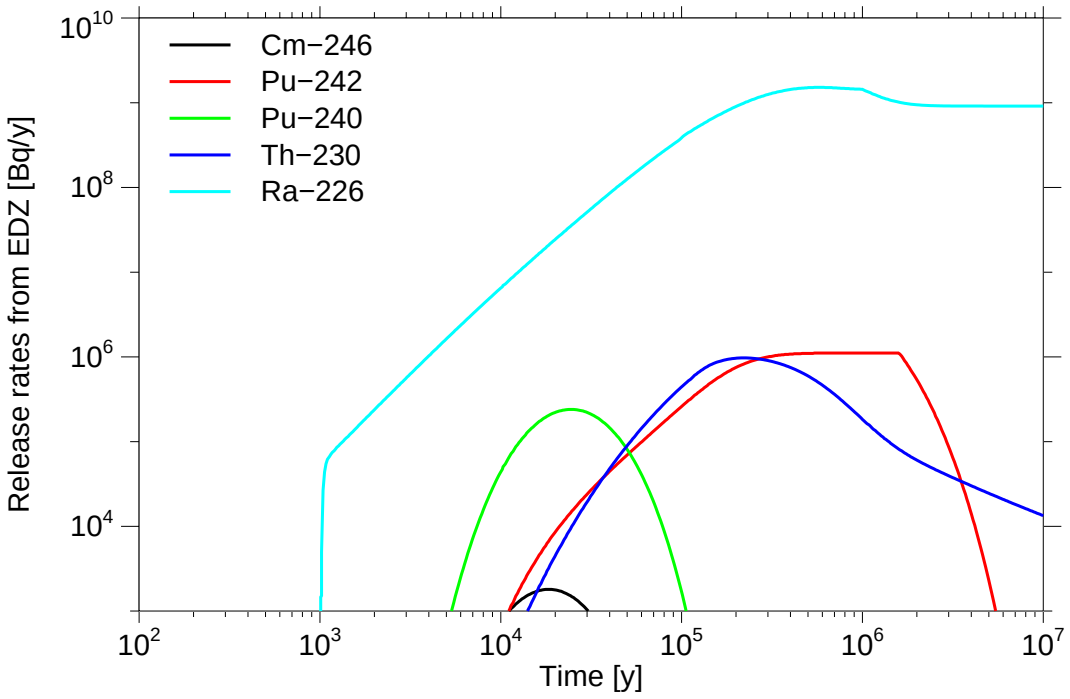

Fig. 4.2 Release rates of the radionuclides in the 4N and 4N+2 nuclide chains from the near-field into the geosphere. LWR, reference case

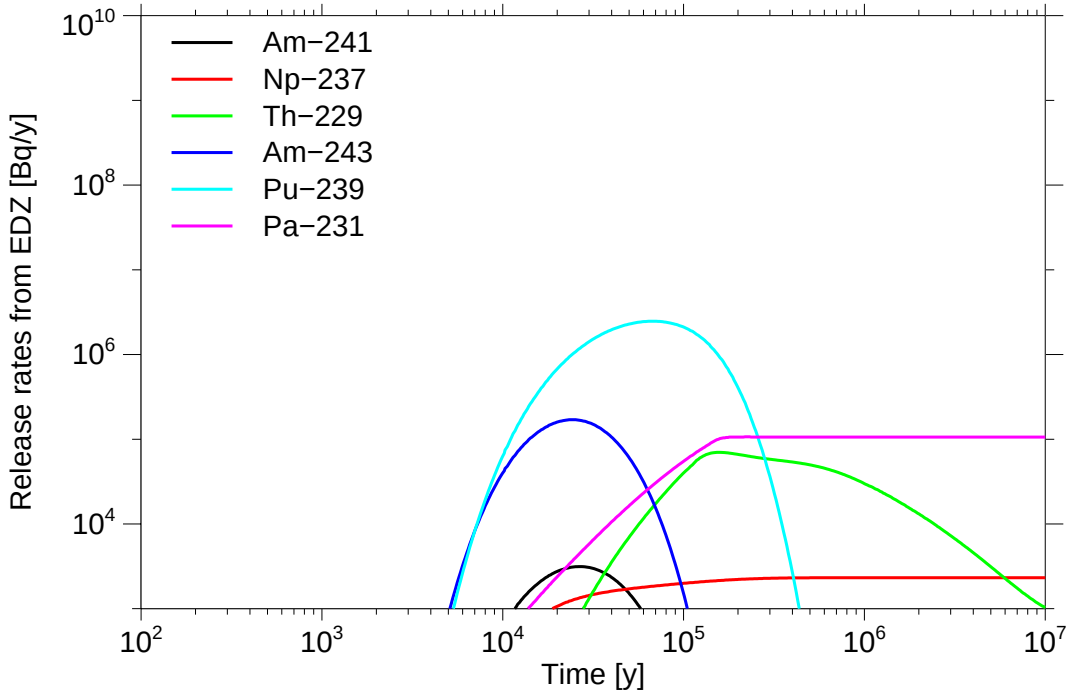

Fig. 4.3 Release rates of the radionuclides in the 4N+1 and 4N+3 nuclide chains from the near-field into the geosphere. LWR, reference case

4.1.2 Far-field and biosphere

The maximum release rates from the geosphere into the biosphere and the maximum radiation exposures are given in Table 4.1. Some short-lived nuclides (Ac-225, Ac-227, Ra-225, Ra-228, Pb-210) are considered in the biosphere calculations only. The radiation exposures caused by these nuclides are calculated by means of the radiation exposures of their parent nuclides assuming both to be in radioactive equilibrium. The release rates from the geosphere into the biosphere and the radiation exposures are shown in Figures 4.4 and 4.5, respectively.

The calculations for the reference case yield the following results:

- The maxima of the total radiation exposures are determined by the contributions of activation and fission products like C-14, Cl-36, I-129, Se-79, and Cs-135.

- In the case of the non-sorbing or weakly sorbing fission products (C-14, Cl-36, Ca-41, Se-79, Pd-107 I-129, Cs-135) the barrier function of the geosphere plays a minor role resulting in maximum release rates and times of occurrence which are only slightly affected by the transport through the geosphere.

- The geosphere is an important transport barrier for the well-sorbing nuclides such as the actinides and their daughter products. The release rates for some of these nuclides are still increasing after 10^7 years. As a consequence, the maximum radiation exposures from the nuclides of the four decay chains are some orders of magnitude lower than those of the relevant activation and fission products.

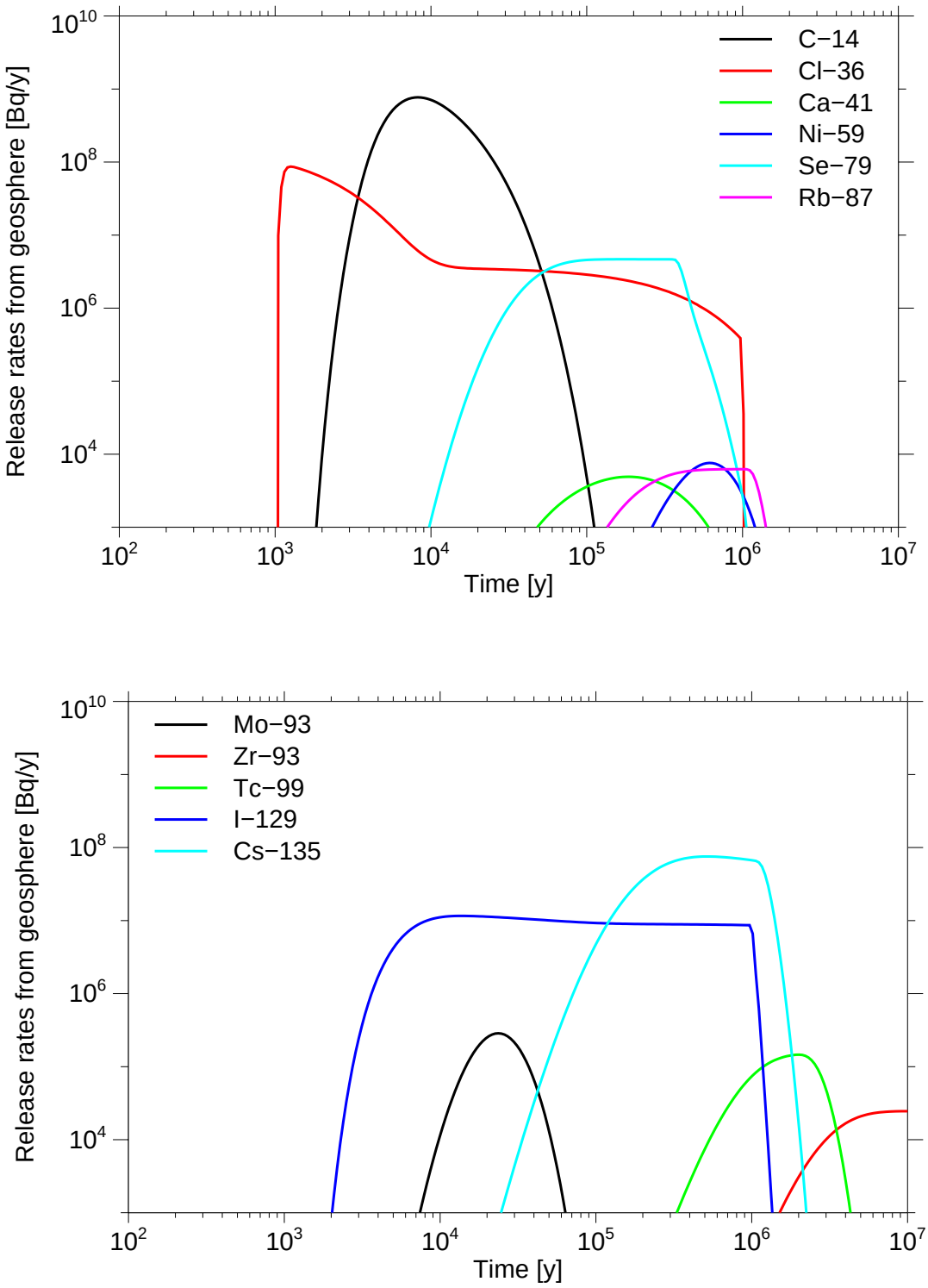

Fig. 4.4 Release rates of fission and activation products from the geosphere into the biosphere. LWR, reference case

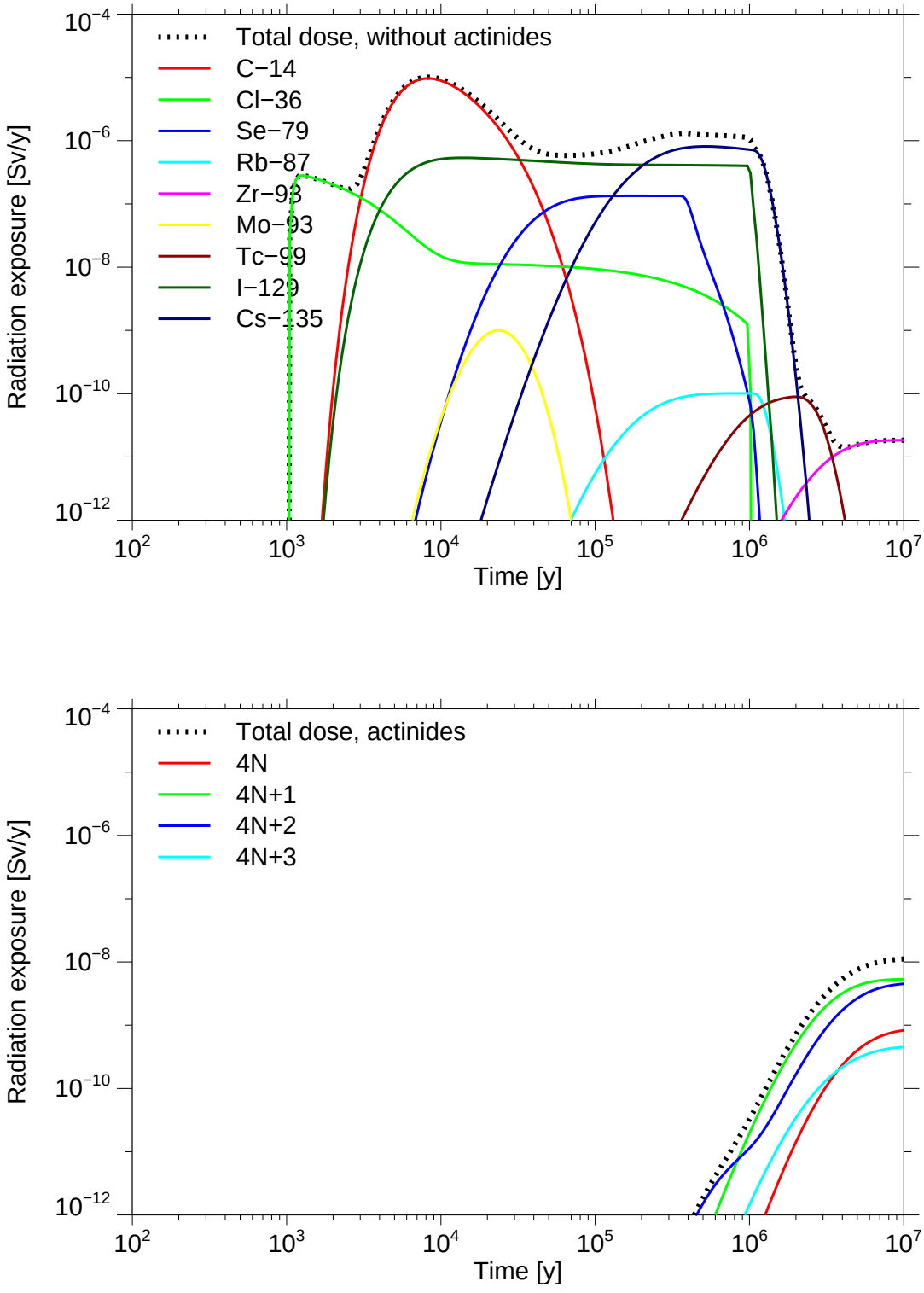

Fig. 4.5 Radiation exposures due to activation and fission products and nuclide chains. LWR, reference case. The dotted lines give the total radiation exposures

Tab. 4.2 Maximum release rates from the near-field and geosphere, and maximum radiation exposures. LWR, reference case

Nuclide	Release from near-field		Release from far-field		Maximum rad.
	t_{max} [y]	[Bq/y]	t_{max} [y]	[Bq/y]	exposure [Sv/y]
C -14	$2.1 \cdot 10^{3}$	$2.1 \cdot 10^{9}$	$8.2 \cdot 10^{3}$	$7.7 \cdot 10^{8}$	$9.6 \cdot 10^{-6}$
Cl-36	$1.0 \cdot 10^{3}$	$9.5 \cdot 10^{7}$	$1.3 \cdot 10^{3}$	$8.7 \cdot 10^{7}$	$2.8 \cdot 10^{-7}$
Ca-41	$1.3 \cdot 10^{5}$	$7.0 \cdot 10^{3}$	$1.9 \cdot 10^{5}$	$4.9 \cdot 10^{3}$	$1.9 \cdot 10^{-12}$
Ni-59	$1.4 \cdot 10^{4}$	$3.7 \cdot 10^{8}$	$6.1 \cdot 10^{5}$	$7.6 \cdot 10^{3}$	$1.6 \cdot 10^{-12}$
Se-79	$1.7 \cdot 10^{3}$	$7.9 \cdot 10^{6}$	$1.7 \cdot 10^{5}$	$4.7 \cdot 10^{6}$	$1.3 \cdot 10^{-7}$
Rb-87	$4.3 \cdot 10^{5}$	$6.2 \cdot 10^{3}$	$9.5 \cdot 10^{5}$	$6.3 \cdot 10^{3}$	$1.0 \cdot 10^{-10}$
Zr-93	$1.1 \cdot 10^{5}$	$1.7 \cdot 10^{5}$	$1.0 \cdot 10^{7}$	$2.5 \cdot 10^{4}$	$1.8 \cdot 10^{-11}$
Mo-93	$2.0 \cdot 10^{3}$	$4.6 \cdot 10^{8}$	$2.4 \cdot 10^{4}$	$2.9 \cdot 10^{5}$	$1.0 \cdot 10^{-9}$
Nb-94	$1.1 \cdot 10^{4}$	$4.5 \cdot 10^{7}$			
Tc-99	$1.2 \cdot 10^{4}$	$2.4 \cdot 10^{7}$	$2.0 \cdot 10^{6}$	$1.5 \cdot 10^{5}$	$8.9 \cdot 10^{-11}$
Pd-107	$1.4 \cdot 10^{5}$	$7.9 \cdot 10^{1}$	$1.0 \cdot 10^{7}$	$6.0 \cdot 10^{1}$	$2.3 \cdot 10^{-15}$
Sn-126	$1.1 \cdot 10^{5}$	$1.4 \cdot 10^{6}$	$8.4 \cdot 10^{5}$	$1.9 \cdot 10^{2}$	$2.1 \cdot 10^{-10}$
I-129	$1.1 \cdot 10^{3}$	$1.2 \cdot 10^{7}$	$1.4 \cdot 10^{5}$	$1.2 \cdot 10^{7}$	$5.4 \cdot 10^{-7}$
Cs-135	$1.8 \cdot 10^{5}$	$8.4 \cdot 10^{7}$	$5.1 \cdot 10^{5}$	$7.5 \cdot 10^{7}$	$8.1 \cdot 10^{-7}$
Sm-147	$1.1 \cdot 10^{6}$	$1.1 \cdot 10^{1}$	$1.0 \cdot 10^{7}$	0.36	$7.3 \cdot 10^{-15}$
Pu-240	$2.4 \cdot 10^{4}$	$2.4 \cdot 10^{5}$			
U-236	$4.5 \cdot 10^{5}$	$1.8 \cdot 10^{3}$	$9.6 \cdot 10^{6}$	$1.3 \cdot 10^{3}$	$3.5 \cdot 10^{-11}$
Th-232	$1.0 \cdot 10^{7}$	$1.8 \cdot 10^{1}$	$1.0 \cdot 10^{7}$	$1.7 \cdot 10^{1}$	$2.4 \cdot 10^{-11}$
Ra-228					$7.9 \cdot 10^{-10}$
Cm-245	$2.6 \cdot 10^{4}$	$3.0 \cdot 10^{3}$			
Pu-241	$2.6 \cdot 10^{4}$	$3.0 \cdot 10^{3}$			
Am-241	$2.6 \cdot 10^{4}$	$3.1 \cdot 10^{3}$			
Np-237	$5.0 \cdot 10^{5}$	$2.3 \cdot 10^{3}$	$1.0 \cdot 10^{7}$	$5.5 \cdot 10^{2}$	$4.3 \cdot 10^{-10}$
U-233	$7.3 \cdot 10^{5}$	$3.8 \cdot 10^{3}$	$1.0 \cdot 10^{7}$	$6.0 \cdot 10^{2}$	$2.1 \cdot 10^{-11}$
Th-229	$1.6 \cdot 10^{5}$	$7.0 \cdot 10^{4}$	$1.0 \cdot 10^{7}$	$6.0 \cdot 10^{2}$	$4.0 \cdot 10^{-10}$
Ra-225					$4.5 \cdot 10^{-9}$
Ac-225					$2.9 \cdot 10^{-12}$

Tab. 4.2 Maximum release rates from the near-field and geosphere, and maximum radiation exposures. LWR, reference case

Nuclide	Release from near-field		Release from far-field		Maximum rad. exposure [Sv/y]
	t_{max} [y]	[Bq/y]	t_{max} [y]	[Bq/y]	
Cm-246	$1.8 \cdot 10^{4}$	$1.8 \cdot 10^{3}$			
Pu-242	$5.4 \cdot 10^{5}$	$1.1 \cdot 10^{6}$	$4.0 \cdot 10^{6}$	1.3	$3.4 \cdot 10^{-13}$
U-238	$7.5 \cdot 10^{5}$	$1.1 \cdot 10^{3}$	$1.1 \cdot 10^{7}$	$1.1 \cdot 10^{3}$	$4.3 \cdot 10^{-11}$
U-234	$1.8 \cdot 10^{5}$	$4.7 \cdot 10^{3}$	$1.1 \cdot 10^{7}$	$1.1 \cdot 10^{3}$	$3.3 \cdot 10^{-11}$
Th-230	$2.2 \cdot 10^{5}$	$9.7 \cdot 10^{5}$	$1.1 \cdot 10^{7}$	$1.1 \cdot 10^{3}$	$3.3 \cdot 10^{-10}$
Ra-226	$5.4 \cdot 10^{5}$	$1.5 \cdot 10^{9}$	$1.1 \cdot 10^{7}$	$2.2 \cdot 10^{3}$	$4.1 \cdot 10^{-9}$
Pb-210					$4.3 \cdot 10^{-11}$
Cm-247	$1.0 \cdot 10^{6}$	$1.5 \cdot 10^{1}$	$1.0 \cdot 10^{7}$	0.32	$1.5 \cdot 10^{-13}$
Am-243	$2.3 \cdot 10^{4}$	$1.7 \cdot 10^{5}$	$1.0 \cdot 10^{7}$	0.32	$1.4 \cdot 10^{-13}$
Pu-239	$6.4 \cdot 10^{4}$	$2.5 \cdot 10^{6}$	$1.0 \cdot 10^{7}$	0.33	$8.9 \cdot 10^{-14}$
U-235	$1.3 \cdot 10^{5}$	$2.8 \cdot 10^{2}$	$1.1 \cdot 10^{7}$	$8.9 \cdot 10^{1}$	$1.0 \cdot 10^{-11}$
Pa-231	$2.2 \cdot 10^{5}$	$1.1 \cdot 10^{5}$	$1.1 \cdot 10^{7}$	$8.9 \cdot 10^{1}$	$1.4 \cdot 10^{-10}$
Ac-227					$3.0 \cdot 10^{-10}$

4.2 CANDU fuel

4.2.1 Near-field

The maximum release rates of the radionuclides from the waste forms into the canister interior (“volume of dissolution”), from the near-field into the geosphere, and from the geosphere into the biosphere are presented in Table 4.3. In Table 4.4, maximum concentrations of the radionuclides in the volume of dissolution, in the geosphere, and in the biosphere are shown. The release rates of the radionuclides from the waste forms into the volume of dissolution are presented in Figure 4.6. The radionuclide release rates into the geosphere are presented in Figures 4.7 to 4.10. The radionuclide inventory released from the container, as well as the inventory trapped in the bentonite buffer and the mobilized inventory in the container water at the end of the scenario ($t = 10^{7}$ y) are compiled in Table 4.5. The maximum outflow from the bentonite shielding and the times when these maxima are attained are compiled in Table 4.6.

The results are presented for a group of 7200 containers, each containing 1.365 t_U. For most of the nuclides, the maximum release rates out of the waste forms (gap, metal parts, and fuel matrix) occur at the time of the container failure (1500 years), as it can also be seen from Table 4.3. The peak in Figure 4.6 is due to the instantaneous release from the gap. After t = 1500 y, the release is controlled by the matrix release fraction, which contains the highest part of the inventory. The release rates out of the waste forms are dominated by actinides (Pu-240, Pu-234 und Am-241), followed by the fission products C-14, Tc-99, Se-79 and Ni-59. The release rates of some actinides (U-236, Th-232, Np-237, U-233, Th-229, Th-230, Ra-226 and Pa-231) continue to raise beyond the moment of container failure due to accumulation from precursors. The release of C-14, Ni-59 and Nb-94 stops at t = 1530 y. For the rest of the nuclides, mobilization stops at $t = 1.15 \cdot 10^4$ y, at the same time with complete dissolution of the matrix.

The maximum release rates of Am-241 and the long-lived nuclide Pu-239 originate from the decay of their parents Cm-245 and Am-243, respectively. The decay of Am-243 released from the waste forms but precipitated in the canister interior results in nearly constant release rates for the daughter nuclides even after the complete degradation of the waste forms (see Figure 4.6 and Table 4.3).

The release rates of the chained nuclides U-233 / Th-229, Th-230 / Ra-226 and Pa-231 are increasing due to accumulation from their parents Np-237, U-234, and U-235 respectively. The parents have constant release rates out of the waste-form into the container interior, due to precipitation in the container water.

The release rates out of the EDZ are shown in Figures 4.7 to 4.10. The maximum release rates out of the EDZ and the times when these maxima are attained are listed in Table 4.3. The maximum release rates from the near-field into the geosphere are dominated by C-14, followed by Tc-99, Se-79, and Ra-226.

The shielding capacity of the bentonite buffer can be inferred from Table 4.5. The release rates of the well sorbed actinides are strongly reduced by the bentonite. This reduction is inversely related to the half-life of the nuclide and to the decrease of the solubility limit (this effect is more pronounced for the short-lived, well sorbed and less soluble nuclides).

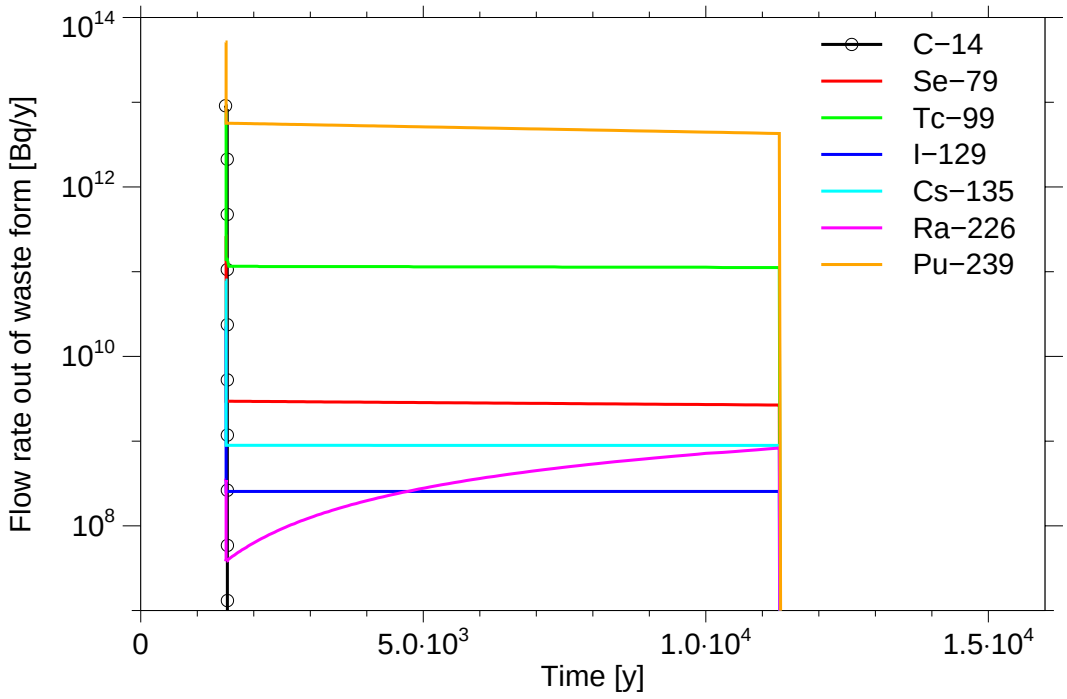

Fig. 4.6 Release rates out of the waste-forms. CANDU. Reference case

The reduction of the release rates is less marked for the soluble, long-lived and weak- or well-sorbed fission and activation products, such as Rb-87, I-129, Se-79 and Ca-41 or for the long-lived and less soluble actinides (Pa-231, Th-232 and Ra-226).

The release rates out the near-field into the geosphere from the non- or weak-sorbing nuclides, and from the non-solubility limited nuclides C-14 and I-129 are reduced by slow diffusion in the bentonite buffer (see Figure 4.7 and Table 4.3) before entering the geosphere. For example, the ratio between the maximum release rates out of the waste-form and out of the geosphere is $1.53 \cdot 10^{-4}$ for I-129 and $2.8 \cdot 10^{-5}$ for C-14.

The release rates of Se, Zr, Tc, Pd, Ra, U, Pu, Np, Th, and Pa are governed by the solubility limits. In the cases of Zr, Th, Pd, U, Np, Ra, and Pa major portions of the nuclides released from the waste forms precipitate in the canister interior.

The solubility limits of Ca, Ni, Nb, Sr and Sn are so high that they do not affect the release rates significantly.

Tab. 4.3 Maximum release rates from the waste-form, from the EDZ and from the geosphere. CANDU. Reference case

Nuclide	Maximum release rates [Bq/y]					
	Time of maximum [y]	Out of the waste form	Time of maximum [y]	Out of the EDZ	Time of maximum [y]	Out of the geosphere
C- 14	$1.50 \cdot 10^{+03}$	$9.09 \cdot 10^{+12}$	$1.87 \cdot 10^{+03}$	$2.50 \cdot 10^{+08}$	$8.24 \cdot 10^{+03}$	$9.07 \cdot 10^{+07}$
Ca- 41	$1.50 \cdot 10^{+03}$	$1.63 \cdot 10^{+08}$	$1.55 \cdot 10^{+04}$	$4.88 \cdot 10^{+04}$	$8.53 \cdot 10^{+04}$	$2.66 \cdot 10^{+04}$
Ni- 59	$1.50 \cdot 10^{+03}$	$1.57 \cdot 10^{+11}$	$2.40 \cdot 10^{+04}$	$3.98 \cdot 10^{+04}$	$6.13 \cdot 10^{+05}$	$8.87 \cdot 10^{-01}$
Se- 79	$1.50 \cdot 10^{+03}$	$2.64 \cdot 10^{+11}$	$1.15 \cdot 10^{+04}$	$3.62 \cdot 10^{+07}$	$7.44 \cdot 10^{+04}$	$1.44 \cdot 10^{+07}$
Rb- 87	$1.50 \cdot 10^{+03}$	$8.91 \cdot 10^{+06}$	$1.18 \cdot 10^{+04}$	$1.13 \cdot 10^{+03}$	$4.25 \cdot 10^{+05}$	$9.40 \cdot 10^{+02}$
Sr- 90	$1.50 \cdot 10^{+03}$	$4.18 \cdot 10^{+00}$	$1.59 \cdot 10^{+03}$	$1.52 \cdot 10^{-06}$	$1.82 \cdot 10^{+03}$	$6.40 \cdot 10^{-27}$
Zr- 93	$1.50 \cdot 10^{+03}$	$7.98 \cdot 10^{+11}$	$2.97 \cdot 10^{+05}$	$2.12 \cdot 10^{+03}$	$9.59 \cdot 10^{+06}$	$3.14 \cdot 10^{+02}$
Nb- 94	$1.50 \cdot 10^{+03}$	$7.75 \cdot 10^{+10}$	$1.62 \cdot 10^{+04}$	$1.23 \cdot 10^{+04}$	$2.13 \cdot 10^{+05}$	$1.07 \cdot 10^{-06}$
Tc- 99	$1.50 \cdot 10^{+03}$	$7.53 \cdot 10^{+12}$	$1.41 \cdot 10^{+04}$	$7.78 \cdot 10^{+07}$	$1.16 \cdot 10^{+06}$	$1.31 \cdot 10^{+05}$
Pd-107	$1.50 \cdot 10^{+03}$	$1.62 \cdot 10^{+10}$	$5.19 \cdot 10^{+04}$	$6.64 \cdot 10^{+04}$	$4.20 \cdot 10^{+06}$	$3.80 \cdot 10^{+04}$
Sn-126	$1.50 \cdot 10^{+03}$	$8.05 \cdot 10^{+10}$	$3.05 \cdot 10^{+04}$	$2.58 \cdot 10^{+05}$	$7.36 \cdot 10^{+05}$	$1.79 \cdot 10^{+01}$
I-129	$1.50 \cdot 10^{+03}$	$2.27 \cdot 10^{+10}$	$1.18 \cdot 10^{+04}$	$3.47 \cdot 10^{+06}$	$2.26 \cdot 10^{+04}$	$3.43 \cdot 10^{+06}$
Cs-135	$1.50 \cdot 10^{+03}$	$7.95 \cdot 10^{+10}$	$1.18 \cdot 10^{+04}$	$6.23 \cdot 10^{+06}$	$3.87 \cdot 10^{+05}$	$4.62 \cdot 10^{+06}$
Cs-137	$1.50 \cdot 10^{+03}$	$5.59 \cdot 10^{+01}$	$1.59 \cdot 10^{+03}$	$2.04 \cdot 10^{-05}$	$1.73 \cdot 10^{+03}$	$1.48 \cdot 10^{-27}$
Sm-147	$1.50 \cdot 10^{+03}$	$1.38 \cdot 10^{+05}$	$2.97 \cdot 10^{+05}$	$6.78 \cdot 10^{-02}$	$1.10 \cdot 10^{+07}$	$3.97 \cdot 10^{-03}$
Cm-248	$1.50 \cdot 10^{+03}$	$2.23 \cdot 10^{+01}$	$1.15 \cdot 10^{+05}$	$2.42 \cdot 10^{-05}$	$2.91 \cdot 10^{+06}$	$4.78 \cdot 10^{-12}$
Pu-244	$1.50 \cdot 10^{+03}$	$4.97 \cdot 10^{+03}$	$2.58 \cdot 10^{+05}$	$7.27 \cdot 10^{-03}$	$1.10 \cdot 10^{+07}$	$3.86 \cdot 10^{-04}$
Pu-240	$1.50 \cdot 10^{+03}$	$6.56 \cdot 10^{+13}$	$3.30 \cdot 10^{+04}$	$1.36 \cdot 10^{+05}$	$1.10 \cdot 10^{+07}$	$3.86 \cdot 10^{-04}$
U-236	$1.51 \cdot 10^{+03}$	$1.95 \cdot 10^{+10}$	$7.88 \cdot 10^{+04}$	$1.42 \cdot 10^{+03}$	$9.16 \cdot 10^{+06}$	$3.10 \cdot 10^{+02}$
Th-232	$1.13 \cdot 10^{+04}$	$1.55 \cdot 10^{+03}$	$9.68 \cdot 10^{+06}$	$1.24 \cdot 10^{+01}$	$1.10 \cdot 10^{+07}$	$1.07 \cdot 10^{+01}$
U-232	$1.50 \cdot 10^{+03}$	$1.70 \cdot 10^{+01}$	$2.88 \cdot 10^{+03}$	$6.62 \cdot 10^{-26}$	$1.00 \cdot 10^{+03}$	$0.00 \cdot 10^{+00}$
Cm-245	$1.50 \cdot 10^{+03}$	$9.53 \cdot 10^{+07}$	$3.36 \cdot 10^{+04}$	$2.16 \cdot 10^{+00}$	$1.55 \cdot 10^{+05}$	$1.96 \cdot 10^{-19}$
Pu-241	$1.50 \cdot 10^{+03}$	$9.55 \cdot 10^{+07}$	$3.36 \cdot 10^{+04}$	$2.16 \cdot 10^{+00}$	$1.55 \cdot 10^{+05}$	$1.97 \cdot 10^{-19}$
Am-241	$1.50 \cdot 10^{+03}$	$2.34 \cdot 10^{+13}$	$3.36 \cdot 10^{+04}$	$2.28 \cdot 10^{+00}$	$1.55 \cdot 10^{+05}$	$2.07 \cdot 10^{-19}$
NP-237	$1.50 \cdot 10^{+03}$	$5.49 \cdot 10^{+10}$	$1.10 \cdot 10^{+06}$	$8.04 \cdot 10^{+03}$	$8.75 \cdot 10^{+06}$	$1.89 \cdot 10^{+03}$
U-233	$1.13 \cdot 10^{+04}$	$3.01 \cdot 10^{+08}$	$9.74 \cdot 10^{+05}$	$4.20 \cdot 10^{+03}$	$8.75 \cdot 10^{+06}$	$2.04 \cdot 10^{+03}$
Th-229	$1.13 \cdot 10^{+04}$	$1.13 \cdot 10^{+08}$	$7.53 \cdot 10^{+05}$	$7.13 \cdot 10^{+03}$	$8.75 \cdot 10^{+06}$	$2.05 \cdot 10^{+03}$
Cm-246	$1.50 \cdot 10^{+03}$	$1.51 \cdot 10^{+07}$	$2.71 \cdot 10^{+04}$	$5.38 \cdot 10^{-02}$	$1.03 \cdot 10^{+05}$	$4.71 \cdot 10^{-24}$

Tab. 4.3 Maximum release rates from the waste-form, from the EDZ and from the geosphere. CANDU. Reference case

Nuclide	Maximum release rates [Bq/y]					
	Time of maximum [y]	Out of the waste form	Time of maximum [y]	Out of the EDZ	Time of maximum [y]	Out of the geosphere
Pu-242	$1.50 \cdot 10^{+03}$	$7.77 \cdot 10^{+10}$	$1.49 \cdot 10^{+05}$	$8.25 \cdot 10^{+04}$	$3.34 \cdot 10^{+06}$	$3.53 \cdot 10^{-02}$
Am-242	$1.50 \cdot 10^{+03}$	$7.66 \cdot 10^{+07}$	$4.12 \cdot 10^{+03}$	$8.30 \cdot 10^{-13}$	$1.00 \cdot 10^{+03}$	$0.00 \cdot 10^{+00}$
U-238	$1.50 \cdot 10^{+03}$	$1.08 \cdot 10^{+11}$	$8.99 \cdot 10^{+05}$	$1.22 \cdot 10^{+03}$	$1.10 \cdot 10^{+07}$	$1.18 \cdot 10^{+03}$
Pu-238	$1.50 \cdot 10^{+03}$	$3.52 \cdot 10^{+08}$	$4.04 \cdot 10^{+03}$	$1.96 \cdot 10^{-12}$	$1.00 \cdot 10^{+03}$	$0.00 \cdot 10^{+00}$
U-234	$1.50 \cdot 10^{+03}$	$9.67 \cdot 10^{+10}$	$1.19 \cdot 10^{+06}$	$1.22 \cdot 10^{+03}$	$1.10 \cdot 10^{+07}$	$1.18 \cdot 10^{+03}$
Th-230	$1.50 \cdot 10^{+03}$	$1.30 \cdot 10^{+09}$	$1.01 \cdot 10^{+06}$	$1.02 \cdot 10^{+05}$	$1.10 \cdot 10^{+07}$	$1.18 \cdot 10^{+03}$
Ra-226	$1.13 \cdot 10^{+04}$	$8.29 \cdot 10^{+08}$	$1.14 \cdot 10^{+06}$	$1.02 \cdot 10^{+07}$	$1.10 \cdot 10^{+07}$	$2.36 \cdot 10^{+03}$
Cm-247	$1.50 \cdot 10^{+03}$	$1.97 \cdot 10^{+01}$	$2.00 \cdot 10^{+05}$	$2.86 \cdot 10^{-05}$	$1.10 \cdot 10^{+07}$	$1.04 \cdot 10^{-06}$
Am-243	$1.50 \cdot 10^{+03}$	$1.48 \cdot 10^{+11}$	$3.17 \cdot 10^{+04}$	$2.27 \cdot 10^{+03}$	$1.10 \cdot 10^{+07}$	$1.04 \cdot 10^{-06}$
Pu-239	$1.50 \cdot 10^{+03}$	$5.14 \cdot 10^{+13}$	$7.56 \cdot 10^{+04}$	$4.16 \cdot 10^{+06}$	$1.10 \cdot 10^{+07}$	$1.04 \cdot 10^{-06}$
U-235	$1.50 \cdot 10^{+03}$	$1.50 \cdot 10^{+09}$	$1.22 \cdot 10^{+05}$	$5.80 \cdot 10^{+02}$	$5.28 \cdot 10^{+06}$	$4.70 \cdot 10^{+01}$
Pa-231	$1.51 \cdot 10^{+03}$	$4.62 \cdot 10^{+07}$	$3.03 \cdot 10^{+05}$	$1.95 \cdot 10^{+04}$	$5.28 \cdot 10^{+06}$	$4.70 \cdot 10^{+01}$

Tab. 4.4 Maximum concentration in the waste-form, in the EDZ and in the geosphere. CANDU. Reference case

Nuclide	Maximum concentration [Bq/m^3]					
	Time of maximum [y]	In the waste form	Time of maximum [y]	In the EDZ	Time of maximum [y]	In the geosphere
C- 14	$1.53 \cdot 10^{+03}$	$3.08 \cdot 10^{-03}$	$1.87 \cdot 10^{+03}$	$1.55 \cdot 10^{+09}$	$8.24 \cdot 10^{+03}$	$5.89 \cdot 10^{+04}$
Ca- 41	$1.15 \cdot 10^{+04}$	$4.76 \cdot 10^{-06}$	$1.55 \cdot 10^{+04}$	$3.03 \cdot 10^{+05}$	$8.53 \cdot 10^{+04}$	$1.73 \cdot 10^{+01}$
Ni- 59	$1.53 \cdot 10^{+03}$	$1.32 \cdot 10^{-04}$	$2.31 \cdot 10^{+04}$	$2.47 \cdot 10^{+05}$	$6.13 \cdot 10^{+05}$	$5.76 \cdot 10^{-04}$
Se- 79	$1.15 \cdot 10^{+04}$	$1.30 \cdot 10^{-03}$	$1.15 \cdot 10^{+04}$	$2.25 \cdot 10^{+08}$	$7.44 \cdot 10^{+04}$	$9.36 \cdot 10^{+03}$
Rb- 87	$1.13 \cdot 10^{+04}$	$2.93 \cdot 10^{-02}$	$1.18 \cdot 10^{+04}$	$6.99 \cdot 10^{+03}$	$4.25 \cdot 10^{+05}$	$6.11 \cdot 10^{-01}$
Sr- 90	$1.51 \cdot 10^{+03}$	$3.52 \cdot 10^{-18}$	$1.59 \cdot 10^{+03}$	$9.43 \cdot 10^{-06}$	$1.82 \cdot 10^{+03}$	$4.16 \cdot 10^{-30}$
Zr- 93	$1.50 \cdot 10^{+03}$	$1.80 \cdot 10^{-06}$	$1.70 \cdot 10^{+05}$	$1.31 \cdot 10^{+04}$	$9.59 \cdot 10^{+06}$	$2.04 \cdot 10^{-01}$
Nb- 94	$1.53 \cdot 10^{+03}$	$1.65 \cdot 10^{-05}$	$1.68 \cdot 10^{+04}$	$7.64 \cdot 10^{+04}$	$2.13 \cdot 10^{+05}$	$6.93 \cdot 10^{-10}$

Tab. 4.4 Maximum concentration in the waste-form, in the EDZ and in the geosphere. CANDU. Reference case

Nuclide	Maximum concentration [Bq/m^3]					
	Time of maximum [y]	In the waste form	Time of maximum [y]	In the EDZ	Time of maximum [y]	In the geosphere
Tc- 99	$1.51\cdot10^{+03}$	$2.34\cdot10^{-02}$	$1.38\cdot10^{+04}$	$4.83\cdot10^{+08}$	$1.16\cdot10^{+06}$	$8.49\cdot10^{+01}$
Pd-107	$1.13\cdot10^{+04}$	$9.46\cdot10^{-04}$	$4.71\cdot10^{+04}$	$4.12\cdot10^{+05}$	$4.20\cdot10^{+06}$	$2.47\cdot10^{+01}$
Sn-126	$1.51\cdot10^{+03}$	$7.15\cdot10^{-05}$	$2.93\cdot10^{+04}$	$1.60\cdot10^{+06}$	$7.36\cdot10^{+05}$	$1.16\cdot10^{-02}$
I-129	$1.15\cdot10^{+04}$	$3.00\cdot10^{-02}$	$1.18\cdot10^{+04}$	$2.16\cdot10^{+07}$	$2.26\cdot10^{+04}$	$2.23\cdot10^{+03}$
Cs-135	$1.15\cdot10^{+04}$	$7.94\cdot10^{-03}$	$1.18\cdot10^{+04}$	$3.87\cdot10^{+07}$	$3.87\cdot10^{+05}$	$3.00\cdot10^{+03}$
Cs-137	$1.51\cdot10^{+03}$	$4.88\cdot10^{-17}$	$1.59\cdot10^{+03}$	$1.27\cdot10^{-04}$	$1.73\cdot10^{+03}$	$9.61\cdot10^{-31}$
Sm-147	$1.51\cdot10^{+03}$	$1.22\cdot10^{-04}$	$2.53\cdot10^{+05}$	$4.21\cdot10^{-01}$	$1.10\cdot10^{+07}$	$2.58\cdot10^{-06}$
Cm-248	$1.13\cdot10^{+04}$	$6.60\cdot10^{-14}$	$1.08\cdot10^{+05}$	$1.50\cdot10^{-04}$	$3.05\cdot10^{+06}$	$3.11\cdot10^{-15}$
Pu-244	$6.47\cdot10^{+04}$	$1.31\cdot10^{-08}$	$2.69\cdot10^{+05}$	$4.52\cdot10^{-02}$	$1.10\cdot10^{+07}$	$2.50\cdot10^{-07}$
Cm-244	$1.50\cdot10^{+03}$	$6.35\cdot10^{-32}$	$1.00\cdot10^{-02}$	$0.00\cdot10^{+00}$	$1.00\cdot10^{+03}$	$0.00\cdot10^{+00}$
Pu-240	$1.50\cdot10^{+03}$	$2.53\cdot10^{-04}$	$3.30\cdot10^{+04}$	$8.42\cdot10^{+05}$	$1.10\cdot10^{+07}$	$2.50\cdot10^{-07}$
U-236	$2.43\cdot10^{+05}$	$5.40\cdot10^{-06}$	$8.19\cdot10^{+04}$	$8.82\cdot10^{+03}$	$8.75\cdot10^{+06}$	$2.01\cdot10^{-01}$
Th-232	$1.09\cdot10^{+07}$	$9.56\cdot10^{-05}$	$1.09\cdot10^{+07}$	$7.73\cdot10^{+01}$	$1.10\cdot10^{+07}$	$6.94\cdot10^{-03}$
U-232	$1.50\cdot10^{+03}$	$7.59\cdot10^{-21}$	$2.88\cdot10^{+03}$	$4.11\cdot10^{-25}$	$1.00\cdot10^{+03}$	$0.00\cdot10^{+00}$
Cm-245	$1.51\cdot10^{+03}$	$6.66\cdot10^{-09}$	$3.30\cdot10^{+04}$	$1.34\cdot10^{+01}$	$1.55\cdot10^{+05}$	$1.27\cdot10^{-22}$
Pu-241	$1.50\cdot10^{+03}$	$8.11\cdot10^{-13}$	$3.30\cdot10^{+04}$	$1.34\cdot10^{+01}$	$1.55\cdot10^{+05}$	$1.28\cdot10^{-22}$
Am-241	$1.51\cdot10^{+03}$	$8.19\cdot10^{-05}$	$3.43\cdot10^{+04}$	$1.42\cdot10^{+01}$	$1.55\cdot10^{+05}$	$1.35\cdot10^{-22}$
NP-237	$1.50\cdot10^{+03}$	$1.00\cdot10^{-05}$	$1.39\cdot10^{+06}$	$5.00\cdot10^{+04}$	$8.75\cdot10^{+06}$	$1.23\cdot10^{+00}$
U-233	$6.05\cdot10^{+05}$	$4.57\cdot10^{-08}$	$9.55\cdot10^{+05}$	$2.61\cdot10^{+04}$	$8.36\cdot10^{+06}$	$1.32\cdot10^{+00}$
Th-229	$5.38\cdot10^{+05}$	$2.29\cdot10^{-05}$	$7.38\cdot10^{+05}$	$4.43\cdot10^{+04}$	$8.75\cdot10^{+06}$	$1.33\cdot10^{+00}$
Cm-246	$1.51\cdot10^{+03}$	$5.86\cdot10^{-10}$	$2.65\cdot10^{+04}$	$3.34\cdot10^{-01}$	$1.03\cdot10^{+05}$	$3.06\cdot10^{-27}$
Pu-242	$6.47\cdot10^{+04}$	$8.61\cdot10^{-04}$	$1.52\cdot10^{+05}$	$5.13\cdot10^{+05}$	$3.34\cdot10^{+06}$	$2.29\cdot10^{-05}$
Am-242	$1.50\cdot10^{+03}$	$9.28\cdot10^{-11}$	$4.12\cdot10^{+03}$	$5.15\cdot10^{-12}$	$1.00\cdot10^{+03}$	$0.00\cdot10^{+00}$
U-238	$1.50\cdot10^{+03}$	$2.99\cdot10^{-03}$	$1.14\cdot10^{+06}$	$7.58\cdot10^{+03}$	$1.10\cdot10^{+07}$	$7.67\cdot10^{-01}$
Pu-238	$1.50\cdot10^{+03}$	$1.82\cdot10^{-11}$	$4.04\cdot10^{+03}$	$1.22\cdot10^{-11}$	$1.00\cdot10^{+03}$	$0.00\cdot10^{+00}$
U-234	$1.19\cdot10^{+06}$	$1.63\cdot10^{-07}$	$1.76\cdot10^{+06}$	$7.58\cdot10^{+03}$	$1.10\cdot10^{+07}$	$7.67\cdot10^{-01}$
Th-230	$1.42\cdot10^{+06}$	$7.99\cdot10^{-05}$	$1.16\cdot10^{+06}$	$6.33\cdot10^{+05}$	$1.10\cdot10^{+07}$	$7.67\cdot10^{-01}$
Ra-226	$5.77\cdot10^{+03}$	$1.00\cdot10^{-06}$	$1.16\cdot10^{+06}$	$6.31\cdot10^{+07}$	$1.10\cdot10^{+07}$	$1.53\cdot10^{+00}$

Tab. 4.4 Maximum concentration in the waste-form, in the EDZ and in the geosphere. CANDU. Reference case

Nuclide	Maximum concentration [Bq/m^3]					
	Time of maximum [y]	In the waste form	Time of maximum [y]	In the EDZ	Time of maximum [y]	In the geosphere
Cm-247	$1.13\cdot10^{+04}$	$2.74\cdot10^{-12}$	$2.08\cdot10^{+05}$	$1.78\cdot10^{-04}$	$1.10\cdot10^{+07}$	$6.75\cdot10^{-10}$
Am-243	$1.51\cdot10^{+03}$	$8.98\cdot10^{-06}$	$3.17\cdot10^{+04}$	$1.41\cdot10^{+04}$	$1.10\cdot10^{+07}$	$6.75\cdot10^{-10}$
Pu-239	$5.63\cdot10^{+04}$	$9.94\cdot10^{-04}$	$7.58\cdot10^{+04}$	$2.58\cdot10^{+07}$	$1.10\cdot10^{+07}$	$6.76\cdot10^{-10}$
U-235	$7.53\cdot10^{+05}$	$1.42\cdot10^{-05}$	$1.24\cdot10^{+05}$	$3.61\cdot10^{+03}$	$5.05\cdot10^{+06}$	$3.05\cdot10^{-02}$
Pa-231	$7.23\cdot10^{+05}$	$2.66\cdot10^{-05}$	$2.69\cdot10^{+05}$	$1.21\cdot10^{+05}$	$5.05\cdot10^{+06}$	$3.05\cdot10^{-02}$

Tab. 4.5 Radionuclide inventory in [Bq] in different parts of the near field at the end of the scenario. CANDU. Reference case

Nuclide	Released from container	Bentonite	Mobilized inventory in the container water
C- 14	$2.98\cdot10^{+08}$	0.0	0.0
Ca- 41	$1.06\cdot10^{+06}$	$1.14\cdot10^{-24}$	$9.78\cdot10^{-28}$
Ni- 59	$7.54\cdot10^{+05}$	0.0	0.0
Se- 79	$4.51\cdot10^{+08}$	0.0	0.0
Rb- 87	$2.43\cdot10^{+05}$	$1.97\cdot10^{+02}$	$3.37\cdot10^{+00}$
Sr- 90	$2.40\cdot10^{-08}$	0.0	0.0
Zr- 93	$3.22\cdot10^{+06}$	$4.47\cdot10^{+07}$	$1.17\cdot10^{+08}$
Nb- 94	$7.40\cdot10^{+04}$	0.0	0.0
Tc- 99	$3.34\cdot10^{+09}$	$2.45\cdot10^{-05}$	$4.20\cdot10^{-08}$
Pd-107	$5.83\cdot10^{+07}$	$4.05\cdot10^{+08}$	$6.95\cdot10^{+04}$
Sn-126	$6.00\cdot10^{+06}$	$5.47\cdot10^{-24}$	$9.40\cdot10^{-28}$
I-129	$3.72\cdot10^{+08}$	$2.14\cdot10^{+02}$	$7.28\cdot10^{+00}$
Cs-135	$9.18\cdot10^{+08}$	$3.99\cdot10^{+04}$	$6.81\cdot10^{+02}$
Cs-137	$3.17\cdot10^{-07}$	0.0	0.0
Sm-147	$1.02\cdot10^{+02}$	$7.02\cdot10^{+03}$	$2.41\cdot10^{-01}$
Cm-248	$1.98\cdot10^{-03}$	$5.92\cdot10^{-10}$	$2.04\cdot10^{-14}$
Pu-244	$1.05\cdot10^{+01}$	$6.89\cdot10^{+02}$	$2.37\cdot10^{-02}$

Tab. 4.5 Radionuclide inventory in [Bq] in different parts of the near field at the end of the scenario. CANDU. Reference case

Nuclide	Released from container	Bentonite	Mobilized inventory in the container water
Cm-244	$3.78 \cdot 10^{-59}$	0.0	0.0
Pu-240	$6.99 \cdot 10^{+05}$	$6.90 \cdot 10^{+02}$	$2.37 \cdot 10^{-02}$
U-236	$5.86 \cdot 10^{+05}$	$3.25 \cdot 10^{+07}$	$4.18 \cdot 10^{+09}$
Th-232	$1.44 \cdot 10^{+04}$	$1.31 \cdot 10^{+06}$	$1.37 \cdot 10^{+06}$
U-232	$8.28 \cdot 10^{-27}$	0.0	0.0
Cm-245	$1.06 \cdot 10^{+01}$	0.0	0.0
Pu-241	$1.06 \cdot 10^{+01}$	0.0	0.0
Am-241	$1.11 \cdot 10^{+01}$	0.0	0.0
NP-237	$1.04 \cdot 10^{+07}$	$2.59 \cdot 10^{+08}$	$8.91 \cdot 10^{+03}$
U-233	$5.23 \cdot 10^{+06}$	$9.71 \cdot 10^{+07}$	$1.83 \cdot 10^{+08}$
Th-229	$6.29 \cdot 10^{+06}$	$1.14 \cdot 10^{+08}$	$1.68 \cdot 10^{+08}$
Cm-246	$1.76 \cdot 10^{-01}$	0.0	0.0
Pu-242	$7.65 \cdot 10^{+06}$	$3.33 \cdot 10^{+01}$	$1.14 \cdot 10^{-03}$
Am-242	$2.00 \cdot 10^{-13}$	0.0	0.0
U-238	$1.83 \cdot 10^{+06}$	$1.28 \cdot 10^{+08}$	$1.65 \cdot 10^{+10}$
Pu-238	$4.76 \cdot 10^{-13}$	0.0	0.0
U-234	$1.83 \cdot 10^{+06}$	$1.28 \cdot 10^{+08}$	$1.65 \cdot 10^{+10}$
Th-230	$1.09 \cdot 10^{+08}$	$5.31 \cdot 10^{+09}$	$1.13 \cdot 10^{+10}$
Ra-226	$1.13 \cdot 10^{+10}$	$4.40 \cdot 10^{+08}$	$1.52 \cdot 10^{+10}$
Cm-247	$3.45 \cdot 10^{-02}$	$1.84 \cdot 10^{+00}$	$6.33 \cdot 10^{-05}$
Am-243	$1.00 \cdot 10^{+04}$	$1.84 \cdot 10^{+00}$	$6.33 \cdot 10^{-05}$
Pu-239	$5.07 \cdot 10^{+07}$	$1.84 \cdot 10^{+00}$	$6.34 \cdot 10^{-05}$
U-235	$7.49 \cdot 10^{+04}$	$3.84 \cdot 10^{+06}$	$4.94 \cdot 10^{+08}$
Pa-231	$2.92 \cdot 10^{+07}$	$4.98 \cdot 10^{+08}$	$5.31 \cdot 10^{+06}$

Tab. 4.6 Maximum outflow from the bentonite shielding [Bq/y]. CANDU. Reference case

Nuclide	Time of maximum outflow [y]	Maximum outflow (bentonite) [Bq/y]
C- 14	$1.90 \cdot 10^{+03}$	$3.48 \cdot 10^{+04}$
Ca- 41	$1.58 \cdot 10^{+04}$	$6.78 \cdot 10^{+00}$
Ni- 59	$2.50 \cdot 10^{+04}$	$5.53 \cdot 10^{+00}$
Se- 79	$1.18 \cdot 10^{+04}$	$5.03 \cdot 10^{+03}$
Rb- 87	$1.20 \cdot 10^{+04}$	$1.56 \cdot 10^{-01}$
Sr- 90	$1.59 \cdot 10^{+03}$	$2.11 \cdot 10^{-10}$
Zr- 93	$4.21 \cdot 10^{+06}$	$2.94 \cdot 10^{-01}$
Nb- 94	$1.72 \cdot 10^{+04}$	$1.71 \cdot 10^{+00}$
Tc- 99	$1.41 \cdot 10^{+04}$	$1.08 \cdot 10^{+04}$
Pd-107	$5.85 \cdot 10^{+04}$	$9.22 \cdot 10^{+00}$
Sn-126	$3.17 \cdot 10^{+04}$	$3.58 \cdot 10^{+01}$
I-129	$1.18 \cdot 10^{+04}$	$4.82 \cdot 10^{+02}$
Cs-135	$1.20 \cdot 10^{+04}$	$8.65 \cdot 10^{+02}$
Cs-137	$1.59 \cdot 10^{+03}$	$2.83 \cdot 10^{-09}$
Sm-147	$3.55 \cdot 10^{+05}$	$9.41 \cdot 10^{-06}$
Cm-248	$1.19 \cdot 10^{+05}$	$3.36 \cdot 10^{-09}$
Pu-244	$3.21 \cdot 10^{+05}$	$1.01 \cdot 10^{-06}$
Cm-244	$1.83 \cdot 10^{+03}$	$1.58 \cdot 10^{-61}$
Pu-240	$3.30 \cdot 10^{+04}$	$1.88 \cdot 10^{+01}$
U-236	$8.20 \cdot 10^{+04}$	$1.97 \cdot 10^{-01}$
Th-232	$1.09 \cdot 10^{+07}$	$1.73 \cdot 10^{-03}$
U-232	$2.88 \cdot 10^{+03}$	$9.20 \cdot 10^{-30}$
Cm-245	$3.43 \cdot 10^{+04}$	$3.00 \cdot 10^{-04}$
Pu-241	$3.43 \cdot 10^{+04}$	$3.01 \cdot 10^{-04}$
Am-241	$3.43 \cdot 10^{+04}$	$3.17 \cdot 10^{-04}$
NP-237	$4.65 \cdot 10^{+06}$	$1.12 \cdot 10^{+00}$
U-233	$1.07 \cdot 10^{+06}$	$5.83 \cdot 10^{-01}$
Th-229	$7.83 \cdot 10^{05}$	$9.90 \cdot 10^{-01}$
Cm-246	$2.71 \cdot 10^{04}$	$7.47 \cdot 10^{-06}$
Pu-242	$1.52 \cdot 10^{05}$	$1.15 \cdot 10^{+01}$
Am-242	$4.12 \cdot 10^{03}$	$1.15 \cdot 10^{-16}$

Tab. 4.6 Maximum outflow from the bentonite shielding [Bq/y]. CANDU. Reference case

Nuclide	Time of maximum outflow [y]	Maximum outflow (bentonite) [Bq/y]
U-238	$1.09 \cdot 10^{07}$	$1.70 \cdot 10^{-01}$
Pu-238	$4.12 \cdot 10^{03}$	$2.73 \cdot 10^{-16}$
U-234	$1.09 \cdot 10^{07}$	$1.70 \cdot 10^{-01}$
Th-230	$1.23 \cdot 10^{06}$	$1.42 \cdot 10^{+01}$
Ra-226	$1.23 \cdot 10^{06}$	$1.41 \cdot 10^{+03}$
Cm-247	$2.39 \cdot 10^{05}$	$3.97 \cdot 10^{-09}$
Am-243	$3.23 \cdot 10^{04}$	$3.15 \cdot 10^{-01}$
Pu-239	$7.73 \cdot 10^{04}$	$5.77 \cdot 10^{+02}$
U-235	$1.24 \cdot 10^{05}$	$8.06 \cdot 10^{-02}$
Pa-231	$3.34 \cdot 10^{05}$	$2.70 \cdot 10^{00}$

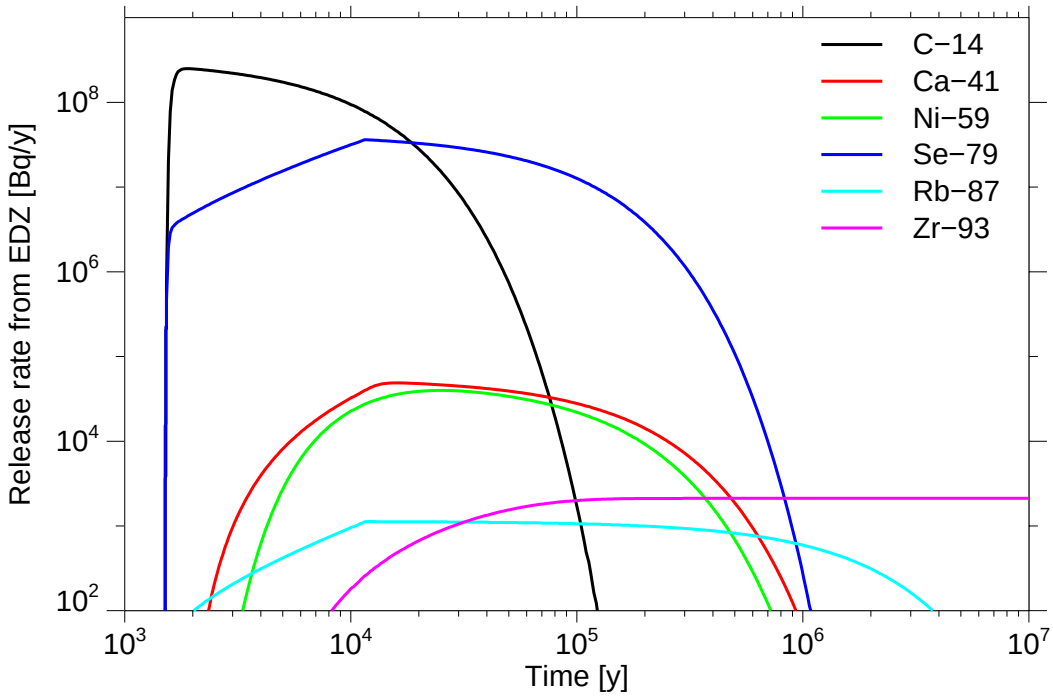

Fig. 4.7 Release rates of fission and activation products from the near-field into the geosphere. CANDU. Reference case

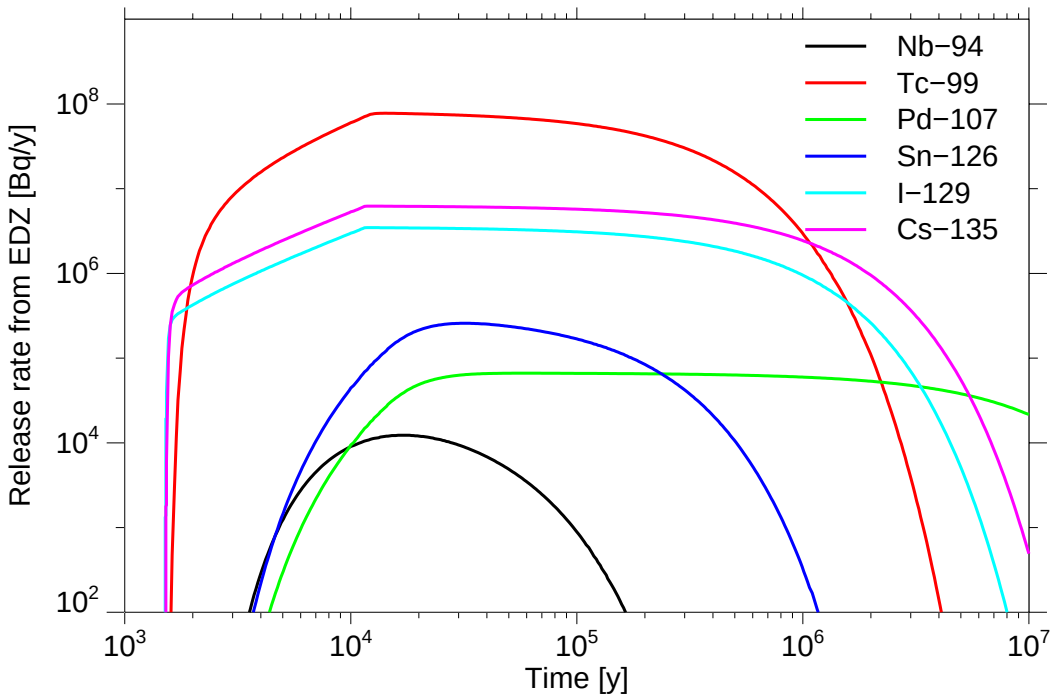

Fig. 4.8 Release rates of fission and activation products from the near-field into the geosphere. CANDU. Reference case

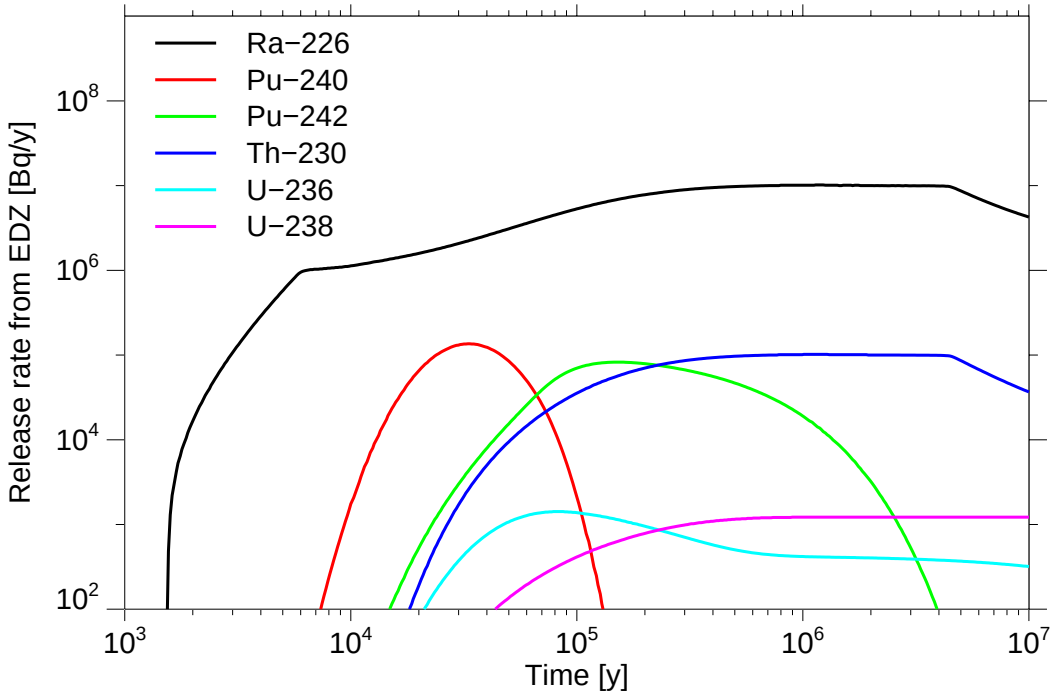

Fig. 4.9 Release rates of the radionuclides in 4N and 4N+2 nuclide chains from the near field into the geosphere. CANDU. Reference case

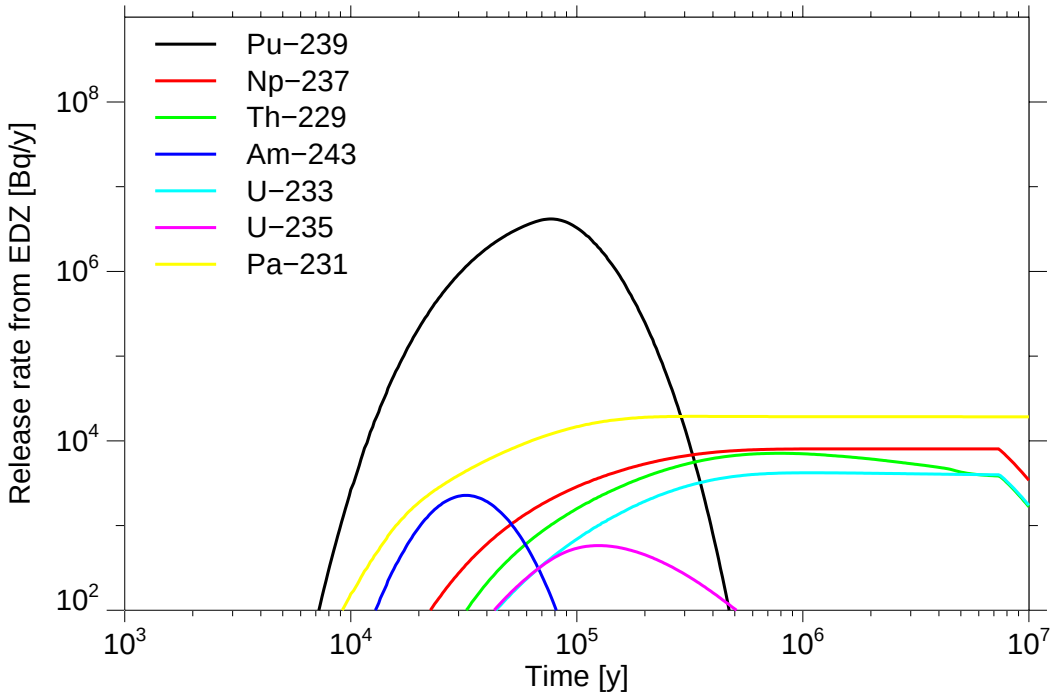

Fig. 4.10 Release rates of the radionuclides in 4N+1 and 4N+3 nuclide chains from the near field into the geosphere. CANDU. Reference case

4.2.2 Far-field and biosphere

The maximum release rates and concentrations from the geosphere into the biosphere are given in Figure 4.11 and Table 4.4, respectively. The maximum individual radiation exposures are given in Table 4.7. Some short-lived nuclides (Ac-225, Ac-227, Ra-225, Ra-228, Pb-210) are considered in the biosphere calculations only. Their radiation exposures are calculated by means of the radiation exposures of their parent nuclides assuming radioactive equilibrium. The individual radiation exposures are shown in Figure 4.12.

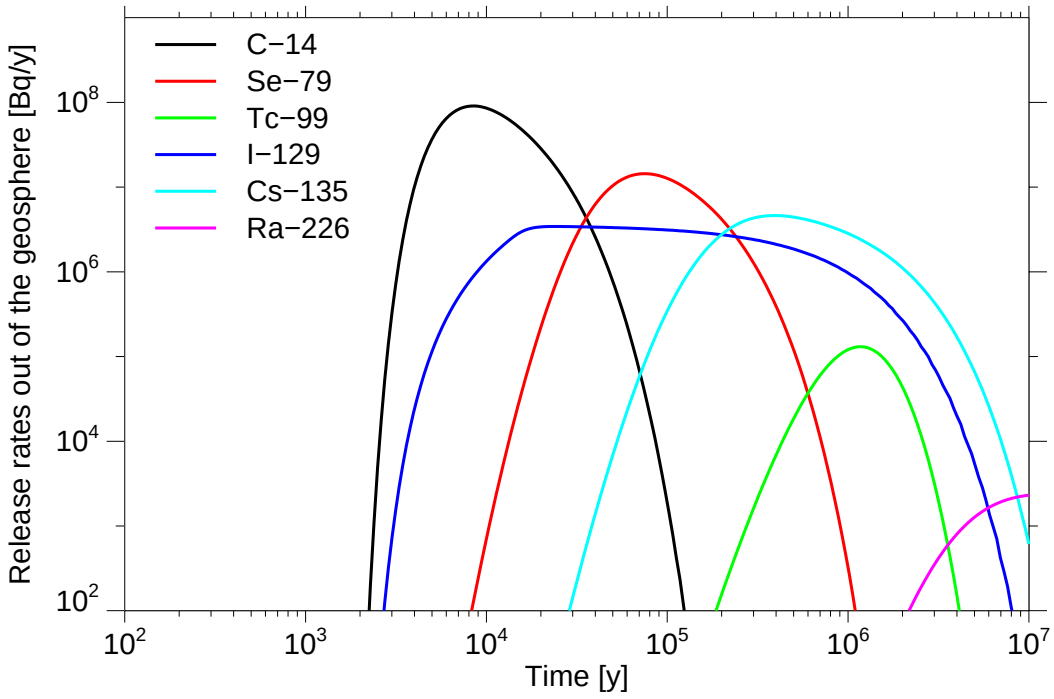

Fig. 4.11 Release rates of relevant radionuclides from the geosphere into the biosphere. CANDU. Reference case

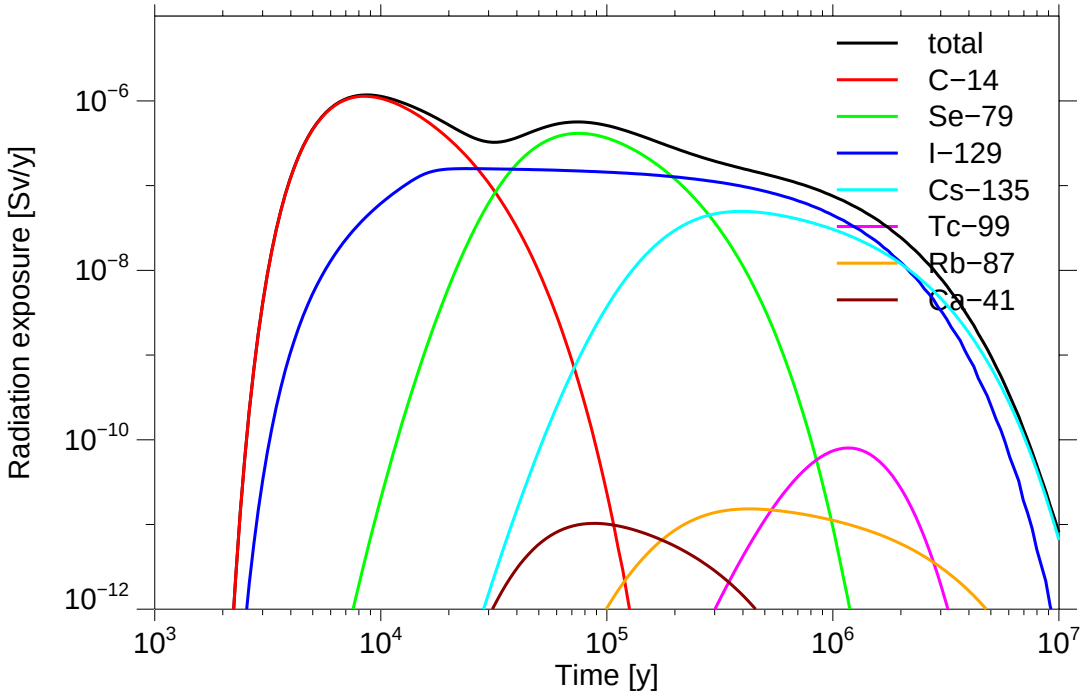

Fig. 4.12 Radiation exposure due to activation/fission products. CANDU. Reference case

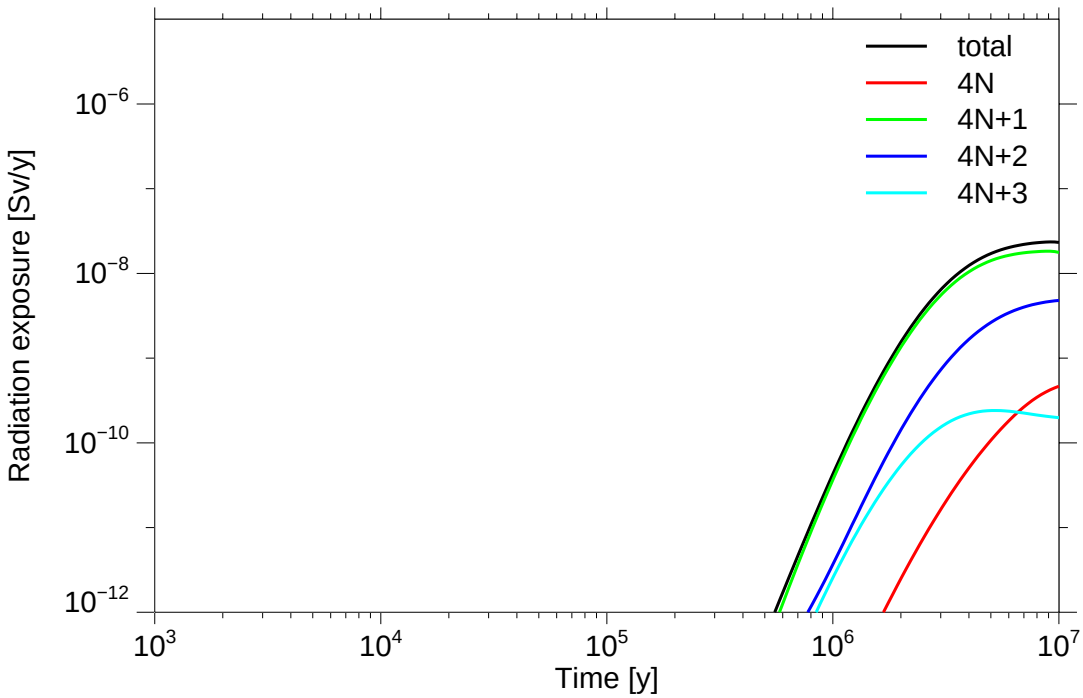

Fig. 4.13 Radiation exposure due to actinides. CANDU. Reference case

Tab. 4.7 Maximum radiation exposure and time of occurrence of maxima. CANDU. Reference case

Nuclide	Time of occurrence [y]	Radiation exposure [Sv/y]
C- 14	$8.62 \cdot 10^{03}$	$1.13 \cdot 10^{-06}$
Se- 79	$7.44 \cdot 10^{04}$	$4.14 \cdot 10^{-07}$
I-129	$2.36 \cdot 10^{04}$	$1.59 \cdot 10^{-07}$
Cs-135	$3.87 \cdot 10^{05}$	$4.97 \cdot 10^{-08}$
Ra-228	$1.10 \cdot 10^{07}$	$4.81 \cdot 10^{-10}$
Np-237	$8.75 \cdot 10^{06}$	$1.46 \cdot 10^{-09}$
Th-229	$8.75 \cdot 10^{06}$	$1.38 \cdot 10^{-09}$
Ra-225	$8.75 \cdot 10^{06}$	$1.54 \cdot 10^{-08}$
Th-230	$1.10 \cdot 10^{07}$	$3.54 \cdot 10^{-10}$
Ra-226	$1.10 \cdot 10^{07}$	$4.43 \cdot 10^{-09}$
Ac-227	$5.28 \cdot 10^{06}$	$1.59 \cdot 10^{-10}$
Total dose	$8.62 \cdot 10^{03}$	$1.18 \cdot 10^{-06}$

The calculations for the reference case yield the following results:

- For the period of the simulation of 10^7 years none of the calculated radiation exposures, including the sum over all radionuclides, exceeds a value of 10^{-6} Sv/a. This value is a factor of 50 lower than the risk limit implied by the Canadian Atomic Energy Control Board (AECB) [1] and a factor of 300 lower than the protection limit implied by the German radiation protection law [2].

- The absolute maxima of the total radiation exposure are determined by the contributions of activation and fission products like C-14, followed by Se-79, I-129 and Cs-135. These maxima occur at early times, between 10^3 and 10^4 years for the first two fission products, and between 10^5 and 10^6 years for the latter, respectively. Much later, between 10^6 and 10^7 years, the radiation exposure is mainly due to nuclides of the 4N+1 chain.

- The geosphere is an important transport barrier for the well-sorbing long-lived actinides and their daughter products and also for some short-lived weakly sorbing fission products, like Sr-90 and Cs-137, and for the well-sorbing actinides having half-

lives below 10^3 years. The release rates for some of these actinides are still increasing after 10^7 years. As a consequence, the maximum radiation exposures from the nuclides of the four decay chains are some orders of magnitude lower than those of the relevant activation and fission products.

4.3 Comparison of results for LWR and CANDU fuel

Due to the earlier release of radionuclides from LWR containers the release rates from the EDZ into the geosphere starts earlier than in the case of CANDU, cf. Figure 4.14. The maxima of the release rates are higher than for CANDU, mainly due to the higher inventories. For Cl-36 no inventory is given for CANDU spent fuel, thus, the corresponding curve is missing.

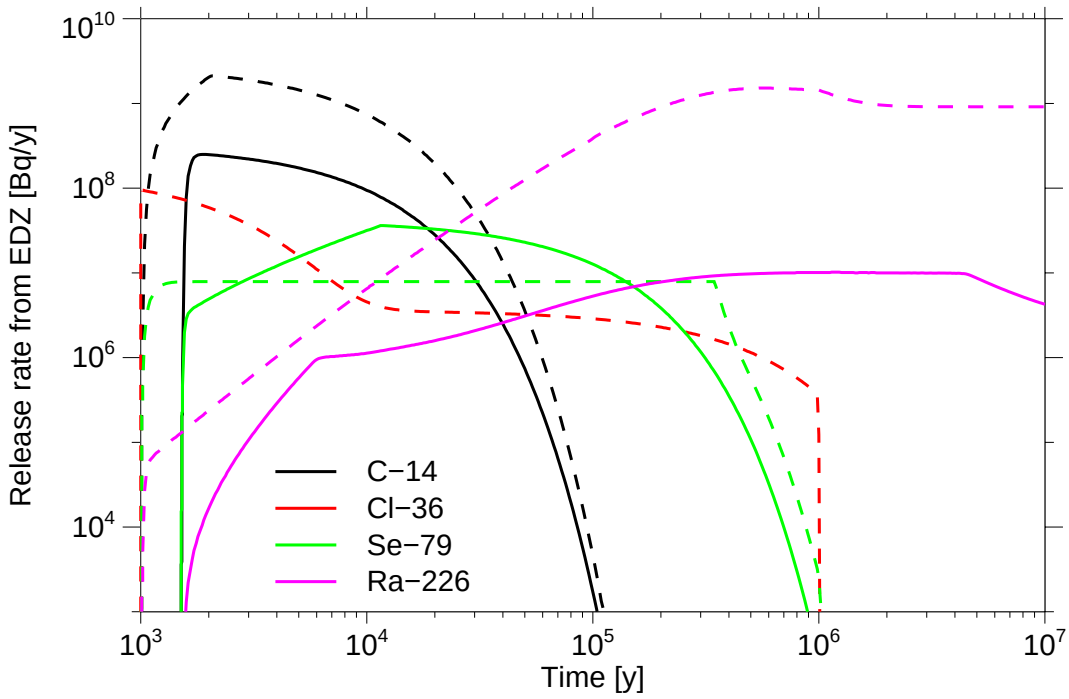

Fig. 4.14 Comparison of release rates into the geosphere for LWR (dashed lines) and CANDU (full lines). Reference case.

The different release behaviour from the near field to the geosphere also influences the radiation exposure in the biosphere. As Figure 4.15 shows, the maxima of the radiation exposures due to decay and activation products are higher in the case of LWR spent fuel, but for actinides the maxima are higher for CANDU spent fuel. This reflects the high amount of Uranium in the CANDU spent fuel compared to LWR spent fuel.

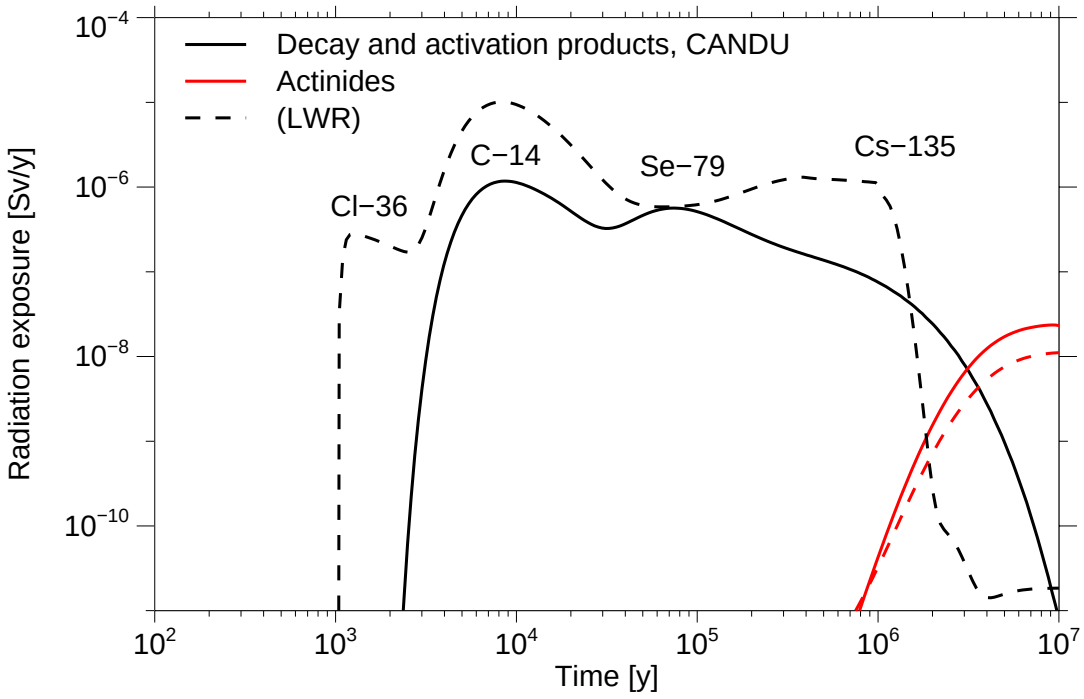

Fig. 4.15 Comparison of radiation exposures for CANDU and LWR spent fuel. Reference case

5 Parameter variations

Parameter variations are performed to investigate the influence of data uncertainties to radiation exposure. In the present study, the procedure applied in [13] is repeated, both for LWR and CANDU spent fuel. Additionally, for the most important parameters combined variations are used to get supplementary information on the impact of parameter uncertainities.

According to the SPIN Report [4], two safety and performance indicators are considered additionally to the radiation exposure: the radiotoxicity and the radiotoxicity flux from compartments. In these investigations, also combined variations of the input parameters are taken into account.

5.1 Single-parameter variations

In this chapter, the impact of one input parameter's value on the maximum total radiation exposure is described. Chapters 5.2 and 5.3 deal with the impacts of many-parameter variations.

5.1.1 LWR spent fuel

The results of single-parameter variations for LWR spent fuel are described in detail in [13], where also the methodology for these variations is discussed. Two groups of varied parameters were used: a set of element-specific parameters and a set of other parameters. In any case, while one parameter was varied, the others were held at the reference values. Figure 5.1 shows the summary of results of these variations. Among the parameters having the highest impact on the maximum radiation exposure are:

- sorption coefficients in bentonite,
- water flow rate through the EDZ,
- bentonite buffer thickness,
- biosphere dilution factor.

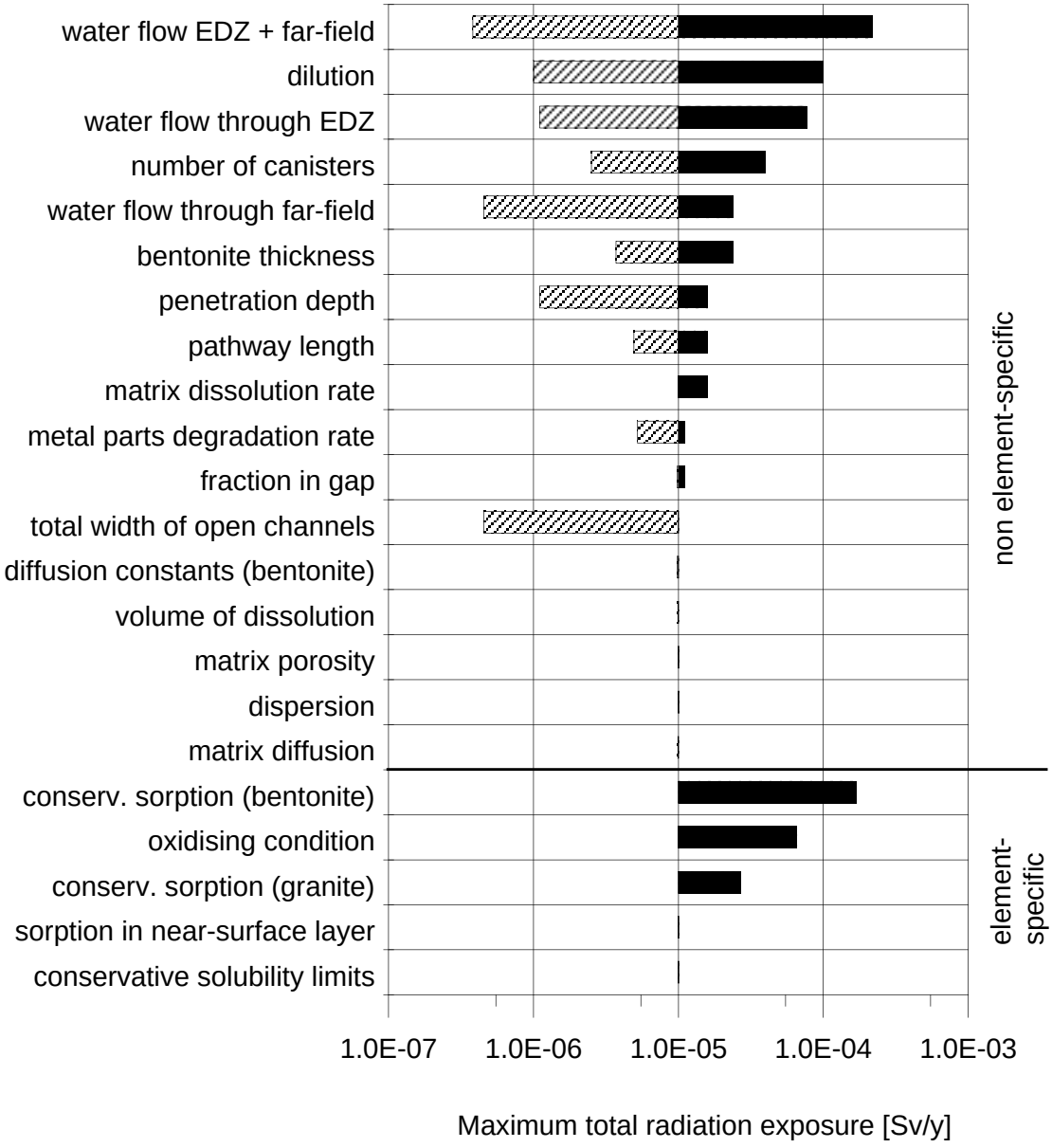

Fig. 5.1 Range of maximum radiation exposures obtained by variation of single model parameters

Four parameters among these, that turn out to be also most sensitive in the case of CAN-DU fuel, are chosen for the many-parameter variations presented in chapters 5.2.1 and 5.2.2. Table 5.1 lists parts of the results in a different representation. The most important radionuclides regarding radiation exposure are, as in the reference case, C-14, Cs-135, and I-129.

Table 5.1: Maximum radiation exposures for single-parameter variations; LWR

Run ID	t_{max} [y]	D_{max} [Sv/y]	1st nuclide	D_{max} [Sv/y]	2nd nuclide	D_{max} [Sv/y]	3rd nuclide	D_{max} [Sv/y]
Ref	$8.2 \cdot 10^{3}$	$1.0 \cdot 10^{-5}$	C-14	$9.6 \cdot 10^{-6}$	Cs-135	$8.1 \cdot 10^{-7}$	I-129	$5.4 \cdot 10^{-7}$
RS-Nbti2	$8.6 \cdot 10^{3}$	$3.7 \cdot 10^{-6}$	C-14	$3.5 \cdot 10^{-6}$	Cs-135	$7.2 \cdot 10^{-7}$	I-129	$4.1 \cdot 10^{-7}$
RS-Nbtd2	$8.2 \cdot 10^{3}$	$2.4 \cdot 10^{-5}$	C-14	$2.3 \cdot 10^{-5}$	I-129	$1.1 \cdot 10^{-6}$	Cs-135	$8.3 \cdot 10^{-7}$
RS-Nfei10	$7.5 \cdot 10^{3}$	$7.7 \cdot 10^{-5}$	C-14	$7.4 \cdot 10^{-5}$	I-129	$2.6 \cdot 10^{-6}$	Cl-36	$1.9 \cdot 10^{-6}$
RS-Nfed10	$8.6 \cdot 10^{3}$	$1.1 \cdot 10^{-6}$	C-14	$9.9 \cdot 10^{-7}$	Cs-135	$4.9 \cdot 10^{-7}$	I-129	$3.7 \cdot 10^{-7}$
RS-Gfri10	$2.9 \cdot 10^{3}$	$2.4 \cdot 10^{-5}$	C-14	$2.3 \cdot 10^{-5}$	Cs-135	$8.9 \cdot 10^{-7}$	Ra-226	$7.1 \cdot 10^{-7}$
RS-Gfrd10	$1.0 \cdot 10^{5}$	$4.5 \cdot 10^{-7}$	I-129	$4.4 \cdot 10^{-7}$	Cs-135	$2.5 \cdot 10^{-7}$	Cl-36	$2.0 \cdot 10^{-7}$
RS-Bdii10	$8.2 \cdot 10^{-3}$	$1.0 \cdot 10^{-6}$	C-14	$9.6 \cdot 10^{-7}$	Cs-135	$8.1 \cdot 10^{-8}$	I-129	$5.4 \cdot 10^{-8}$
RS-Bdid10	$8.2 \cdot 10^{-3}$	$1.0 \cdot 10^{-4}$	C-14	$9.6 \cdot 10^{-5}$	Cs-135	$8.1 \cdot 10^{-6}$	I-129	$5.4 \cdot 10^{-6}$

The times of occurrences of the maxima are omitted for individual nuclides in the table, although the times are sometimes different to the times for the maximum of the total dose. The meaning of the abbreviations is as follows:

- Ref: the LWR or CANDU reference case,
- RS-Nfei10: water flow rate through EDZ increased 10 times,
- RS-Nfed10: water flow rate through EDZ decreased 10 times,
- RS-Nbti2: bentonite thickness increased 2 times,
- RS-Nbtd2: bentonite thickness decreased 2 times,
- RS-Gfri10: water flow rate through the geosphere increased 10 times,
- RS-Gfrd10: water flow rate through the geosphere decreased 10 times,
- RS-Bdii10: biosphere dilution factor increased 10 times,
- RS-Bdid10: biosphere dilution factor decreased 10 times.

5.1.2 CANDU spent fuel

The same parameter variations as for LWR are performed for CANDU spent fuel. The parameters having the highest impact on the maximum radiation exposure are in this order:

- water flow rate through the EDZ,

- bentonite buffer thickness,
- geosphere water flow rate,
- biosphere dilution factor.

The results of these single-parameter variations are compiled in Table 5.2. The most important radionuclides are, as in the reference case, C-14, Se-79, and I-129.

Tab. 5.2 Maximum radiation exposures for 1-parameter variations; CANDU

Run ID	t_{max} [y]	D_{max} [Sv/y]	1st nuclide	D_{max} [Sv/y]	2nd nuclide	D_{max} [Sv/y]	3rd nuclide	D_{max} [Sv/y]
Ref	$8.6 \cdot 10^{+3}$	$1.2 \cdot 10^{-6}$	C- 14	$1.1 \cdot 10^{-6}$	Se- 79	$4.1 \cdot 10^{-7}$	I-129	$1.6 \cdot 10^{-7}$
RS-Nfei10	$8.6 \cdot 10^{+3}$	$1.2 \cdot 10^{-5}$	C- 14	$1.1 \cdot 10^{-5}$	Se- 79	$3.2 \cdot 10^{-6}$	I-129	$1.4 \cdot 10^{-6}$
RS-Nfed10	$8.6 \cdot 10^{+3}$	$1.2 \cdot 10^{-7}$	C- 14	$1.1 \cdot 10^{-7}$	Se- 79	$4.3 \cdot 10^{-8}$	I-129	$1.6 \cdot 10^{-8}$
RS-Nbti2	$9.0 \cdot 10^{+3}$	$4.6 \cdot 10^{-7}$	C- 14	$4.4 \cdot 10^{-7}$	Se- 79	$1.7 \cdot 10^{-7}$	I-129	$6.5 \cdot 10^{-8}$
RS-Nbtd2	$8.6 \cdot 10^{+3}$	$2.7 \cdot 10^{-6}$	C- 14	$2.6 \cdot 10^{-6}$	Se- 79	$8.8 \cdot 10^{-7}$	I-129	$3.4 \cdot 10^{-7}$
RS-Gfri10	$2.9 \cdot 10^{+3}$	$2.8 \cdot 10^{-6}$	C- 14	$2.7 \cdot 10^{-6}$	Se- 79	$9.1 \cdot 10^{-7}$	I-129	$1.6 \cdot 10^{-7}$
RS-Gfrd10	$1.2 \cdot 10^{+5}$	$1.5 \cdot 10^{-7}$	I-129	$1.5 \cdot 10^{-7}$	Cs-135	$1.4 \cdot 10^{-8}$	C- 14	$1.3 \cdot 10^{-8}$
RS-Bdii10	$8.6 \cdot 10^{+3}$	$1.2 \cdot 10^{-7}$	C- 14	$1.1 \cdot 10^{-7}$	Se- 79	$4.1 \cdot 10^{-8}$	I-129	$1.6 \cdot 10^{-8}$
RS-Bdid10	$8.6 \cdot 10^{+3}$	$1.2 \cdot 10^{-5}$	C- 14	$1.1 \cdot 10^{-5}$	Se- 79	$4.1 \cdot 10^{-6}$	I-129	$1.6 \cdot 10^{-6}$

The times of occurrences of the maxima are omitted for individual nuclides in the table, although the times are sometimes different to the times for the maximum of the total dose. The meaning of the abbreviations is as for LWR spent fuel.

In a second step, the most important parameters are varied over the entire range of values. The results are shown in Figures 5.2 to 5.5. The maximum radiation exposure increases, when the bentonite barrier thickness and the dilution are reduced, and when the water flow through the EDZ and through the geosphere are increased.

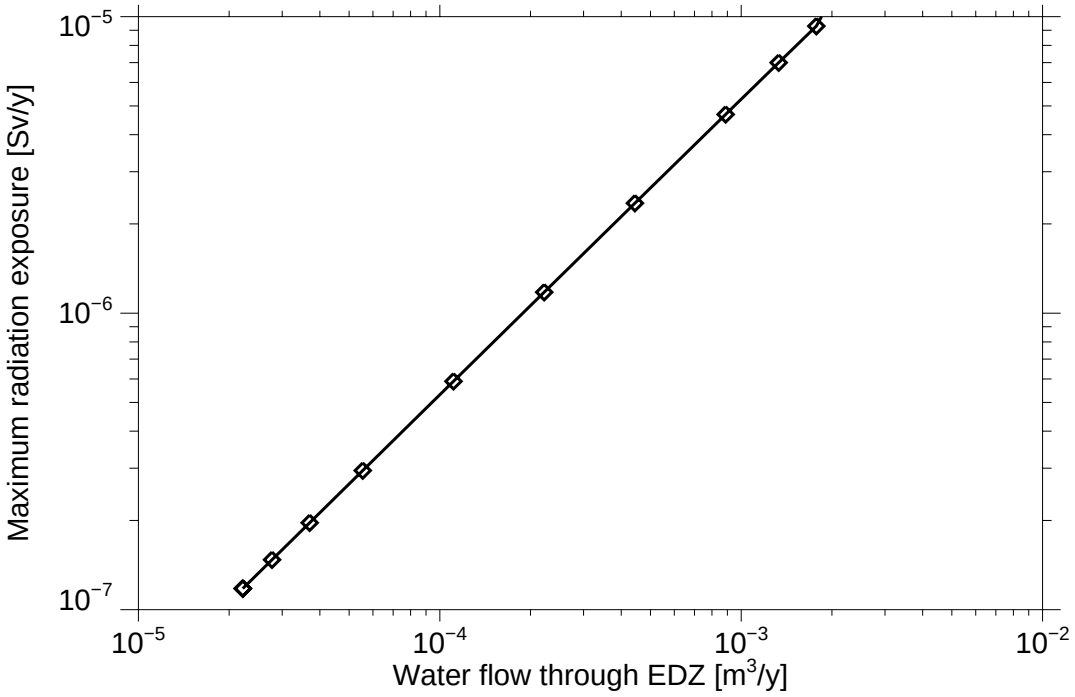

Fig. 5.2 Total radiation exposure as function of water flow rate through EDZ. CANDU

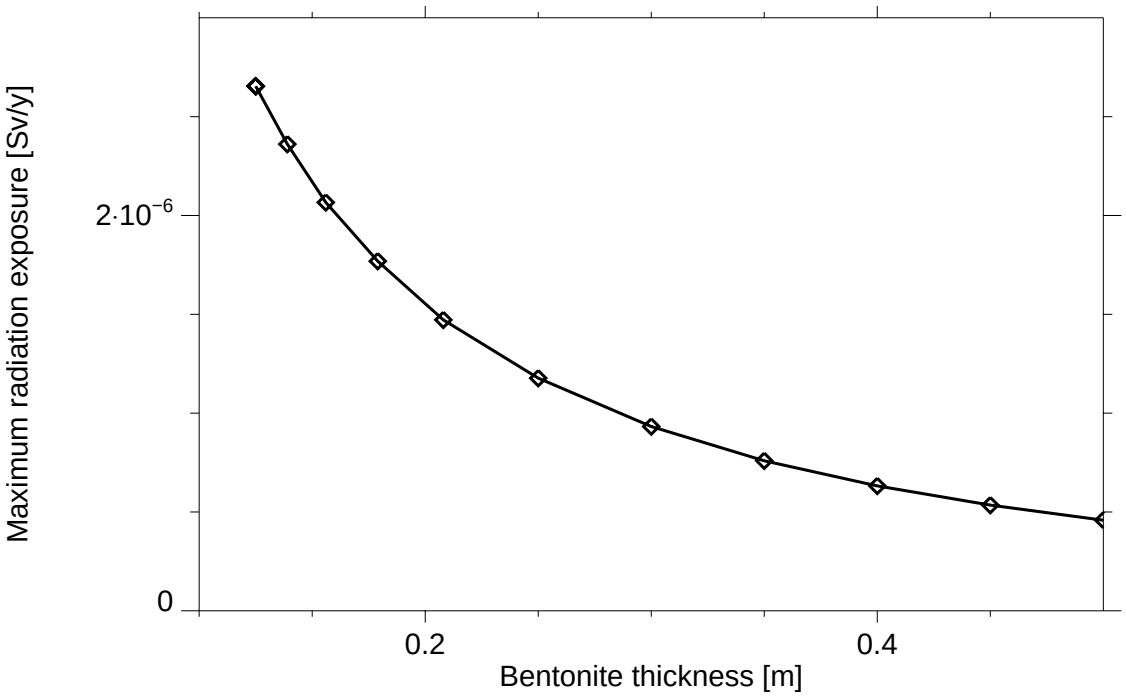

Fig. 5.3 Total radiation exposure as function of bentonite thickness. CANDU

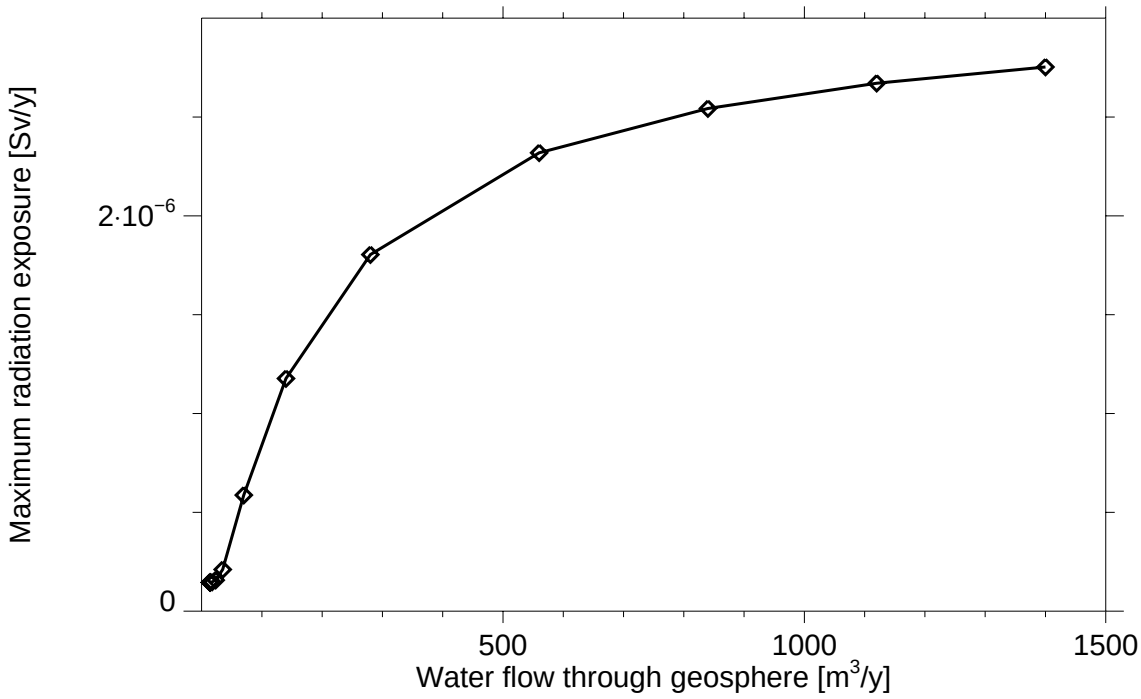

Fig. 5.4 Radiation exposure as function of water flow rate through geosphere. CANDU

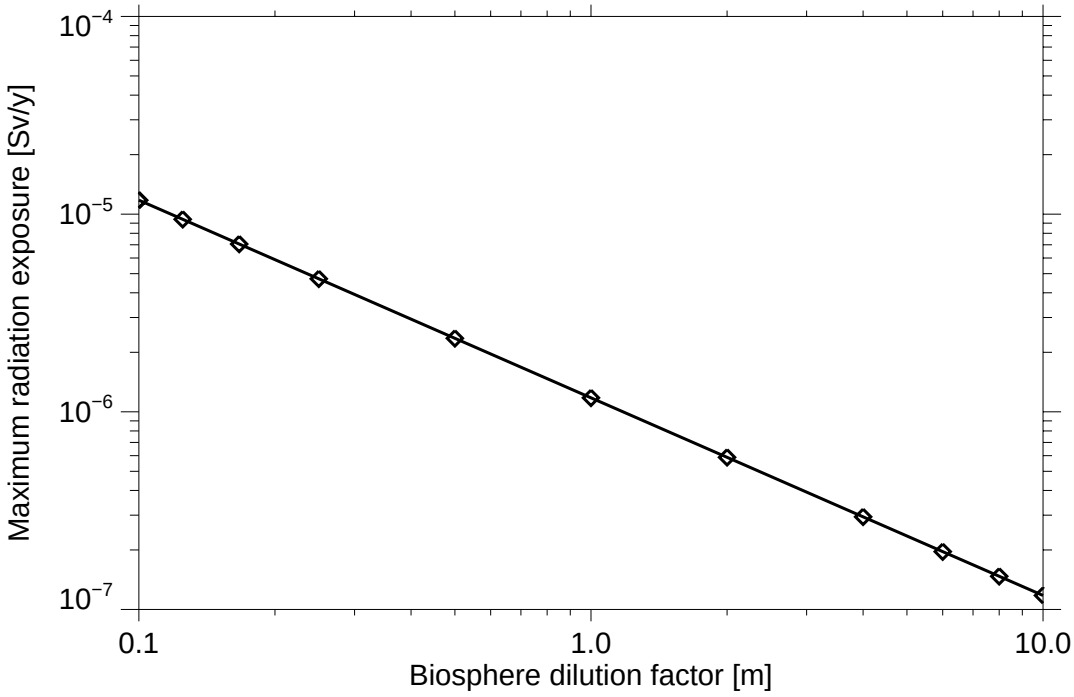

Fig. 5.5 Total radiation exposure as function of biosphere dilution factor. CANDU

In detail, the maximum radiation exposure is reduced compared to the reference case by

- 38 %, if the bentonite thickness is twice the reference value,
- 10 %, if the flow rate in the EDZ is reduced by a factor of 10,
- 10 %, if the dilution factor is increased by a factor of 10,
- 12.5 %, if the flow rate in the geosphere is reduced by a factor of 10.

The maximum radiation exposure increases compared to the reference case by

- 225 %, if the bentonite thickness is half of the reference value,
- 1000 %, if the flow rate in the EDZ is increased by a factor of 10,
- 233 %, if the dilution factor is increased by a factor of 10,
- 233 %, if the flow rate in the geosphere is increased by a factor of 10.

The times when these maxima are attained are not influenced by the parameter values, with one exception: The reduction of the water flow through the geosphere results in a retardation of the maximum, while an increase of the water flow rate results in maxima at earlier times.

5.2 Many-parameter variations

This kind of analysis is used to identify the influence of a combination of the input parameters' uncertainties on the maximum radiation exposure. It is performed for LWR and CANDU spent fuel. In both cases, four parameters are varied simultaneously. Only the upper and lower bounds of the parameter values are used.

Four highly sensitive parameters of those investigated in detail in chapter 5.1 are used to perform the combined sensitivity analysis. Either two or three of these parameters are varied, while the third and/or fourth are held to their reference values, or all the four parameters are varied simultaneously. The indicator for comparison of results is the maximum total radiation exposure and the maximum radiation exposure of the most relevant nuclides.

The four varied parameters are:

- water flow rate through the EDZ,
- bentonite buffer thickness,
- geosphere water flow rate, and
- biosphere dilution factor.

To identify the different runs, the naming scheme in Table 5.3 is used. The run ID is a 4-digits number, calculated by

$$ID = F*1000 + T*100 + G*10 + D, \qquad (5.1)$$

where F, T, G and D take the following values:

0, if the parameter value is the same as in the reference case;
1, if the parameter value is higher than in the reference case;
2, if the parameter value is lower than in the reference case.

For example, the run ID for the water flow rate increased by a factor of 10, the bentonite thickness left as in the reference case, the water flow rate through the geosphere left as in the reference case, and the biosphere dilution factor decreased by a factor of 10 is D=1002.

Tab. 5.3 Naming scheme for run IDs

Parameter ID	Parameter description
F	water **F**low rate through EDZ (increased/decreased by a factor of 10)
T	bentonite **T**hickness (increased/decreased by a factor of 2)
G	water flow through **G**eosphere (increased/decreased by a factor of 10)
D	biosphere **D**ilution factor (increased/decreased by a factor of 10)

5.2.1 LWR spent fuel

Table 5.4 lists the calculated maximum radiation exposures for those combinations of input parameter values, which lead to a maximum value differing from the reference case by a factor of 10 or more.

Tab. 5.4 Maximum radiation exposures for many-parameter variations; LWR

Run ID	t_{max} [y]	D_{max} [Sv/y]	1st nuclide	D_{max} [Sv/y]	2nd nuclide	D_{max} [Sv/y]	3rd nuclide	D_{max} [Sv/y]
0000	$8.24 \cdot 10^{+3}$	$1.0 \cdot 10^{-5}$	C-14	$9.7 \cdot 10^{-6}$	Cs-135	$8.1 \cdot 10^{-7}$	I-129	$5.4 \cdot 10^{-7}$
1212	$2.74 \cdot 10^{+3}$	$3.5 \cdot 10^{-3}$	C- 14	$3.4 \cdot 10^{-3}$	Ra-226	$8.3 \cdot 10^{-5}$	I-129	$7.4 \cdot 10^{-5}$
1012	$2.74 \cdot 10^{+3}$	$2.1 \cdot 10^{-3}$	C- 14	$2.1 \cdot 10^{-3}$	Ra-226	$5.6 \cdot 10^{-5}$	I-129	$4.7 \cdot 10^{-5}$
1202	$7.18 \cdot 10^{+3}$	$1.2 \cdot 10^{-3}$	C- 14	$1.1 \cdot 10^{-3}$	I-129	$3.4 \cdot 10^{-5}$	Cl- 36	$2.6 \cdot 10^{-5}$
1112	$3.01 \cdot 10^{+3}$	$1.1 \cdot 10^{-3}$	C- 14	$1.0 \cdot 10^{-3}$	Ra-226	$2.6 \cdot 10^{-5}$	I-129	$2.4 \cdot 10^{-5}$
1002	$7.52 \cdot 10^{+3}$	$7.8 \cdot 10^{-4}$	C- 14	$7.5 \cdot 10^{-4}$	I-129	$2.6 \cdot 10^{-5}$	Cl- 36	$1.9 \cdot 10^{-5}$
0212	$2.87 \cdot 10^{+3}$	$4.2 \cdot 10^{-4}$	C- 14	$4.1 \cdot 10^{-4}$	Ra-226	$1.1 \cdot 10^{-5}$	Cs-135	$1.0 \cdot 10^{-5}$
1102	$7.87 \cdot 10^{+3}$	$4.1 \cdot 10^{-4}$	C- 14	$4.0 \cdot 10^{-4}$	I-129	$1.7 \cdot 10^{-5}$	Se- 79	$1.2 \cdot 10^{-5}$
1210	$2.74 \cdot 10^{+3}$	$3.5 \cdot 10^{-4}$	C- 14	$3.4 \cdot 10^{-4}$	Ra-226	$8.3 \cdot 10^{-6}$	I-129	$7.4 \cdot 10^{-6}$
0012	$3.01 \cdot 10^{+3}$	$2.4 \cdot 10^{-4}$	C- 14	$2.3 \cdot 10^{-4}$	Cs-135	$8.9 \cdot 10^{-6}$	Ra-226	$6.6 \cdot 10^{-6}$
1010	$2.74 \cdot 10^{+3}$	$2.1 \cdot 10^{-4}$	C- 14	$2.1 \cdot 10^{-4}$	Ra-226	$5.6 \cdot 10^{-6}$	I-129	$4.7 \cdot 10^{-6}$
0202	$8.24 \cdot 10^{+3}$	$1.7 \cdot 10^{-4}$	C- 14	$1.7 \cdot 10^{-4}$	I-129	$8.4 \cdot 10^{-6}$	Cs-135	$8.3 \cdot 10^{-6}$
1200	$7.18 \cdot 10^{+3}$	$1.2 \cdot 10^{-4}$	C- 14	$1.1 \cdot 10^{-4}$	I-129	$3.4 \cdot 10^{-6}$	Cl- 36	$2.6 \cdot 10^{-6}$
0112	$3.01 \cdot 10^{+3}$	$1.1 \cdot 10^{-4}$	C- 14	$1.1 \cdot 10^{-4}$	Cs-135	$8.1 \cdot 10^{-6}$	I-129	$4.1 \cdot 10^{-6}$
1110	$3.01 \cdot 10^{+3}$	$1.1 \cdot 10^{-4}$	C- 14	$1.0 \cdot 10^{-4}$	Ra-226	$2.6 \cdot 10^{-6}$	I-129	$2.4 \cdot 10^{-6}$
0002	$8.24 \cdot 10^{+3}$	$1.0 \cdot 10^{-4}$	C- 14	$9.7 \cdot 10^{-5}$	Cs-135	$8.1 \cdot 10^{-6}$	I-129	$5.4 \cdot 10^{-6}$
0000	$8.24 \cdot 10^{+3}$	$1.0 \cdot 10^{-5}$	C- 14	$9.7 \cdot 10^{-6}$	Cs-135	$8.1 \cdot 10^{-7}$	I-129	$5.4 \cdot 10^{-7}$
0001	$8.24 \cdot 10^{+3}$	$1.0 \cdot 10^{-6}$	C- 14	$9.7 \cdot 10^{-7}$	Cs-135	$8.1 \cdot 10^{-8}$	I-129	$5.4 \cdot 10^{-8}$
1020	$3.26 \cdot 10^{+4}$	$9.8 \cdot 10^{-7}$	C- 14	$6.3 \cdot 10^{-7}$	I-129	$6.2 \cdot 10^{-7}$	Cl- 36	$6.0 \cdot 10^{-7}$
1120	$3.91 \cdot 10^{+4}$	$7.1 \cdot 10^{-7}$	I-129	$6.0 \cdot 10^{-7}$	Cl- 36	$4.9 \cdot 10^{-7}$	C- 14	$3.8 \cdot 10^{-7}$
2100	$1.01 \cdot 10^{+6}$	$5.8 \cdot 10^{-7}$	C- 14	$4.6 \cdot 10^{-7}$	Cs-135	$3.1 \cdot 10^{-7}$	I-129	$2.9 \cdot 10^{-7}$
0220	$7.44 \cdot 10^{+4}$	$5.2 \cdot 10^{-7}$	I-129	$5.1 \cdot 10^{-7}$	Cl- 36	$2.7 \cdot 10^{-7}$	Cs-135	$2.5 \cdot 10^{-7}$
0101	$8.62 \cdot 10^{+3}$	$4.8 \cdot 10^{-7}$	C- 14	$4.6 \cdot 10^{-7}$	Cs-135	$7.5 \cdot 10^{-8}$	I-129	$4.1 \cdot 10^{-8}$
0020	$1.03 \cdot 10^{+5}$	$4.5 \cdot 10^{-7}$	I-129	$4.4 \cdot 10^{-7}$	Cs-135	$2.5 \cdot 10^{-7}$	Cl- 36	$2.0 \cdot 10^{-7}$
0120	$1.01 \cdot 10^{+6}$	$4.3 \cdot 10^{-7}$	I-129	$4.1 \cdot 10^{-7}$	Cs-135	$2.4 \cdot 10^{-7}$	Cl- 36	$1.2 \cdot 10^{-7}$

Tab. 5.4 Maximum radiation exposures for many-parameter variations; LWR

Run ID	t_{max} [y]	D_{max} [Sv/y]	1st nuclide	D_{max} [Sv/y]	2nd nuclide	D_{max} [Sv/y]	3rd nuclide	D_{max} [Sv/y]
2211	$2.87 \cdot 10^{+3}$	$4.3 \cdot 10^{-7}$	C- 14	$4.1 \cdot 10^{-7}$	Cs-135	$6.6 \cdot 10^{-8}$	I-129	$4.0 \cdot 10^{-8}$
2220	$1.01 \cdot 10^{+6}$	$4.1 \cdot 10^{-7}$	I-129	$3.9 \cdot 10^{-7}$	Cs-135	$2.0 \cdot 10^{-7}$	Cl- 36	$4.4 \cdot 10^{-8}$
2020	$1.01 \cdot 10^{+6}$	$3.8 \cdot 10^{-7}$	I-129	$3.7 \cdot 10^{-7}$	Cs-135	$1.7 \cdot 10^{-7}$	Cl- 36	$2.9 \cdot 10^{-8}$
2120	$1.06 \cdot 10^{+6}$	$2.9 \cdot 10^{-7}$	I-129	$2.8 \cdot 10^{-7}$	Cs-135	$1.1 \cdot 10^{-7}$	Cl- 36	$1.5 \cdot 10^{-8}$
2011	$3.01 \cdot 10^{+3}$	$2.5 \cdot 10^{-7}$	C- 14	$2.4 \cdot 10^{-7}$	Cs-135	$5.4 \cdot 10^{-8}$	I-129	$3.7 \cdot 10^{-8}$
2201	$8.24 \cdot 10^{+3}$	$1.9 \cdot 10^{-7}$	C- 14	$1.7 \cdot 10^{-7}$	Cs-135	$6.2 \cdot 10^{-8}$	I-129	$4.0 \cdot 10^{-8}$
1221	$3.11 \cdot 10^{+4}$	$1.2 \cdot 10^{-7}$	C- 14	$8.3 \cdot 10^{-8}$	Cl- 36	$6.6 \cdot 10^{-8}$	I-129	$6.3 \cdot 10^{-8}$
2111	$3.15 \cdot 10^{+3}$	$1.1 \cdot 10^{-7}$	C- 14	$1.1 \cdot 10^{-7}$	Cs-135	$3.4 \cdot 10^{-8}$	I-129	$2.9 \cdot 10^{-8}$
2001	$8.62 \cdot 10^{+3}$	$1.1 \cdot 10^{-7}$	C- 14	$9.9 \cdot 10^{-8}$	Cs-135	$5.0 \cdot 10^{-8}$	I-129	$3.7 \cdot 10^{-8}$
1021	$3.26 \cdot 10^{+4}$	$9.8 \cdot 10^{-8}$	C- 14	$6.3 \cdot 10^{-8}$	I-129	$6.2 \cdot 10^{-8}$	Cl- 36	$6.0 \cdot 10^{-8}$
1121	$3.91 \cdot 10^{+4}$	$7.1 \cdot 10^{-8}$	I-129	$6.0 \cdot 10^{-8}$	Cl- 36	$4.9 \cdot 10^{-8}$	C- 14	$3.8 \cdot 10^{-8}$
2101	$1.01 \cdot 10^{+6}$	$5.8 \cdot 10^{-8}$	C- 14	$4.6 \cdot 10^{-8}$	Cs-135	$3.1 \cdot 10^{-8}$	I-129	$2.9 \cdot 10^{-8}$
0221	$7.44 \cdot 10^{+4}$	$5.2 \cdot 10^{-8}$	I-129	$5.1 \cdot 10^{-8}$	Cl- 36	$2.7 \cdot 10^{-8}$	Cs-135	$2.5 \cdot 10^{-8}$
0021	$1.03 \cdot 10^{+5}$	$4.5 \cdot 10^{-8}$	I-129	$4.4 \cdot 10^{-8}$	Cs-135	$2.5 \cdot 10^{-8}$	Cl- 36	$2.0 \cdot 10^{-8}$
0121	$1.01 \cdot 10^{+6}$	$4.3 \cdot 10^{-8}$	I-129	$4.1 \cdot 10^{-8}$	Cs-135	$2.4 \cdot 10^{-8}$	Cl- 36	$1.2 \cdot 10^{-8}$
2221	$1.01 \cdot 10^{+6}$	$4.1 \cdot 10^{-8}$	I-129	$3.9 \cdot 10^{-8}$	Cs-135	$2.0 \cdot 10^{-8}$	Cl- 36	$4.4 \cdot 10^{-9}$
2021	$1.01 \cdot 10^{+6}$	$3.8 \cdot 10^{-8}$	I-129	$3.7 \cdot 10^{-8}$	Cs-135	$1.7 \cdot 10^{-8}$	Cl- 36	$2.9 \cdot 10^{-9}$
2121	$1.06 \cdot 10^{+6}$	$2.9 \cdot 10^{-8}$	I-129	$2.8 \cdot 10^{-8}$	Cs-135	$1.1 \cdot 10^{-8}$	Cl- 36	$1.5 \cdot 10^{-9}$

The combination of parameter values leading to the highest effect is

- increase of the water flow rate through the EDZ by a factor of 10,
- reduction of the bentonite thickness by a factor of 2,
- increase of the geosphere water flow rate by a factor of 10, and
- decrease of the biosphere dilution factor by 10.

In this case, the maximum radiation exposure increases by a factor of about 350 compared to the reference value.

The combination of parameter values leading to the minumum effect is

- decrease of the water flow rate through the EDZ by a factor of 10,

- increase of the bentonite thickness by a factor of 2,
- decrease of the geosphere water flow rate by a factor of 10, and
- increase of the biosphere dilution factor by 10.

In this case, the maximum radiation exposure decreases by a factor of about 340.

The most important radionuclide concerning radiation exposure in these variations is C-14, which contributes to the maximum total radiation exposure by more than 40 % in all cases. The next important radionuclides are Cs-135, Ra-226, Cl-36, and I-129, respectively.

5.2.2 CANDU spent fuel

Table 5.5 lists the results for those combinations of input parameter values, which lead to a maximum radiation exposure differing from the reference case by a factor of 10 or more.

Tab. 5.5 Maximum radiation exposures for many-parameter variations; CANDU

Run ID	t_{max} [y]	D_{max} [Sv/y]	1st nuclide	D_{max} [Sv/y]	2nd nuclide	D_{max} [Sv/y]	3rd nuclide	D_{max} [Sv/y]
0000	$8.6\cdot10^{+3}$	$1.2\cdot10^{-6}$	C- 14	$1.1\cdot10^{-6}$	Se- 79	$4.1\cdot10^{-7}$	I-129	$1.6\cdot10^{-7}$
1212	$2.7\cdot10^{+3}$	$6.2\cdot10^{-4}$	C- 14	$6.1\cdot10^{-4}$	Se- 79	$1.6\cdot10^{-4}$	I-129	$3.0\cdot10^{-5}$
1012	$2.9\cdot10^{+3}$	$2.7\cdot10^{-4}$	C- 14	$2.7\cdot10^{-4}$	Se- 79	$8.3\cdot10^{-5}$	I-129	$1.5\cdot10^{-5}$
1202	$8.2\cdot10^{+3}$	$2.6\cdot10^{-4}$	C- 14	$2.5\cdot10^{-4}$	Se- 79	$5.5\cdot10^{-5}$	I-129	$2.8\cdot10^{-5}$
1002	$8.6\cdot10^{+3}$	$1.2\cdot10^{-4}$	C- 14	$1.1\cdot10^{-4}$	Se- 79	$3.2\cdot10^{-5}$	I-129	$1.4\cdot10^{-5}$
1112	$3.4\cdot10^{+3}$	$1.0\cdot10^{-4}$	C- 14	$1.0\cdot10^{-4}$	Se- 79	$3.6\cdot10^{-5}$	I-129	$6.4\cdot10^{-6}$
0212	$2.9\cdot10^{+3}$	$6.2\cdot10^{-5}$	C- 14	$6.2\cdot10^{-5}$	Se- 79	$2.0\cdot10^{-5}$	I-129	$3.5\cdot10^{-6}$
1210	$2.7\cdot10^{+3}$	$6.2\cdot10^{-5}$	C- 14	$6.1\cdot10^{-5}$	Se- 79	$1.6\cdot10^{-5}$	I-129	$3.0\cdot10^{-6}$
1102	$9.0\cdot10^{+3}$	$4.5\cdot10^{-5}$	C- 14	$4.4\cdot10^{-5}$	Se- 79	$1.5\cdot10^{-5}$	I-129	$6.2\cdot10^{-6}$
0012	$2.9\cdot10^{+3}$	$2.8\cdot10^{-5}$	C- 14	$2.7\cdot10^{-5}$	Se- 79	$9.1\cdot10^{-6}$	I-129	$1.6\cdot10^{-6}$
1010	$2.9\cdot10^{+3}$	$2.7\cdot10^{-5}$	C- 14	$2.7\cdot10^{-5}$	Se- 79	$8.3\cdot10^{-6}$	I-129	$1.5\cdot10^{-6}$
0202	$8.6\cdot10^{+3}$	$2.7\cdot10^{-5}$	C- 14	$2.6\cdot10^{-5}$	Se- 79	$8.8\cdot10^{-6}$	I-129	$3.4\cdot10^{-6}$
1200	$8.2\cdot10^{+3}$	$2.6\cdot10^{-5}$	C- 14	$2.5\cdot10^{-5}$	Se- 79	$5.5\cdot10^{-6}$	I-129	$2.8\cdot10^{-6}$
1222	$6.8\cdot10^{+4}$	$1.5\cdot10^{-5}$	I-129	$1.5\cdot10^{-5}$	C- 14	$2.6\cdot10^{-6}$	Se- 79	$5.5\cdot10^{-7}$

Tab. 5.5 Maximum radiation exposures for many-parameter variations; CANDU

Run ID	t_{max} [y]	D_{max} [Sv/y]	1st nuclide	D_{max} [Sv/y]	2nd nuclide	D_{max} [Sv/y]	3rd nuclide	D_{max} [Sv/y]
0002	$8.6 \cdot 10^{+3}$	$1.2 \cdot 10^{-5}$	C- 14	$1.1 \cdot 10^{-5}$	Se- 79	$4.1 \cdot 10^{-6}$	I-129	$1.6 \cdot 10^{-6}$
2000	$8.6 \cdot 10^{+3}$	$1.2 \cdot 10^{-7}$	C- 14	$1.1 \cdot 10^{-7}$	Se- 79	$4.3 \cdot 10^{-8}$	I-129	$1.6 \cdot 10^{-8}$
0001	$8.6 \cdot 10^{+3}$	$1.2 \cdot 10^{-7}$	C- 14	$1.1 \cdot 10^{-7}$	Se- 79	$4.1 \cdot 10^{-8}$	I-129	$1.6 \cdot 10^{-8}$
2110	$3.4 \cdot 10^{+3}$	$1.1 \cdot 10^{-7}$	C- 14	$1.0 \cdot 10^{-7}$	Se- 79	$3.8 \cdot 10^{-8}$	I-129	$6.6 \cdot 10^{-9}$
0111	$3.4 \cdot 10^{+3}$	$1.0 \cdot 10^{-7}$	C- 14	$1.0 \cdot 10^{-7}$	Se- 79	$3.7 \cdot 10^{-8}$	I-129	$6.6 \cdot 10^{-9}$
1021	$8.2 \cdot 10^{+4}$	$9.5 \cdot 10^{-8}$	I-129	$9.5 \cdot 10^{-8}$	C- 14	$1.2 \cdot 10^{-8}$	Se- 79	$3.9 \cdot 10^{-9}$
2122	$3.2 \cdot 10^{+5}$	$6.7 \cdot 10^{-8}$	I-129	$6.5 \cdot 10^{-8}$	Cs-135	$9.0 \cdot 10^{-9}$	C- 14	$4.9 \cdot 10^{-9}$
0120	$1.4 \cdot 10^{+5}$	$6.2 \cdot 10^{-8}$	I-129	$6.2 \cdot 10^{-8}$	Cs-135	$7.3 \cdot 10^{-9}$	C- 14	$4.9 \cdot 10^{-9}$
2211	$2.9 \cdot 10^{+3}$	$6.2 \cdot 10^{-8}$	C- 14	$6.2 \cdot 10^{-8}$	Se- 79	$2.0 \cdot 10^{-8}$	I-129	$3.5 \cdot 10^{-9}$
1121	$9.4 \cdot 10^{+4}$	$4.9 \cdot 10^{-8}$	I-129	$4.9 \cdot 10^{-8}$	C- 14	$4.8 \cdot 10^{-9}$	Cs-135	$2.6 \cdot 10^{-9}$
2100	$9.0 \cdot 10^{+3}$	$4.6 \cdot 10^{-8}$	C- 14	$4.4 \cdot 10^{-8}$	Se- 79	$1.7 \cdot 10^{-8}$	I-129	$6.6 \cdot 10^{-9}$
0101	$9.0 \cdot 10^{+3}$	$4.6 \cdot 10^{-8}$	C- 14	$4.4 \cdot 10^{-8}$	Se- 79	$1.7 \cdot 10^{-8}$	I-129	$6.5 \cdot 10^{-9}$
2220	$2.4 \cdot 10^{+5}$	$3.5 \cdot 10^{-8}$	I-129	$3.4 \cdot 10^{-8}$	Cs-135	$4.5 \cdot 10^{-9}$	C- 14	$2.8 \cdot 10^{-9}$
0221	$1.1 \cdot 10^{+5}$	$2.9 \cdot 10^{-8}$	I-129	$2.9 \cdot 10^{-8}$	C- 14	$2.8 \cdot 10^{-9}$	Cs-135	$2.2 \cdot 10^{-9}$
2011	$2.9 \cdot 10^{+3}$	$2.8 \cdot 10^{-8}$	C- 14	$2.7 \cdot 10^{-8}$	Se- 79	$9.2 \cdot 10^{-9}$	I-129	$1.6 \cdot 10^{-9}$
2201	$8.6 \cdot 10^{+3}$	$2.7 \cdot 10^{-8}$	C- 14	$2.6 \cdot 10^{-8}$	Se- 79	$9.3 \cdot 10^{-9}$	I-129	$3.5 \cdot 10^{-9}$
2020	$2.8 \cdot 10^{+5}$	$1.6 \cdot 10^{-8}$	I-129	$1.6 \cdot 10^{-8}$	Cs-135	$2.1 \cdot 10^{-9}$	C- 14	$1.3 \cdot 10^{-9}$
0021	$1.2 \cdot 10^{+5}$	$1.5 \cdot 10^{-8}$	I-129	$1.5 \cdot 10^{-8}$	Cs-135	$1.4 \cdot 10^{-9}$	C- 14	$1.3 \cdot 10^{-9}$
2001	$8.6 \cdot 10^{+3}$	$1.2 \cdot 10^{-8}$	C- 14	$1.1 \cdot 10^{-8}$	Se- 79	$4.3 \cdot 10^{-9}$	I-129	$1.6 \cdot 10^{-9}$
2111	$3.4 \cdot 10^{+3}$	$1.1 \cdot 10^{-8}$	C- 14	$1.0 \cdot 10^{-8}$	Se- 79	$3.8 \cdot 10^{-9}$	I-129	$6.6 \cdot 10^{-10}$
2120	$3.2 \cdot 10^{+5}$	$6.7 \cdot 10^{-9}$	I-129	$6.5 \cdot 10^{-9}$	Cs-135	$9.0 \cdot 10^{-10}$	C- 14	$4.9 \cdot 10^{-10}$
0121	$1.4 \cdot 10^{+5}$	$6.2 \cdot 10^{-9}$	I-129	$6.2 \cdot 10^{-9}$	Cs-135	$7.3 \cdot 10^{-10}$	C- 14	$4.9 \cdot 10^{-10}$
2101	$9.0 \cdot 10^{+3}$	$4.6 \cdot 10^{-9}$	C- 14	$4.4 \cdot 10^{-9}$	Se- 79	$1.7 \cdot 10^{-9}$	I-129	$6.6 \cdot 10^{-10}$
2221	$2.4 \cdot 10^{+5}$	$3.5 \cdot 10^{-9}$	I-129	$3.4 \cdot 10^{-9}$	Cs-135	$4.5 \cdot 10^{-10}$	C- 14	$2.8 \cdot 10^{-10}$
2021	$2.8 \cdot 10^{+5}$	$1.6 \cdot 10^{-9}$	I-129	$1.6 \cdot 10^{-9}$	Cs-135	$2.1 \cdot 10^{-10}$	C- 14	$1.3 \cdot 10^{-10}$
2121	$3.2 \cdot 10^{+5}$	$6.7 \cdot 10^{-10}$	I-129	$6.5 \cdot 10^{-10}$	Cs-135	$9.0 \cdot 10^{-11}$	C- 14	$4.9 \cdot 10^{-11}$

The combination of parameter values leading to the maximum effect is the same as in the case of LWR spent fuel:

- increase of the water flow rate through the EDZ by a factor of 10,
- reduction of the bentonite thickness by a factor of 2,

- increase of the geosphere water flow rate by a factor of 10, and
- decrease of the biosphere dilution factor by 10.

In this case, the maximum radiation exposure increases by a factor of about 600 compared to the reference value.

The combination of parameter values leading to the minimum effect is again the same as in the case of LWR spent fuel:

- decrease of the water flow rate through the EDZ by a factor of 10,
- increase of the bentonite thickness by a factor of 2,
- decrease of the geosphere water flow rate by a factor of 10, and
- increase of the biosphere dilution factor by 10.

In this case, the maximum radiation exposure decreases by a factor of about 1500.

The most important radionuclides concerning radiation exposure in these variations are C-14 and I-129. The next important radionuclides are Se-79 and Cs-135, respectively.

5.3 Other indicators

Recent developments in performance assessments for repositories with radioactive wastes aim towards different indicators for the long-term safety. In the following, suggestions of the EU project SPIN [4] regarding safety and performance indicators are applied to the actual project. The following indicators are considered:

- safety indicator: radiotoxicity flux (release) from the geosphere.
- performance indicator: radiotoxicity flux (release) from the EDZ.

The calculations are performed only for CANDU spent fuel, but also taking into account 4-parameter variations. The radiotoxicity flux from the waste forms was also considered, but no effect to the radiation exposure with regards to the four input parameters was observed. The radiotoxicity is calculated applying the ingestion dose coefficients given in Table 3.9.

5.3.1 Radiotoxicity flux from the geosphere

In the reference case, this safety indicator takes its maximum value of about 0.4 Sv/y after about 50 000 years from the beginning of the scenario. Both the maximum value and the corresponding time of occurrence are influenced by the four sensitive parameters discussed above (water flow through the EDZ, bentonite buffer thickness, flow rate of geosphere water and biosphere dilution factor): If all the parameters are decreased by the known factors (10, 2, 10, 10), i.e. run ID: 2222, the maximum radiotoxicity flux occurs about 70 000 years later than in the reference case and the maximum value is decreased to about 0.08 Sv/y. If all the parameters are increased, i.e. run ID: 1111, the maximum radiotoxicity flux occurs about 35 000 years earlier than in the reference case and the maximum value is increased to about 2 Sv/y.

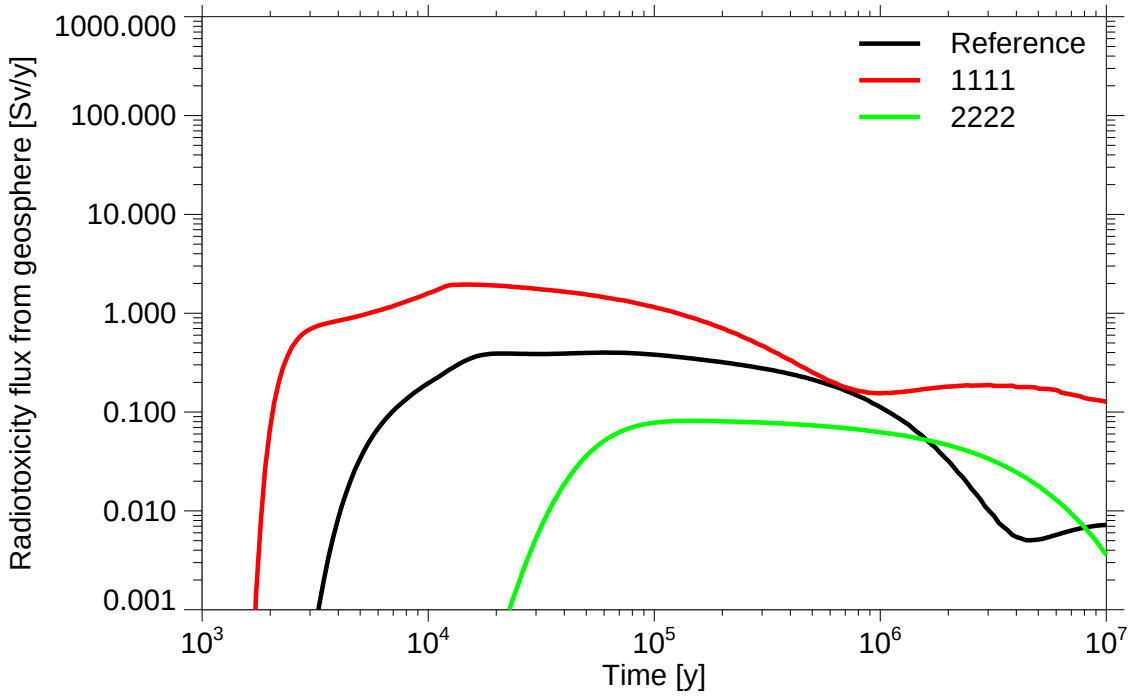

Fig. 5.6 Radiotoxicity release from geosphere (4-parameter variation)

5.3.2 Radiotoxicity flux from the EDZ

In the reference case, this performance indicator reaches its maximum value of about 22 Sv/y after about $1.2 \cdot 10^{+6}$ years from the beginning of the scenario. If all the parameter values are decreased, i.e. run ID: 2222, the maximum flux occurs at about the same time

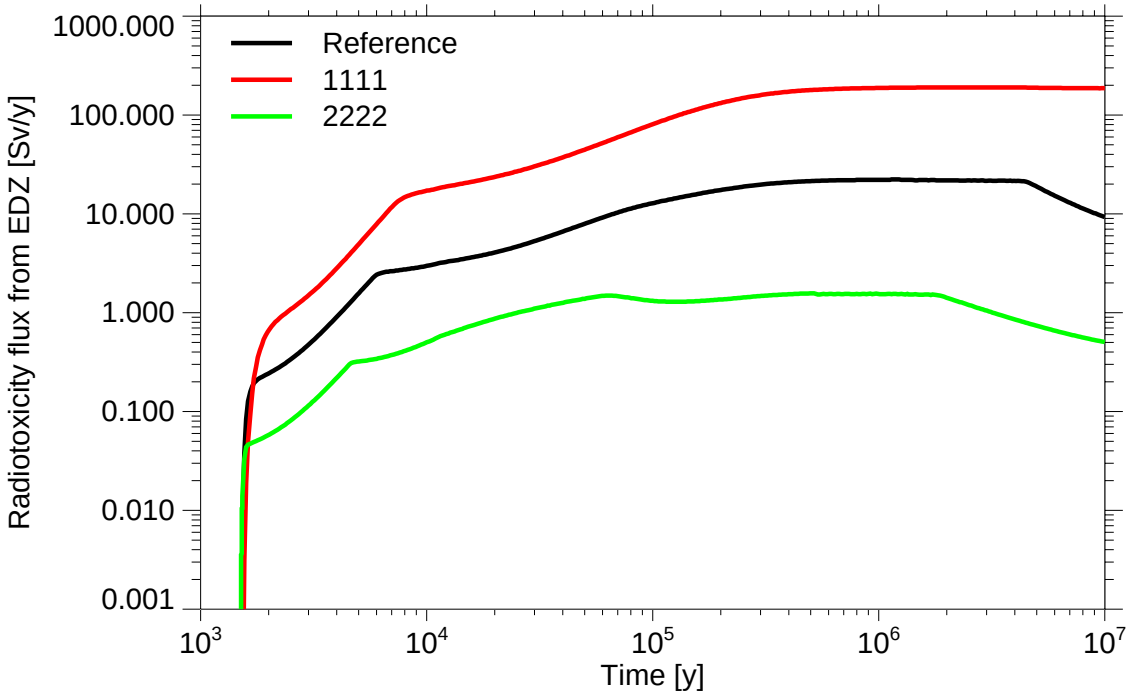

Fig. 5.7 Radiotoxicity release from EDZ (4-parameter variation)

as in the reference case, but the maximum value is decreased to about 1.5 Sv/y. If all the parameters are increased, i.e. run ID: 1111, the maximum flux again occurs at about the same time as in the reference case, but the maximum value is increased to about 190 Sv/y.

5.4 Conclusions from parameter variations

Parameter variations have been used to identify sensitive parameters regarding radiation exposure. Among the most sensitive parameters are for both fuel types:

- the water flow rate through the EDZ,
- the bentonite buffer thickness,
- the flow rate of geosphere water,
- and the biosphere dilution factor.

If these parameters are varied separately over the specified range, the calculated maximum radiation exposures change by about one order of magnitude.

If the parameter values are varied simultaneously, the changes in the radiation exposures are more than one order of magnitude. These investigations give additional information about the relevance of parameter uncertainties. E.g. they can be used to identify ’worst’ cases and ’best’ cases of parameter values, to give an impression of the possible range of radiation exposures.

6 Conclusions

A long-term safety analysis for a repository in hard rock has been performed for both types of spent fuel, CANDU or LWR. The investigations were based on previous results for LWR spent fuel. All the results for CANDU spent fuel are presented here for the first time. For LWR spent fuel, the results of many-parameter variations are presented for the first time.

The main differences in the parameter values for CANDU and LWR spent fuel are the initial inventories, the number of waste containers, and the geometrical dimensions of the near field. While the inventory of CANDU spent fuel is higher than for LWR, the geometrical dimensions of the waste packages are smaller. This results in a smaller flow rate of groundwater in the surroundig EDZ of a CANDU disposal borehole.

In the reference case, the total radiation exposure is higher for LWR spent fuel than for CANDU. This is mainly due to the very low groundwater flow rate in the case of CANDU.

Two kinds of parameter variations have been performed, single-parameter variations and many-parameter variations. In the single-parameter variations the most sensitive parameters turned out to be the water flow rates through the EDZ and through the geosphere, the dilution factor in the biosphere, and the bentonite buffer thickness. The sorption coefficients in bentonite are the most important element-specific parameters. For LWR spent fuel, the most important radionuclides regarding radiation exposure are C-14, Cs-135, and I-129, while for CANDU spent fuel C-14, Se-79, and I-129 are most important.

The non element-specific parameters, which turned out to be important in the single-parameter variations, were chosen as a basis for the many-parameter variations. In these calculations four parameters have been varied simultaneously. Compared to the reference case, the calculated maximum radiation exposures differ up to a factor of 1500. This is an almost linear behaviour in the case of unfavourable parameter values.

The calculated maximum radiation exposures are for both waste types below 10^{-5} Sv/a in the reference case. This value is more than one order of magnitude lower than the German and Canadian radiation protection limits. Assuming unfavourable values of some

sensitive input parameters, these limits may be exceeded. Thus, for future performance assessments of repositories in hard rock a global sensitivity analysis on the basis of e.g. Monte-Carlo simulations is recommended.

Acknowledgements

The authors gratefully acknowledge financial support by the Scientific and Environmental Affairs Division of NATO under contract number LG 977810.

7 References

[1] AECB (Atomic Energy Control Board). Regulatory policy statement. Regulatory objectives, requirements and guidelines for the disposal of radioactive wastes - long-term aspects. AECB document R-104, Ottawa, June 1987.

[2] Allgemeine Verwaltungsvorschrift zu § 45 Strahlenschutzverordnung: Ermittlung der Strahlenexposition durch die Ableitung radioaktiver Stoffe aus kerntechnischen Anlagen oder Einrichtungen. Bundesanzeiger, 42. Jg, Nummer 64a, 1990.

[3] Baudoin P.; Gay, D.; Certes, C.; Serres, C.; Alonso, J.; Lührmann, L.; Martens, K.H.; Dodd, D.; Marivout, J.; Vieno, T.: Spent fuel disposal Performance Assessment (SPA project). Final Report; European Commission, EUR 19132 EN, Brussels 2000.

[4] Becker, D.-A.; Buhmann, D.; Storck, R.; Alonso, J.; Cormenzana, J.-L.; Hugi, M.; van Gemert, F.; O'Sullivan, P.; Laciok, A.; Marivoet, J.; Sillen, X.; Nordman, H.; Vieno, T.; Niemeyer, M.: Testing of Safety and Performance Indicators (SPIN), European Commission, EUR 19965 EN, Brussels 2003.

[5] Buhmann, D.: Das Programmpaket EMOS. Ein Instrumentarium zur Analyse der Langzeitsicherheit von Endlagern. Gesellschaft für Anlagen- und Reaktorsicherheit (GRS) mbH, GRS-159, Braunschweig 1999.

[6] Buhmann, D.; Ionescu, A.; Pavelescu, M.; Storck, R.: Comparison of safety assessments for spent CANDU or LWR fuels in repositories in rock salt. Gesellschaft für Anlagen- und Reaktorsicherheit (GRS) mbH, GRS-168, Institute of Nuclear Research Pitesti, SCN-N.T. 250/2000, Braunschweig 2000.

[7] Curti, E.: Modelling bentonite pore waters for the Swiss high level waste repository. PSI-report 93-05. Würrenlingen and Villigen 1993.

[8] International Commission on Radiological Protection: Limits for intakes of radionuclides by workers. ICRP 30. Pergamon Press. Oxford 1979

[9] International Commission on Radiological Protection: The metabolism of plutonium and related elements. ICRP 48. Pergamon Press. Oxford 1986

[10] International Commission on Radiological Protection: Age-dependent doses to members of the public from intake of radionuclides: Part 5 Compilation of ingestion and inhalation dose coefficients. ICRP 72. Pergamon Press. Oxford 1996

[11] Johnson, L. H.; LeNeveau, D. M.; Shoesmith, D. W..; Oscarson, D. W..; Gray, M. N.; Lemire, R. J.; Garisto, N. C.: The Disposal of Canada's Nuclear Fuel Waste: The Vault Model for Postclosure Assessment, AECL-10714, COG-93-4 1994.

[12] Kristallin-I Safety Assessment Report, NAGRA TECHNICAL REPORT 93-22, 1994.

[13] Lührmann, L.; Noseck, U.; Storck, R.: Spent Fuel Performance Assessment (SPA) for a hypothetical repository in crystalline formations in Germany. Gesellschaft für Anlagen- und Reaktorsicherheit (GRS) mbH, GRS-154, Braunschweig 2000.

[14] NUCLEARELECTRICA S.A. – Annual report 2001, Bucharest 2001.

[15] Papp, R.: GEISHA: Gegenüberstellung von Endlagerkonzepten in Salz und Hartgestein. FZKA-PTE Nr. 3, Forschungszentrum Karlsruhe GmbH, Karlsruhe 1997.

[16] Stenhouse, M.J.: Sorption Database for Crystalline, Marl, and Bentonite for Performance Assessments. NAGRA Technical Report NTB 93-06, Wettingen, July 1995.

List of Figures

List of Tables

Gesellschaft für Anlagen- und Reaktorsicherheit (GRS) mbH

Schwertnergasse 1
50667 Köln
Telefon +49 221 2068-0
Telefax +49 221 2068-888

Forschungsinstitute
85748 Garching b. München
Telefon +49 89 32004-0
Telefax +49 89 32004-300

Kurfürstendamm 200
10719 Berlin
Telefon +49 30 88589-0
Telefax +49 30 88589-111

Theodor-Heuss-Straße 4
38122 Braunschweig
Telefon +49 531 8012-0
Telefax +49 531 8012-200

www.grs.de

ISBN 3-931995-64-X